

**EPIGENETIC REGULATION OF QUIESCENT HERPES SIMPLEX VIRUS TYPE 1
GENE EXPRESSION**

by

Michael William Ferenczy

Bachelor of Science in Engineering, Tufts University, 2002

Submitted to the Graduate Faculty of
School of Medicine in partial fulfillment
of the requirements for the degree of
Doctor of Philosophy

University of Pittsburgh

2010

UNIVERSITY OF PITTSBURGH

SCHOOL OF MEDICINE

This dissertation was presented

by

Michael William Ferenczy

It was defended on

September 3rd, 2010

and approved by

J. Richard Chaillet, Associate Professor,
Department of Microbiology and Molecular Genetics

Fred Homa, Associate Professor,
Department of Microbiology and Molecular Genetics

Larry Kane, Associate Professor,
Department of Immunology

Saleem Khan, Professor,
Department of Microbiology and Molecular Genetics

Dissertation Advisor: Neal DeLuca, Professor,
Department of Microbiology and Molecular Genetics

A modified version of data presented in Chapter 2 appeared in “Epigenetic Modulation of Gene Expression from Quiescent Herpes Simplex Virus Genomes.” Michael W. Ferenczy and Neal A. DeLuca, *Journal of Virology*, 2009, volume 83(17), pages 8514-8524, copyright © 2009. Reproduced/amended with permission from American Society for Microbiology. All rights reserved.

Copyright © by Michael William Ferenczy

2010

EPIGENETIC REGULATION OF QUIESCENT HERPES SIMPLEX VIRUS TYPE 1

GENE EXPRESSION

Michael William Ferenczy, Ph.D.

University of Pittsburgh, 2010

HSV-1 is a ubiquitous human pathogen with a biphasic lifecycle. During latency, gene expression is globally repressed, most likely due to epigenetic mechanisms. The HSV protein ICP0 is a promiscuous transactivator of gene expression, and is required for efficient viral reactivation from latency. Evidence indicates that ICP0 interacts with a number of cellular pathways that mediate chromatin structure. Using a cell culture model of latency, the effects of cell-type, ICP0 expression, and ICP0 functional domains on the chromatin structure of viral genomes was examined. During viral entry into quiescence, ICP0 expression increased gene expression and histone hyperacetylation, while limiting the association of histones and heterochromatin with the viral genome. In the absence of ICP0, expression from viral promoters was rapidly repressed, and heterochromatin formed on viral promoters in a cell-type specific manner. Once quiescence was fully established, HSV genomes were found in a highly heterochromatic state. Heterochromatin, measured by the presence of heterochromatin protein 1 γ and trimethylation of histone H3 lysine 9, was rapidly removed upon provision of ICP0 *trans*. The changes in epigenetic structure were global, and preceded reactivation of gene expression. Overexpression of ICP0 resulted in the removal of histones from the quiescent genome, an effect not seen when ICP0 was expressed at physiological levels. This indicated that ICP0 may be mediating its effects through multiple functions, potentially through the enzymatic

function of its RING finger (RF) E3 ubiquitin ligase domain when expressed at low levels, and through physical protein-protein interaction when overexpressed. The effects on chromatin structure and gene activation of quiescent HSV were determined by superinfection with mutants of the RF domain and the C-terminus, which is important for the disruption of the CoREST/HDAC repressor complex. The RF domain was necessary and sufficient for reactivation of gene expression, but full transcriptional activation and removal of heterochromatin and histones required both the RF and C-terminus of ICP0. These results indicate that ICP0 relieves repression of gene expression through interactions with multiple cellular pathways. Expression of ICP0 removes epigenetic repression at multiple levels of chromatin, including heterochromatin, histone deposition, and the acetylation of histones.

TABLE OF CONTENTS

1.0	INTRODUCTION.....	1
1.1	OVERVIEW.....	1
1.2	PATHOLOGY, EPIDEMIOLOGY, GENOME STRUCTURE, AND LIFE CYCLE OF HSV-1	2
	1.2.1 Pathology and Epidemiology	2
	1.2.2 Structure and Life Cycle.....	3
1.3	CHROMATIN AND THE HISTONE CODE.....	4
1.4	ESTABLISHMENT OF QUIESCENCE.....	6
	1.4.1 Localization of the quiescent genome	6
	1.4.2 ND10 bodies	7
	1.4.3 Circularization of the Genome	7
	1.4.4 Methylation of viral DNA is not a means to repress transcription.....	8
	1.4.5 Deposition of histones on viral DNA and the formation of nucleosomes ...	9
	1.4.6 Histone tail modifications on the quiescent viral genome – entry into heterochromatin	15
	1.4.7 Higher order chromatin structure	18
1.5	MAINTENANCE OF QUIESCENCE.....	19
	1.5.1 Differences between maintenance of cell culture quiescence and latency	19

1.5.2	The structure of quiescent HSV and the maintenance of latency	20
1.6	EXIT FROM QUIESCENCE/REACTIVATION	23
1.6.1	Differences between cell types and states of latency.....	23
1.6.2	Changes in epigenetic structure upon reactivation	26
1.7	METHODS TO STUDY LATENCY AND QUIESCENCE	27
1.8	RATIONALE	30
2.0	EPIGENETIC MODULATION OF GENE EXPRESSION FROM QUIESCENT HSV GENOMES.....	35
2.1	ABSTRACT.....	35
2.2	INTRODUCTION	36
2.3	MATERIALS AND METHODS.....	39
2.3.1	Cells and viruses	39
2.3.2	ChIP	40
2.3.3	Micrococcal nuclease digestion.....	41
2.3.4	RNA isolation and reverse transcription.....	41
2.3.5	Real-time PCR	42
2.4	RESULTS	43
2.4.1	RNA expression from quiescent genomes	43
2.4.2	Histone deposition on the viral genome as a function of cell type and ICP0	46
2.4.3	Acetylation of histone H3 on quiescent viral genomes is a function of ICP0	50
2.4.4	Effects of cell type and ICP0 on repressive chromatin structure.....	53

2.5	DISCUSSION.....	56
2.5.1	Gene expression as a function of IE proteins.....	56
2.5.2	Deposition of nucleosomes and histone H3 as a function of ICP0.....	57
2.5.3	The formation of repressive chromatin.....	60
3.0	REVERSAL OF HETEROCHROMATIC SILENCING OF QUIESCENT HSV-1 BY ICP0.....	63
3.1	ABSTRACT.....	63
3.2	INTRODUCTION.....	64
3.3	MATERIALS AND METHODS.....	66
3.3.1	Cells and viruses.....	66
3.3.2	ChIP.....	66
3.3.3	Micrococcal nuclease digestion.....	68
3.3.4	RNA isolation and reverse transcription.....	69
3.3.5	qPCR.....	69
3.4	RESULTS.....	70
3.4.1	RNA expression from quiescent genomes upon reactivation by ICP0.....	70
3.4.2	Removal of higher order chromatin structure and repressive epigenetic marks upon expression of ICP0.....	73
3.4.3	Removal of histones upon expression of ICP0.....	75
3.4.4	Hyperacetylation of histones is a result of ICP0 expression.....	80
3.5	DISCUSSION.....	84
3.5.1	Gene expression upon ICP0 induced reactivation.....	84
3.5.2	Removal of heterochromatin as a function of ICP0.....	85

3.5.3	The abundance of ICP0 may affect the removal and acetylation of histones from quiescent genomes.....	87
4.0	FUNCTIONAL DOMAINS OF ICP0 INVOLVED IN REVERSAL OF EPIGENETIC SILENCING OF QUIESCENT HSV-1	90
4.1	ABSTRACT.....	90
4.2	INTRODUCTION	91
4.3	MATERIALS AND METHODS	94
4.3.1	Cells and viruses	94
4.3.2	ChIP	95
4.3.3	RNA isolation and reverse transcription.....	96
4.3.4	qPCR.....	97
4.4	RESULTS	98
4.4.1	Plaque-forming ability of ICP0 mutants	98
4.4.2	RNA expression from quiescent genomes upon reactivation by ICP0 mutants.....	99
4.4.3	Changes in chromatin structure of highly repressed quiescent d109 induced by ICP0 mutants	105
4.5	DISCUSSION.....	111
5.0	SUMMARY AND GENERAL DISCUSSION	118
5.1	SUMMARY OF RESULTS	118
5.2	ICP0 ACTS AT THE INTERSECTION OF INTERFERON, CHROMATIN, CELL-CYCLE, AND DNA DAMAGE RESPONSE PATHWAYS	125
	BIBLIOGRAPHY.....	130

LIST OF TABLES

Table 1. Primers used for RT-PCR.....	43
Table 2. Comparison of plaque-forming ability in L7 and Vero cells.....	99

LIST OF FIGURES

Figure 1. Levels of epigenetic repression of HSV-1 transcription.	10
Figure 2. Structure of the wild-type HSV-1 genome and the mutants d109, d106, and d105.	32
Figure 3. Functional domains attributed to ICP0, and ICP0 mutants RF, R8507, and R8508.	34
Figure 4. Abundance of GFP, tk, and gC mRNAs in KOS-, d109-, and d106-infected Vero and HEL cells.	45
Figure 5. MN digestion of d109- and d106-infected cells.	48
Figure 6. Binding of histone H3 to the tk, gC, and HCMV promoters of d109 and d106 in Vero and HEL cells.	49
Figure 7. Binding of AcH3 to the tk, gC, and HCMV promoters of d109 and d106 in Vero and HEL cells.	51
Figure 8. Binding of H3K9Ac to the tk, gC, and HCMV promoters of d109 and d106 in Vero and HEL cells.	53
Figure 9. Repressive chromatin modifications associated with the tk, gC, and HCMV promoters of d109 and d106 in Vero and HEL cells.	55
Figure 10. Abundance of GFP, tk, or gC mRNA in d109-infected MRC-5 cells after superinfection.	72
Figure 11. Repressive chromatin modifications associated with the tk, gC and HCMV promoters, and GFP 5' region of d109 in MRC-5 cells after superinfection.	75

Figure 12. Binding of histones H3 and H4 to the HCMV promoter of d109 in MRC-5 cells after superinfection with d105.....	77
Figure 13. Micrococcal nuclease digestion of d109-infected MRC-5 cells after superinfection.	78
Figure 14. Binding of histones H3 and H4 to the tk and gC promoters and GFP 5' region of d109 in MRC-5 cells after superinfection with adenovirus.....	79
Figure 15. Binding of hyperacetylated histone H3 and hyperacetylated H4 to the HCMV promoter of d109 in MRC-5 cells after superinfection with d105.....	82
Figure 16. Binding of hyperacetylated histone H3 and hyperacetylated H4 to the tk and gC promoters and GFP 5' region of d109 in MRC-5 cells after superinfection with adenovirus.....	83
Figure 17. Abundance of GFP mRNA in d109-infected MRC-5 cells (A) or Vero cells (B) after superinfection.....	100
Figure 18. Abundance of GFP mRNA in d109-infected MRC-5 cells (A) or Vero cells (B) after superinfection.....	103
Figure 19. Abundance of GFP mRNA in d109-infected MRC-5 cells (A) or Vero cells (B) after superinfection.....	104
Figure 20. Repressive chromatin modifications associated with the HCMV promoter of d109 in MRC-5 cells after superinfection.....	106
Figure 21. Binding of histones H3 and H4 to the HCMV promoter of d109 in MRC-5 cells after superinfection.....	108
Figure 22. Binding of hyperacetylated histone H3 (AcH3) and hyperacetylated H4 (AcH4) to the HCMV promoter of d109 in MRC-5 cells after superinfection.....	110
Figure 23. Binding of histone H3 dimethyl lysine 4 (H3K4me2) to the HCMV promoter of d109 in MRC-5 cells after superinfection.....	111

PREFACE

The six years or so that it takes to earn a Ph.D. may seem like a long and lonely odyssey, but I would not have been able to complete mine without a number of people. First, I want to thank my advisor, Dr. Neal DeLuca, who took me into his lab as a wandering graduate student and provided me with numerous professional opportunities. He taught me scientific techniques and, more importantly, how to think like a scientist. I would also like to thank Padma Sampath for teaching me the ChIP technique, and all of my lab-mates, especially Lauren Wagner and Fran Sivrich, for valuable discussions, both scientific and decidedly unscientific. They have helped to make working in the DeLuca lab a great experience. A number of my friends deserve special mention. Lauren Wagner and Tammer Farid independently suggested a troubleshooting fix for my experiments that allowed me to finish the research for Chapters 3 and 4. Dr. Anna Kusche proofed parts of my thesis, immediately read what I sent her, and made helpful suggestions and equally helpful jokes. Erik Moskowitz, Nick Deifel, Tammer Farid, Bryan Rivard, and Bill McCarthy helped me maintain some level of professional and personal sanity through this process, mostly by listening to me vent about various frustrations; I can't even imagine how boring that must have been for all of them, and for that I both apologize and thank them profusely.

I would especially like to thank my family, particularly my brothers Stefan and Philip – the best brothers anyone could ever ask for – and my stepfather Dr. Richard Cheney – who has been a wonderful addition to our family. My biggest role model has always been my father, both during life, and since his passing. He pushed me to only accept my best in sports, school, and all other aspects of life. Above all, he taught me to be a good man. I hope I have made him proud. Mostly, however, my completion of doctoral study; as well as high school and college, and pretty much everything in between, is due to the presence of my Mom. As a single mother for many of my developing years, she provided the love, encouragement, and (probably above all) discipline that I needed to develop into a strong, caring, and successful person. No amount of words can ever express the depth of my gratitude for everything she has sacrificed to help me on my journey.

1.0 INTRODUCTION

1.1 OVERVIEW

Herpes simplex virus type 1 (HSV-1) is arguably the most successful human pathogen. It infects the vast majority of the population, with which it has coevolved for thousands of years (206). HSV-1 is highly infectious, but does not greatly impair the normal function of its host, and may in fact be beneficial to its host's survival (9).

This success is due to the biphasic life cycle of HSV-1. Following infection of epithelial cells, HSV undergoes a burst of lytic replication and infects the sensory neurons innervating the site of infection. The viral DNA then establishes life-long latent infection in neuronal nuclei, where productive cycle gene expression is repressed, except in rare instances of reactivation. The global shutdown of gene expression allows the virus to evade the immune response and avoid viral clearance, and is most likely due to epigenetic mechanisms employed by the host cellular antiviral defense. During reactivation and subsequent replication, the virus must counteract the suppression of gene expression.

ICP0 is a viral protein required for efficient HSV establishment of infection, as well as reactivation from latency. A large number of functions have been attributed to ICP0, including, but not limited to, activation of gene expression (49, 84) and interactions with cellular proteins involved in: transcription (44, 115), translation (114), cell cycle regulation (44, 257), the

interferon response (41, 169), and the double-stranded break repair mechanism (108, 188). As a multifunctional activator of viral gene expression, ICP0 plays a key role in viral transcription, and may act as a molecular switch between the lytic and latent phases of the HSV-1 life cycle.

There is mounting evidence that the functions of ICP0 are due to multiple interactions with cellular signaling pathways that affect chromatin structure. The study presented here uses a cell culture model of quiescence that mimics aspects of *in vivo* latency, allowing for a detailed molecular study of the chromatin structure and kinetics of viral entry and exit from quiescence. The roles of cell type and functional regions of ICP0 upon the viral chromatin structure were explored, in addition to the effects that the abundance of ICP0 has on the epigenetic structure of the viral genome. This study begins to elucidate the cellular metabolic pathways that are involved in control of HSV-1 through epigenetic mechanisms.

1.2 PATHOLOGY, EPIDEMIOLOGY, GENOME STRUCTURE, AND LIFE CYCLE OF HSV-1

1.2.1 Pathology and Epidemiology

HSV-1 is a double-stranded DNA virus that establishes life-long infection in its host. Almost 100% of the human population is infected with HSV-1 (140) and approximately one third of people display clinical manifestations of infection (265). HSV-1 is transmitted through direct skin to skin contact (264), and causes visible, painful, and embarrassing skin lesions, primarily in the region surrounding the mouth (207, 263). HSV ocular diseases are among the leading infectious causes of blindness in many developed countries (141) and infection of the central

nervous system causes encephalitis, which can lead to brain damage and death (264). HSV-1 infection also increases the risk of HIV transmission (215).

1.2.2 Structure and Life Cycle

HSV-1 is an enveloped virus containing an icosahedral capsid that packages the viral genome. Between the capsid and envelope is an amorphous tegument layer that contains proteins which are important for the early stages of infection (10, 24, 238). Glycoprotein spikes which mediate entry are embedded in the envelope (206). The encapsidated HSV-1 genome is a linear double-stranded DNA molecule composed of approximately 152,000 base pairs, with single-stranded nicks and gaps (204). The genome is composed of two segments, the unique long (U_L) and unique short (U_S), which are bracketed by inverted repeats (147). The U_L and U_S sequences are joined by internal repeat sequences. The U_L and U_S sequences can invert relative to one another, such that the genome can be found in four equimolar configurations (42, 94).

Upon infection, HSV-1 undergoes an initial round of lytic replication in epithelial cells. HSV-1 encodes approximately 80 genes (204), which are grouped into three classes, and are expressed as a cascade during productive infection: immediate-early (IE), early (E), and late (L) (99, 100). All viral genes are transcribed by the host RNA polymerase II machinery (207). Upon entry into a cell, the transcription of the IE genes is induced by the tegument-associated virion protein 16 (VP16) in complex with cellular host cell factor (HCF) and Oct-1 (10, 24), which recognize the IE gene promoters (71). The five IE genes encode proteins that are primarily involved in the regulation of host cell metabolism and activation of viral gene transcription. Infected Cell Protein 4 (ICP4) is required for the activated transcription of E and L

genes (260). The E genes encode proteins involved in viral DNA replication, while the L genes produce mainly viral structural proteins (207).

After infection of the mucosa or an epithelial abrasion, HSV-1 enters the endings of sensory nerves adjacent to the site of infection, and moves via retrograde axonal transport to cell bodies, where, after limited replication, it establishes a latent infection (250). Primary lytic infection probably involves irregular histone association with viral genomes, although this is not conclusive (95, 96, 117, 136, 172). In contrast, latent HSV-1 genomes are associated with heterochromatin and express little or no protein (43), although a class of mRNAs called latency-associated transcripts (LATs) are expressed (230, 231).

Because of the global nature of transcriptional repression during latency, HSV-1 probably relies on epigenetic control of expression to prevent gene expression. DNA methylation is probably not the major means of control of HSV-1 gene expression because latent HSV-1 DNA is not extensively methylated (19, 128). In contrast, a number of studies have implicated chromatin structure and specific histone tail modifications in the control of HSV-1 latency, reactivation, and replication (1, 20, 117, 128, 255, 259).

1.3 CHROMATIN AND THE HISTONE CODE

Eukaryotic DNA is associated in a chromatin structure with nucleosomes, which are octamers composed of two each of the histones H2A, H2B, H3 and H4 (123). DNA wraps approximately 1.65 times around each nucleosome (154), and may additionally be associated with the linker histone H1 between nucleosomes. Thus, each nucleosomal structure of DNA is composed of 145-200 base pairs of DNA.

Epigenetic regulation of gene expression entails the control of access to the DNA by regulatory elements such as transcription factors. The occupational density of histones on DNA influences transcription because less occupied DNA is more open to transcription factors and the RNA polymerase II (pol II) is less impeded in its travel along the DNA. Modifications of the N-terminal histone tails, which protrude from the nucleosome, are also associated with control of transcription. Modifications to the chromatin structure of DNA to control transcription have been elucidated in a “histone code” hypothesis (112). Acetylation of lysines of histones H3 and H4 is associated with increased transcription. This may be due to decreased positive charge of the histones, which bind less tightly to negatively charged DNA, thus allowing greater access to the DNA by transcription factors. Some transcription factors contain bromodomains that bind acetyl-lysine. Methylation of histone tail residues is more complicated. For example, methylation of histone H3 lysine 4 is associated with transcription activation, while methylation of histone H3 lysine 9 is associated with transcriptional repression. Proteins with chromodomains can bind methylated lysines and cause repression or activation of transcription (202). Other modifications of histones include phosphorylation, ubiquitylation and SUMOylation (276).

Histone tail modifications may also influence their ability to bind to the major or minor groove of DNA on their own or neighboring nucleosomes, which influences accessibility to transcription factors (251). These modifications also recruit proteins that are involved in forming a higher order chromatin structure, known as heterochromatin, which is extremely repressive to transcription. Proteins such as heterochromatin protein 1 (HP1), which binds to methylated histone H3 lysine 9, help nucleosomes form this more compact and dense heterochromatin (177, 251).

Cells use a regulatory control network of histone chaperones and modifying enzymes to control the epigenetic state of their genes. Deposition of histones on DNA is controlled by histone chaperones such as ASF and CAF1 (187). Chromatin can be modified by remodeling enzymes such as members of the SWI/SNF family (276). The modifications of histone tails are controlled by numerous enzymes, including histone acetyltransferases (HATs), histone deacetylases (HDACs), histone methyltransferases (HMTs), and histone lysine demethylases such as LSD1 (221).

There is crosstalk between histone modifications at one residue of the histone tail and those at another (40), as well as between histone tails and DNA (227), such that modification of a specific residue of a histone influences the modification state of other histone residues. This crosstalk extends to the DNA. Repressive histone modifications are linked to the methylation of DNA, which also represses transcription (227).

1.4 ESTABLISHMENT OF QUIESCENCE

1.4.1 Localization of the quiescent genome

Latent infection is established in the nuclei of infected neurons (76). A more detailed determination of viral genome nuclear localization in neuronal cells has been difficult due to the lack of suitable antibodies for immunofluorescence studies in mouse and rat neuronal cells (101). Using cell culture systems, it has been determined that HSV genomes localize to the periphery of newly formed Nuclear Domain 10 (ND10) structures during the early stages of lytic infection (59, 64, 105, 161). This is consistent with the observation that other DNA viruses are deposited

near ND10 sites (105, 159). Quiescent HSV genomes are also associated with ND10 in human fibroblasts (60).

1.4.2 ND10 bodies

ND10 (or PML) bodies are small structures found in the nucleus that are organized by the protein PML. ND10 bodies are thought to be part of the innate cellular defense against viral infection (50), and in fact, overexpression of the ND10 components PML and Sp100 is able to cause repression of HSV-1 in the absence of ICP0. Upon expression of ICP0, PML and Sp100 are degraded (25, 57). Numerous other proteins localize to ND10 bodies, including HP1, which is associated with heterochromatin (56), as well as hDaxx (56, 107), and ATRX (107), which are members of transcriptionally repressive chromatin modifying complexes. These observations support the hypothesis that ND10 bodies repress viral transcription through epigenetic mechanisms.

1.4.3 Circularization of the Genome

Upon entry into the nucleus, HSV begins its gene expression cascade. If it is able to replicate, genomes can be found in many complex configurations, including full length linear genomes, complicated branched structures, and circular forms (70, 109), but all available evidence points to a circular episomal latent form of HSV DNA.

In latently infected mice, HSV DNA can be found in an “endless” configuration, determined by an increase in the joint fragments and a decrease in the terminal fragments in Southern blots of mouse neuronal tissue (46, 203). All four isomeric arrangements of the

genome were found and these results extended to analysis of human trigeminal ganglia (46). This increase in joint fragments has been found in quiescently infected PC12 cells (239) and Vero cells (108). A decrease of genomic termini could also mean that the quiescent genome is integrated into cellular DNA, but there is no evidence to support this possibility (164). Vero cells also showed an increase of circular DNA in relation to linear DNA in Gardella gel analysis (108). Circular HSV DNA is also extremely stable in cell culture, detectable 3-4 weeks post infection (108, 239). It is likely that latent viral DNA is found in a circular episome, both *in vitro* and *in vivo*.

The appearance of circular DNA occurs in the absence of *de novo* viral protein synthesis (108, 193). This suggests that cellular factors, such as DNA repair proteins, are responsible for the circularization of the quiescent viral genome. In fact, the ATM DNA damage response is activated upon infection of some cell types by HSV (142, 226); cellular recombination and repair proteins are recruited to sites of HSV DNA replication (275); and Mre11, a downstream effector of ATM, is degraded upon HSV infection of some cell types (77).

1.4.4 Methylation of viral DNA is not a means to repress transcription

Gene expression of circular latent viral genomes is generally repressed, except for LAT mRNA. The global nature of HSV gene repression suggests an epigenetic mechanism of transcriptional silencing. One possible mechanism is the methylation of DNA. HSV DNA has a very high CG content (206), which if methylated, could be silenced by the physical barrier to transcription, as well as the recruitment of methyl-CpG-binding domain proteins. This is not the case, however, as HSV DNA is not extensively methylated *in vivo* (45, 128). Thus, in the most sophisticated study of latent HSV DNA methylation to date, regions of the HSV genome likely to be

methyated were identified by bioinformatic analysis, and these regions were tested for methylation using bisulfite sequencing of latently infected mouse dorsal root ganglia (128). This study also found that chromatin structure correlated with gene activity. Histone modifications indicative of active gene expression were found within the active LAT region and modifications correlating with repression of transcription were found at the inactive HSV-1 DNA polymerase gene.

1.4.5 Deposition of histones on viral DNA and the formation of nucleosomes

Mounting evidence indicates that chromatin structure is a major determinant of HSV gene expression, both during lytic and latent infection. Chromatin structure exists on a number of levels, including deposition of histones on DNA, covalent modification of the histone tails, recruitment of non-histone proteins to the chromatin fiber, and folding into higher order chromatin structures (Figure 1).

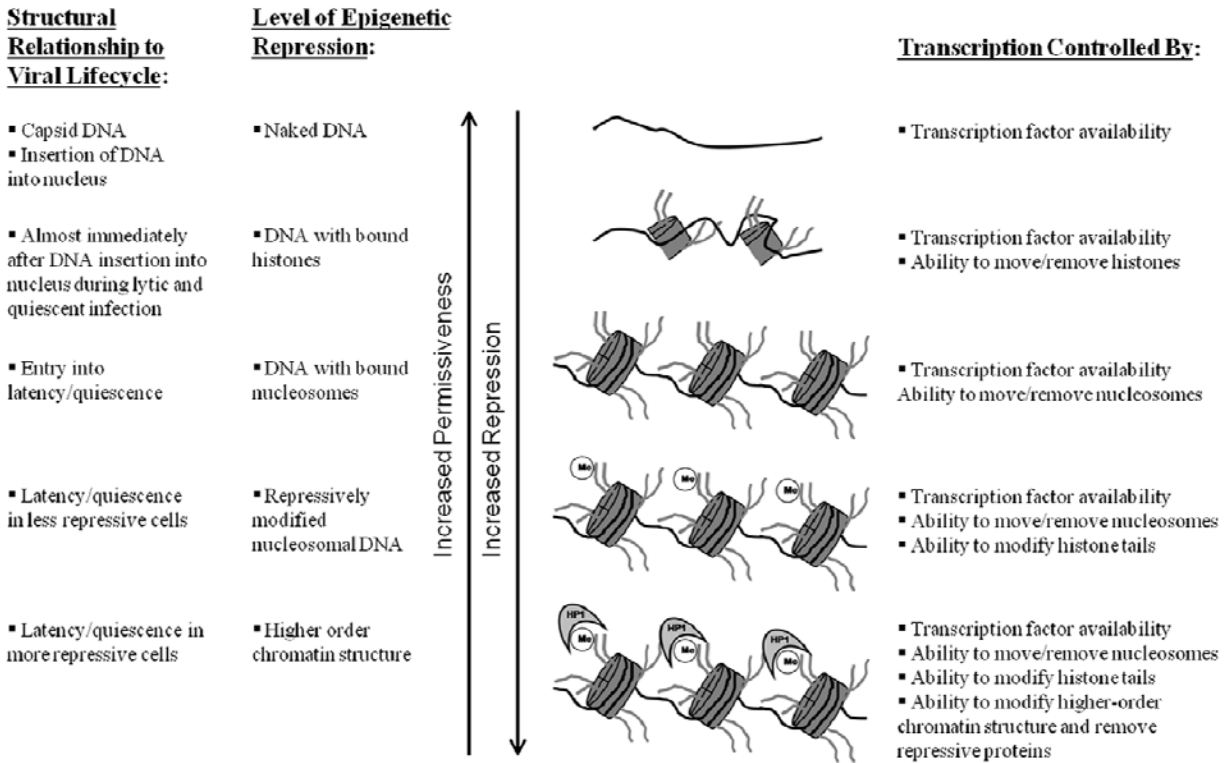


Figure 1. Levels of epigenetic repression of HSV-1 transcription.

As the viral genome enters quiescence, it acquires increasingly higher-order chromatin structure. The order of heterochromatin acquisition is not fully defined, but higher amounts of heterochromatin are associated with greater repression.

Initial studies of the chromatin structure of HSV utilized micrococcal nuclease digestion of radiolabelled DNA of cultured cells. Lytic infection of rat liver cells – labeled with [³H]thymidine either pre- or post-infection – revealed that the chromatin structure of replicating virus differed from that of cellular chromatin, producing a “smeared” pattern upon limited digestion while the pattern of cellular DNA did not change (171). This indicated that replicating viral DNA either did not associate with nucleosomes, or that there was random association of nucleosomes with viral DNA. These results were similar in nature to a more in-depth study of the betaherpesvirus Epstein Barr Virus (EBV). Micrococcal nuclease digestion and Southern

hybridization of EBV-infected non-producing (i.e. quiescent) Raji cells showed that the quiescent genomes were in a nucleosomal structure similar to that of cellular DNA. However, EBV-producing (i.e. lytic) P3HR-1 cells, containing replicating virus, were only minimally associated with nucleosomes (222), as demonstrated by a faint banding pattern superimposed upon a smear of viral DNA.

By pulse labeling DNA upon infection of Vero cells, it was found that parental HSV DNA is at least partially nucleosomal, while progeny DNA is found in a similar bands-on-a-smear pattern as replicating EBV DNA (136). A high molecular weight band of DNA was found, even after micrococcal nuclease digestion. This is presumably encapsidated DNA protected from enzymatic cleavage. Southern blotting with a full HSV DNA probe in this system also found a pattern of bands on a smear (136). In another study, complete micrococcal nuclease digestion of lytically infected Sy5y cells, a human neuroblastoma line, showed a band of mononucleosomal length, indicating that there is at least minimal association of nucleosomes with HSV DNA during lytic infection (117).

The cell culture micrococcal nuclease data of lytic infection was confirmed in an animal model system. Comparing lytic infection of the C1300 neuroblastoma cell line and the brainstems of acutely infected female BALB/c mice, it was found that most viral DNA from productive infection digested in a bands-on-a-smear pattern, indicating that both *in vitro* and *in vivo* lytic infection results in a population of viral genomes largely devoid of nucleosomal structure (172). These results cannot, however, distinguish between a single population of genomes with irregular nucleosome association and two distinct populations of genomes – one nucleosome-free, the other consisting of genomes regularly associated with nucleosomes.

Additionally, this study also concluded that encapsidated viral DNA was protected from micrococcal nuclease digestion (172).

A study of latently infected female BALB/c mice corroborated the previous cell culture EBV data. HSV genomes during lytic infection are partially or irregularly nucleosomal, while latent HSV DNA is found in a nucleosomal structure similar to that of cellular chromatin, as determined by the typical banding pattern of nucleosomal DNA upon incomplete micrococcal nuclease digestion. Both full-length HSV genomic probes and subgenomic probes spanning different regions of the genome were tested, indicating that nucleosomal association is regular across the genome (43). Additionally, micrococcal nuclease digested DNA from latently infected mice did not contain a high molecular weight band, indicating that no encapsidated genomes were present (43). A more recent study of quiescently infected human fibroblasts came to different conclusions about the nucleosomal association of the tk gene. Cells were treated with interferon- α and AraC to induce quiescence of a and a mutant virus deleted for the VP16 gene. It was found that quiescent DNA of the tk gene was not associated with nucleosomes in a regular pattern (110). Upon micrococcal nuclease digestion, a smear was seen when DNA was probed for the viral tk gene. This may have been due to low-level expression of viral genes in the fibroblast quiescence model. Additionally, viral DNA was more protected from digestion than the cellular DNA. This may indicate that quiescent infection of fibroblasts results in denser, higher order chromatin structure that is more resistant to micrococcal nuclease digestion than simple nucleosomal DNA.

These micrococcal nuclease digestion data indicate that the cell culture model is a good model for the epigenetic structure of latent HSV *in vivo*. The data indicate that the quiescent and

latent HSV genome is circular and found in a chromatin arrangement that is at least as protected from micrococcal nuclease digestion as bulk cellular DNA, and possibly more so.

The encapsidated viral genome is not associated with histones (183). As a result, when the capsid reaches the nucleus of the infected cell, it injects naked, linear DNA into the nucleus. This DNA may be recognized as foreign, which will initiate the innate immune response of the cell, or it may be recognized as damaged DNA. Recognition of this naked DNA prompts the cell to deposit histones on the incoming genome. Histone deposition is mediated by histone chaperones, such as Chz1 (which binds the H2A/H2B dimer) and CAF1 (which binds H3/H4) (187). In order to initiate the lytic cycle, HSV expresses proteins that either prevent histone deposition or remove deposited histones from the viral genome.

In order to gain a more detailed understanding of the chromatin state of latent HSV, chromatin immunoprecipitation (ChIP) has been utilized. ChIP consists of four basic steps: (i) *in situ* crosslinking of protein to DNA, generally using formaldehyde, (ii) isolation and shearing of DNA to slightly larger than nucleosomal size, (iii) selective immunoprecipitation of proteins of interest, to the resolution of specific histone tail modifications, followed by isolation of the bound DNA and (iv) amplification of DNA sequences of interest by qPCR to determine the percent bound by the protein of interest (129). The following studies utilized ChIP to better understand the regulation of HSV gene expression.

Lytic HSV infection does not affect the total amount of cellular histone H3 in Sy5y cells (117), but it encodes a number of proteins that may prevent histone deposition on the genome. VP22 is one of the most abundant tegument proteins, and is available to the virus immediately upon infection. In COS-1 cells VP22 binds to and colocalizes with the histone chaperones template-activating factor I α and β (TAF-I α and -I β) (255), which have been reported to

facilitate nucleosome formation on naked DNA (184). VP22 was also found to prevent the ability of TAF-I to reconstitute nucleosomes on plasmid DNA *in vitro* (255). VP22 may act in a nonspecific manner to prevent histone deposition.

Another tegument protein, VP16, activates the transcription of immediate early genes and recruits the chromatin remodeling proteins and transcriptional activators BRG1 and BRM to viral promoters in HeLa cells. VP16 also causes the underrepresentation of histone H3 in an activation domain-dependent manner (95); this effect is targeted to the promoters of IE genes. Transcription of IE genes allows the expression of ICP0, the promiscuous viral transactivating protein. ICP0 is a multifunctional protein that causes the proteosomal degradation of a number of proteins through its E3 ubiquitin ligase domain (48, 256). Expression of ICP0 increases the expression of all classes of viral genes, at least partially by manipulating the host chromatin modifying machinery. Recently it has been reported that ICP0 removes histone H3 from the viral genome during lytic infection of HeLa cells (29).

Because of the numerous strategies HSV employs to prevent histone deposition on its genome, it seems likely that latent genomes are generally associated with high levels of histones, which could help to physically block the transcriptional machinery. In male Cd-1 mice, histone H3 association with the ICP4 and tk promoters does not increase during the first 5 days post-infection, while the initial infection replicates. After 5 days post infection, however, histone H3 on the ICP4 promoter increased by over 10-fold, and histone H3 association with viral promoters increased through day 30 post infection (259).

ChIP and micrococcal nuclease digestion experiments *in vitro* and *in vivo* show that latent HSV is found in a nucleosomal structure during latency. This implicates histone and nucleosomal association with the viral genome as methods of cellular control of viral gene

transcription. Transcription can still occur, despite histone association with the virus, but this is the first cellular level of defense. Modifications of histone tails are a major determinant of whether the virus enters the lytic cycle or latency.

1.4.6 Histone tail modifications on the quiescent viral genome – entry into heterochromatin

During latency, the lytic cascade is abrogated and LAT expression predominates. In an *in vitro* neuronal culture utilizing viruses with reporter genes under control of lytic cycle or LAT promoters, it was seen that initial expression from lytic cycle promoters was gradually shut down over time, while expression from the LAT promoter was found at early times post infection and is stably maintained in culture (4).

It has been found that chromatin structure is necessary to block gene expression of quiescent DNA. In addition to prevention of histone deposition, HSV encodes a number of functions to block heterochromatin-associated histone modifications from occurring on its genome. Lytic HSV infection of Sy5y cells modestly increases the total cellular amount of the transcriptionally active histone modifications H3 acetyl lysine 9 (H3K9Ac) and H3 acetyl lysine 14 (H3K14Ac) by 1.5- to 2-fold, while decreasing the amount of dimethylated H3 lysine 9 (H3K9me2), a mark of inactive transcription, by approximately 2-fold (117). The same study found that lytic HSV increased its association with histones bearing the active chromatin marks H3K9Ac, H3K14Ac, and H3K4me3, while maintaining low levels of association of the repressive mark H3K9me2 (117). It was later found that inhibition of methylation by the histone H3K4 methyltransferase reduces the amount of H3K4me3 on the HSV genome and also results in decrease replication and transcription of HSV (103). These observation in lytic cell culture

models indicate that the latent HSV genome is likely to be hypoacetylated on inactive genes and hyperacetylated on active genes.

VP16 plays a role in recruiting the HATs p300 and CBP to immediate early promoters during infection of HeLa cells, which results in an increase in hyperacetylated H3 (AcH3) relative to total H3 at these promoters (95). The viral Us3 kinase has also been reported to increase gene transcription in a manner similar to the HDAC inhibitor sodium butyrate in SK-N-Sh cells by causing the phosphorylation and redistribution of HDAC1 (194).

Most of the research on HSV interference with chromatin modification machinery has focused on ICP0. Viruses lacking ICP0 are poorly replicating in most cell types, and show significantly decreased expression of viral genes (210, 237). ICP0 is a key activator of the lytic cycle. In HeLa cells, the ICP8 gene is associated with hyperacetylated histones in the presence of ICP0 (29). This effect may be mediated by the reported interaction of ICP0 with class II HDACs (153), or its disruption of the neuronal REST/CoREST/HDAC1/HDAC2 repressor complex in HeLa, SK-N-SH, HEL, and HEK293 cells (78, 81). The REST/NRSF DNA binding site has been reported to be in proximity of the ICP22 and ICP4 IE genes. Transient transfection assays in HEK293 cells indicate that REST/NRSF reduces transcription from the ICP4 and ICP22 promoters, and binds in the proximity of and reduces histone H4 acetylation of the ICP4 promoter (190). The REST/NRSF binding site is not necessary, however, for entry into quiescence. A mutant lacking the REST/NRSF binding site, which does not express any IE genes, can stably enter quiescence in Vero and HEL cells (211).

Multiple studies have also determined that HDAC inhibitors can at least partially substitute for ICP0, relieving transcriptional repression in the absence of the protein (4, 39, 97, 195). In certain cell types, however, as quiescence progresses HDAC inhibitors decrease in their

ability to functionally substitute for ICP0, indicating the ICP0 has functions in addition to HDAC inhibition (246).

In quiescently infected MRC-5 cells, the ICP0 promoter was enriched in the repressive chromatin marks H3K9me and H3K9me3 prior to reactivation induced by superinfection. Concurrently, the ICP0, ICP27, gC, and LAT promoters were hypoacetylated on histone H3 prior to superinfection (32). In contrast, in latently infected female Swiss Webster mice, the LAT promoter is enriched in hyperacetylated H3 (AcH3), which may reflect differences between LAT expression *in vitro* and *in vivo*. The findings that lytic gene promoters are associated with hypoacetylated histone H3 concurred with the *in vitro* data (128). Another *in vivo* study using male CD-1 mice has also determined by CHIP that LAT expression affects the histone modifications on viral promoters. LAT expression was associated with an increase of the heterochromatic modification dimethyl H3 lysine 9 (H3K9me3) and a reduction of the transcriptionally active H3K9me2 on lytic gene promoters (259).

Studies of the histone changes associated with lytic virus suggest that histone modifications play a major role in viral expression. Hyperacetylation of histones and methylation of histone H3K4 are modifications associated with active chromatin, and are associated with gene expression from the lytic HSV genome. The ability of HDAC inhibitors to partially substitute for ICP0 highlights the importance of acetylated histones to viral transcription. These studies also suggest that quiescent HSV, in addition to being associated with hypoacetylated histones, is further repressed in a manner that is insensitive to HDAC inhibitors.

1.4.7 Higher order chromatin structure

The decreasing ability of HDAC inhibitors such as trichostatin A (TSA) to reactivate quiescent HSV in mouse TG explant cultures as the infection proceeds (246) implies that there are additional barriers to gene expression in the chromatin state of the repressed genome. Additionally, quiescent genomes lacking ICP0 in HEL cells are not reactivated upon superinfection with virus also lacking ICP0, despite the replication of the superinfecting genome (168). ICP0 is required for reactivation of these quiescent genomes.

Few studies have addressed the higher order chromatin structure of quiescent virus, but some aspects of its structure can be inferred by studies of lytic virus. An early study of nuclear sedimentation rates of chromosomal DNA in HeLa cells indicated that infection by HSV induced disruption of higher-order chromatin structure (3). HSV has also been reported to mobilize linker histone H1, a key component of the 30nm fiber of higher order DNA folding (90), in Vero cells (33).

ICP0 expression induces the degradation of the centromeric histone H3 variants CENP-A in HeLa, HFL, and Hep2 cells (152), CENP-B in HeLa and NIH3T3 cells (151), and CENP-C in Hep2 cells (55). These proteins help to form the kinetochore and begin assembly of the centromere (219). This may be a strategy by the virus to stall the cell cycle of actively dividing cells (97, 150), or it may be a byproduct of the destruction of ND10, as a significant number of proteins can be found in both ND10 and centromeres (56). It may also interfere with the formation of heterochromatin on the viral genome, a prospect that requires further study. The ICP0 promoter of quiescent genomes lacking VP16, ICP0 and ICP4 expression in MRC-5 cells is associated with HP1 α (32), which is a constituent of heterochromatin (149).

Both *in vitro* and *in vivo* studies have found that the quiescent genome is found in a circular episome. The quiescent genome is also associated with nucleosomes containing histones with modifications corresponding to transcriptional repression. Specifically, histones are hypoacetylated, there is a decrease of the active mark H3K4me, and an increase in the repressive modifications H3K9me, H3K9me₂, and H3K9me₃. This modification is known to recruit the HP1 chromodomain, and the HP1 γ isoform is recruited to quiescent HSV genomes in at least some cell types. The cumulative results of these studies demonstrate that as the genome enters quiescence, it acquires increasing chromatin structure, until it is tightly packaged in a higher-order chromatin structure.

1.5 MAINTENANCE OF QUIESCENCE

1.5.1 Differences between maintenance of cell culture quiescence and latency

There are a number of differences between *in vitro* quiescence and *in vivo* latency. Quiescent genomes in human fibroblast cultures are associated with ND10 (60), and while there is a dearth of data corresponding to specific cellular location of the latent viral genome, some evidence has shown that neurons either lack ND10, or have limited or different ND10 structures in comparison to fibroblasts in cell culture (101, 106, 175). ND10 structures have a role in the repression of HSV replication, but the mechanism by which ND10 exert their influence is unclear.

Mutants of HSV used to establish quiescent cell culture infections almost invariably have ICP0 mutations, truncations, or complete knockouts. These methods to suppress gene expression

necessarily also interfere with the structure of the LAT gene. The function of the LAT gene and its transcripts has been the subject of some controversy. In the mouse it has been reported that LAT expression promotes the assembly of heterochromatin on lytic genes (128, 259), while in the rabbit it has been shown to promote euchromatin assembly on, and increase transcription of, lytic genes during latency (73). These two sets of results may be due to the different models used. LAT also reportedly prevents splicing of the primary ICP0 transcript (156), protects neurons of the TG from apoptosis (18), and encodes a microRNA responsible for reduction in ICP0 protein expression, in both Vero cells and mice (252). To complicate matters, it appears that LAT, and most viral proteins, are dispensable for establishing quiescence in cell culture (209, 211). Clearly, more study of the function of LAT is required, and quiescent cell culture models containing intact LAT could help by providing a less complex system.

Additionally, cell culture models examining maintenance of quiescent HSV infection are only poorly able to mimic immune conditions found *in vivo*. Addition of interferon to cultures has been used to establish quiescent infection, but it is not absolutely necessary. Some *in vivo* studies of latent HSV have shown an activated immune response in latently infected mice, which helps to prevent HSV reactivation (67, 118, 223, 247). It appears that through immune activation, the host contributes to the perpetuation of the latent state. This may be beneficial to both host and virus, as it allows viral survival, while also minimizing immune-mediated damage to the host.

1.5.2 The structure of quiescent HSV and the maintenance of latency

Despite their limitations, cell culture models of latency can give us insights into both the viral and cellular mechanisms involved in maintaining quiescence. One of the major characteristics of

HSV is its ability to maintain lifelong infection of its host. This is accomplished through latency, during which the virus is able to effectively maintain its genome in non-dividing sensory neurons while “hiding” from the immune system. The virus is able to accomplish this in part through the structure of the quiescent genome. In cell culture, circular episomes are more stable than their linear counterparts (108, 239), and “endless” circular configurations are found *in vivo* as well (46, 203).

The shutdown of activated expression of lytic transcripts during latency may be part of a viral strategy to evade the immune system and prevent long term damage to its host. The chromatin structure of the virus may be able to block activated gene expression, which limits viral toxicity to its host cell and activation of the immune system. Quiescent infection of Vero cells with a viral mutant lacking all IE gene expression did not affect cell survival, and infection of HFL cells did not disrupt ND10 (211).

In a rat neuronal culture system utilizing various replication-defective reporter mutants, lytic promoters were found to be active upon infection and shut down over time, while LAT expression was evident in neurons at early times post infection and was stably maintained for several weeks (4). Together with the data finding that LAT expression, at least in some animal models, is able to down-regulate lytic gene expression through both miRNA and chromatin structure (252, 259), it appears that lytic gene shutdown is part of a viral strategy to maintain latency.

LAT expression plays an important, if poorly understood role in HSV latency *in vivo*. In order to express LAT while globally repressing the genome, the virus must have a mechanism to maintain LAT in a more open chromatin structure. An early cell culture study of the Pseudorabies Virus LAT promoter inserted into differing regions of the HSV genome suggested

a positional effect on expression (102). When inserted into the LAT promoter region of HSV, expression was seen in cells of neuronal origin, but when inserted in the place of gC, expression was greatly repressed.

A study of latently infected female Swiss Webster mice revealed that the LAT enhancer is associated with hyperacetylated histones, but that this pattern does not extend into the ICP0 promoter region; indeed, no lytic genes tested contained regions of hyperacetylated histones (127). This effect was maintained in the presence or absence of LAT transcription, indicating that HSV employs a mechanism independent of transcription to maintain an active chromatin state on LAT during latency. This study suggested that a boundary element was present to maintain two distinct chromatin domains on the latent HSV genomes. Further *in vitro* and *in vivo* studies, while disagreeing slightly, found that there is a CTCF-dependent chromatin insulator element between LAT and the ICP0 promoter, allowing LAT to maintain an active chromatin state, while ICP0 and other lytic genes are found in heterochromatin (2, 26).

In order to maintain latency, the HSV genome adopts a stable, circular, episomal structure that is bound by nucleosomes. Expression from the LAT region appears to promote the assembly of heterochromatin on lytic regions of the genome, which are globally repressed by their structure. The LAT promoter is bounded by an insulator that allows it to remain associated with hyperacetylated histones and continue expression, while the bulk of the latent genome remains repressed, effectively allowing it to evade the immune system and maintain infection throughout the life of the host.

1.6 EXIT FROM QUIESCENCE/REACTIVATION

1.6.1 Differences between cell types and states of latency

Multiple levels of control regulate gene expression in eukaryotic cells. Availability of transcription factors and specific DNA sequences regulate expression from naked DNA. Nucleosome and histone binding and placement require additional cofactors to aid transcription and remove histones from the path of the RNA polymerase II holoenzyme (138). Specific histone tail modification can further regulate transcription, either positively or negatively, and greater DNA folding due to linker histone association and non-histone proteins associated with chromatin can limit access of transcriptional machinery to the genome and further repress gene expression.

Despite its repressive chromatin structure, some expression of lytic genes from latent HSV is observed, both *in vitro* and *in vivo* (66, 126). Additionally, chronic immune activation of latently infected hosts implies that at least some protein expression occurs during latency *in vivo*. The mechanism that changes the viral expression pattern from the latent program to the lytic cycle is unclear. Cellular stress (36, 38, 148, 197, 274) and decrease in immune function can both reactivate HSV (67). The exact order of gene expression upon reactivation is unclear, but latently infected explanted mouse TG were shown to express genes out of the order of the lytic cascade (242), while there is reportedly a decrease in LAT prior to, or concurrent with, lytic gene expression (231, 274).

One hypothesis explaining reactivation is that during latent infection, some genomes are found in a less repressed state, allowing for stochastic gene expression and less restricted reactivation. This would help to explain chronic immune activation during latent infection, as

there would be low level antigen present throughout infection. Using a GFP reporter gene under control of the HCMV promoter, it has been found that cell types vary greatly in their ability to repress expression from quiescent genomes expressing no IE genes. The osteosarcoma cell line U2OS expressed GFP in 99% of cells, while HEL cells expressed GFP in less than 1% of cells. Additionally, in primary cultures of murine TG, neurons expressed GFP during quiescent infection, while support cells rarely demonstrated GFP expression (246).

Even cells of the same type within the same culture differentially repress quiescent virus. Low MOI infection of human fibroblasts with a mutant HSV strain lacking ICP0 expression established quiescent infection. Nonproductive infection varied greatly between cells, with some expressing no detectable viral protein, others expressing some IE proteins, still others expressing all IE proteins, and some stalling at an early protein expression phase, prior to DNA replication (53). Similarly, reactivation of HSV in quiescently infected PC12 cells in response to stress only moderately increases expression of the viral genes ICP0, ICP4, or LAT, and does not increase average expression of VP16 and ICP27 (38). This lack of global viral transactivator expression indicated that virus from only a small proportion of cells initiated reactivation.

These *in vitro* studies of differing states of latency correlate with *in vivo* studies. In male Swiss Webster mice, it was found that few latently infected neurons were able to reactivate in response to hyperthermic stress (214). Another study of latently infected ICR mice demonstrated differing populations of neurons, with reactivation by explant cultivation occurring specifically in those neurons expressing *cdk2* (216).

These results, which show levels of expression differing between cell type and even between neighboring cells of the same type in culture, suggest that repression of viral gene expression varies. This variation of repression is likely to be the result of differences in

epigenetic structure. Cellular chromatin varies from cell to cell in its protein association, nuclear position, and three dimensional structure, even at the same locus (74). It seems likely that viral chromatin behaves similarly.

In order to undergo reactivation of gene expression, quiescent viral genomes likely must change chromatin structure. HDAC inhibitors such as TSA and sodium butyrate can induce reactivation of replication competent quiescent virus in PC12 cells (39). TSA can also induce reactivation of gene expression in quiescently infected neurons in explant cultures from mice (246) and rats (4). TSA induced reactivation was limited in both cases to reporter gene expression from neurons. It appears that HSV in quiescently infected support cells requires more than histone acetylation to reactivate gene expression. Provision of ICP0 by superinfecting virus was able to reactivate gene expression in mouse neuronal cultures (246). This indicates that the functions of ICP0 include more than HDAC inhibition, and that quiescent virus in some cell types is in a higher order chromatin structure refractory to activation by histone acetylation alone.

The presence of ICP0 is critical for effective viral reactivation from latency (21-23, 85, 86, 113). Using a reporter gene controlled by the ICP0 promoter in quiescently infected rat neuronal culture, it was determined that the ICP0 promoter is able to reactivate expression upon addition of TSA. It has been shown in HEL cell culture that levels of ICP0 1000-fold less than typical lytic infection levels are able to efficiently reactivate reporter gene expression from quiescent genomes (96). These observations suggest that perturbation of the chromatin structure of ICP0 in a small number of viral genomes can initiate ICP0 expression, which can further alter chromatin of the quiescent viral genome, allowing viral reactivation without significant changes in gene expression or average chromatin structure of the quiescent viral genomes.

Cell type differences in chromatin structure of latent HSV are likely to allow a minority of latent virus to reactivate. Upon reactivation, these viruses may spread and provide the impetus to begin reactivation in cells previously refractory to reactivation. In order to express viral lytic genes and eventually replicate the genome, latent HSV must undergo structural changes.

1.6.2 Changes in epigenetic structure upon reactivation

Few studies have investigated the changes to viral chromatin upon reactivation of quiescent or latent virus. One study employed a fibroblast model of quiescence utilizing replication-deficient HSV mutants, followed by derepression due to the provision of ICP0 (32). Upon ICP0-mediated derepression, histone levels remained essentially the same on quiescent genomes, as determined by ChIP. After superinfection with an adenovirus providing ICP0, an increase in AcH3 was found on the ICP0, ICP4, ICP27, VP16, gC and LAT promoters, and a decrease in the repressive modification H3K9me3 was found on the ICP0, ICP27, VP16, and gC promoters. These results demonstrate that derepression of quiescent genomes by ICP0 induces a global change in chromatin structure, specifically the acetylation of histones associated with quiescent viral genomes.

Corresponding to this *in vitro* study, in a BALB/c mouse model, it was found that sodium butyrate treatment of latently infected mice induced reactivation. Using ChIP, it was determined that acetylation of histones at the LAT promoter decreased soon after sodium butyrate treatment, with a corresponding decrease in LAT expression, while the ICP0 and ICP4 promoters became hyperacetylated (176). These findings agree with those of a previous ChIP study of latently infected mouse dorsal root ganglia explants, in which the LAT promoter became hypoacetylated

post explant, corresponding to decreased LAT expression, while the ICP0 promoter became hyperacetylated (1).

The discrepancy between the *in vitro* and *in vivo* data on the structural changes to LAT chromatin induced by reactivation can be explained in several ways. It is possible that there is an *in vivo* mechanism by which LAT is treated differently than the bulk of the viral genome in cell culture. This may be a consequence of immune interaction with latently infected cells. Alternatively, since the ChIP technique measures an average across a population, it may be that discrepancies exist due to multiple infected cell types or states of latency *in vivo*, while the more uniform cell culture infection gives a different average association of acetylated histones with viral genomes. More study on the consequences of structural changes to viral chromatin upon reactivation is clearly needed.

1.7 METHODS TO STUDY LATENCY AND QUIESCENCE

Study of viral genome structure during latency has proved to be difficult. Various viral mutants have been studied for their ability to establish and reactivate from latency (12, 13, 28, 104, 111, 124, 163, 192, 232, 254). Reactivation and viral shedding has been studied by stressing mice or using mice deficient in various aspects of the immune system (167, 185, 186). Elucidating the structure of the latent genome requires sacrifice and dissection of the animal, followed by biochemical analysis.

As with all model systems, there are a number of drawbacks to studying latency *in vivo*. Changes may occur in viral genome structure during the manipulation of the animal and its dissected cells. The act of explantation can itself reactivate latent virus (120, 233). Additionally,

dissection of the TG does not isolate neuronal cells; various support cells are necessarily included when harvesting the TG, and it is difficult to isolate specific cell types in high enough purity to use for biochemical analysis.

In order to overcome these limitations, cell culture models of HSV latency, known as quiescence, have been developed. Cell culture models offer a number of advantages in the study of quiescence. Primarily, they confer the ability to study the state of the genome in a uniform cell type. They also bypass difficulties in determining the quantitative establishment of infection that may be due to varied infection efficiency, immune responses, or scarification of the eye. Cell culture techniques also allow for study of cells in the absence of an immune system, allowing a focus on innate cellular mechanisms of viral expression and control.

Various cell culture systems have been used to study HSV quiescence including explanted mouse and rat neuronal cultures, which include support cells (228, 246, 266, 270-274); neuronally derived cell lines (101, 122, 132, 178, 253); rat-derived pheochromocytoma (PC12) cells, which are thought to mimic the behavior of neurons, (11, 37); and even isolated human fetal neurons (267). More exotic model systems have also been used, such as T-lymphoid lines (87, 88) and three dimensional keratinocyte cultures (241).

The most extensively utilized human cell culture system for the study of quiescence has been human fibroblasts, generally of fetal origin. These cells offer the advantage of being human in origin, thus having a vast array of compatible reagents available. Primary fibroblasts also provide a uniform cell culture to study mechanistic details of quiescence and are amenable to quiescent infection, possibly due to their low metabolic rate (which may make them more similar to neurons than immortalized cell lines) or intrinsic factors that suppress lytic infection

(89, 168). Fibroblasts are more repressive to gene expression in the absence of the viral transactivating protein ICP0 than most immortalized cell lines (246).

The use of fibroblasts to support quiescent wild-type infection has required elevated temperature (34, 35, 98, 162, 181, 199, 261, 262); serum starvation (162); viral irradiation prior to infection (179); treatment with inhibitors of replication (30, 31, 181, 217, 268, 269), interferon (199, 217, 269), or various other chemicals (225). Additionally, many of these techniques required infection at low multiplicity of infection (92, 208, 282), limiting the sensitivity of various assays.

An alternative to the above techniques has been the use of viral mutants lacking essential genes to establish quiescent infection. These mutants allow high multiplicity infection of cells, establishment of quiescence, and reactivation of expression or replication through the provision of one or more complementing genes in *trans*. Mutants of VP16 are reduced in the ability to activate expression from IE genes (93, 110, 170, 199). ICP4 is required to activate E and L genes (209). ICP27, like ICP4, is essential for virus replication. ICP0, though not absolutely required for viral replication, is a promiscuous transactivator of gene expression, and is required for efficient replication in a MOI and cell-type dependent manner (53, 96, 209). Many viral systems used to establish quiescent infection contain lesions in multiple genes (60, 96, 170, 198, 211, 212).

Cell culture systems have advanced the understanding of HSV genetics and cellular mechanisms that regulate viral gene expression and replication, and have allowed for a mechanistic study of quiescence. Viruses deficient in ICP0 necessarily cause deletions or truncations of LAT (206). Since LAT is the predominant mRNA expressed by latent virus *in vivo*, this is a major drawback to such systems. The true test of any model system, however, is

its ability to mimic *in vivo*, physiologically relevant situations. Viral mutants have been used to establish latency in animal systems (28, 158, 232, 254), and viral mutant infection of fibroblasts have mimicked key aspects of latency and reactivation, establishing the use of cell culture systems as a valid system to investigate quiescent genomes.

1.8 RATIONALE

Due to the complications inherent in studying latency and genome structure in a complex animal system, cell culture techniques to investigate quiescence have been developed, and provide a robust, if imperfect, model for latency. Models of quiescence give insight into the cellular mechanisms involved in viral transcriptional repression, as well as epigenetic control of gene transcription generally. The epigenetic structure of the HSV genome is intimately linked to the establishment, maintenance, and reactivation from, quiescence. Circular forms of the genome are more stable in cell culture, and are the predominant form of the genome found during *in vivo* latency.

Shortly after infection and during entry into quiescence, the HSV genome becomes associated with histones. These histones are modified with epigenetic marks of heterochromatin, including hypoacetylation of histones H3 and H4, hypomethylation of H3K4, and methylation of H3K9 on lytic gene promoters. The kinetics of acquisition of these modifications vary between viral strains, mutants of specific viral genes, culture conditions, and cell type. As establishment of quiescence proceeds and increasing repression of expression occurs, the viral genome is further packaged into a higher order chromatin structure, at least partially due to the association of HP1 with methylated H3K9. The LAT promoter appears to maintain euchromatic

modifications in animal models, due to the presence of a chromatin boundary element. It is probable that other proteins involved in the formation of higher-order chromatin structure, as well as other chromatin modifying proteins are associated with the quiescent genome. More work is needed to fully elucidate the structure and maintenance of quiescent HSV.

Reactivation provides insight into how the epigenetic structure of the viral genome is related to increased gene expression, as well as to the state of the genome before reactivation. The state of viral epigenetic repression varies between cell types, and likely even between cells of the same type. The extent of heterochromatin may even vary between repressed genomes in the same cell. Upon reactivation, quiescent genomes undergo structural changes, including a decrease in HP1 association and methylation of H3K9, and a corresponding increase of hyperacetylation at lytic promoters.

HSV-1 reactivation from the latent state occurs during increased physical or emotional stress in an infected host (14) or following loss of immune function (215). Efficient reactivation from latency requires the IE protein ICP0 (135). ICP0 is a 775 amino acid protein (189) that is a promiscuous transactivator of gene expression. It does not bind DNA, but rather causes an increase in transcription by interfering with host cell pathways ranging from the DNA damage response, the interferon response, and the cell cycle. ICP0 is a critical viral protein that influences viral chromatin structure and host cell metabolism through multiple mechanisms. Therefore, we propose to characterize the histone modifications induced by ICP0, the mechanisms by which ICP0 causes these effects, and the structural motifs of ICP0 necessary for these effects.

In order to facilitate studies of the chromatin changes induced by cell type and ICP0 expression upon the entry into viral quiescence, the viruses d109 and d106 will be used. d109 is

a viral mutant that is defective for all five IE genes and expresses GFP under control of the hCMV promoter. d106 expresses ICP0 and the GFP transgene, but none of the other IE proteins. Infection of either Vero or HEL cells, followed by RT-PCR, ChIP, or micrococcal nuclease digestion will give insight into the role of chromatin structure and its effect on viral gene expression during the establishment of quiescence.

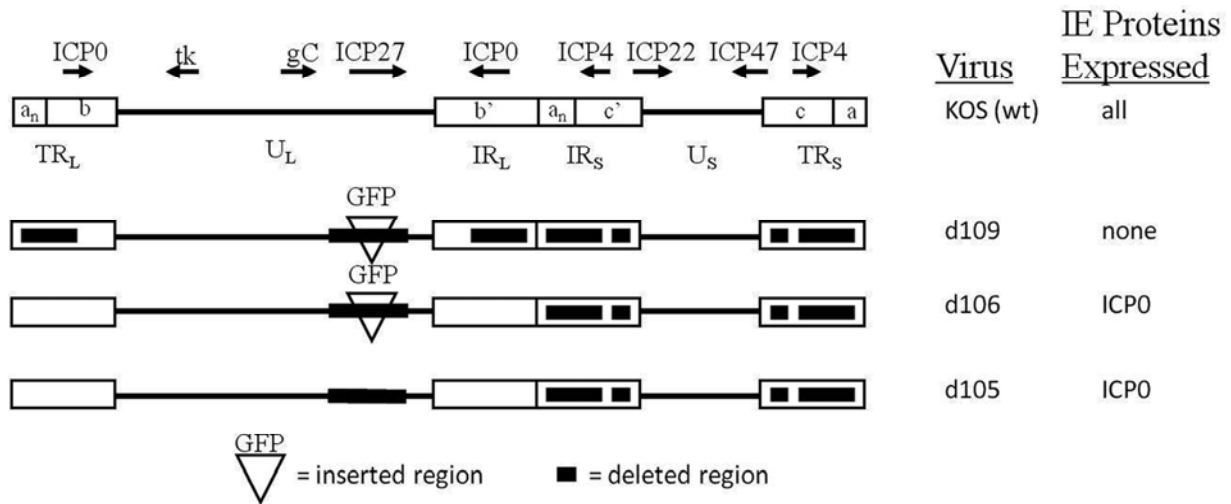


Figure 2. Structure of the wild-type HSV-1 genome and the mutants d109, d106, and d105.

The unique long (U_L) and unique short (U_S) segments of the genome are flanked by inverted repeats: the long and short terminal repeats (TR_L and TR_S), and the long and short internal repeats (IR_L and IR_S). The location of deleted IE genes is shown, as well as the inserted GFP transgene cassette, and the representative E and L genes tk and gC.

d109 establishes long-term quiescence in cell culture, and gene expression from d109 can be reactivated by supplying ICP0 in *trans*, modeling reactivation from latency. Quiescence will be established with d109, and gene expression will be reactivated by providing ICP0 in *trans* by superinfection with various viruses and mutants of ICP0. By modeling reactivation with the virus d105, which is an isogenic variant of d106 that does not contain the GFP transgene cassette, the kinetics of chromatin changes and reactivation of gene expression will be measured

by RT-PCR, ChIP and micrococcal nuclease digestion. Adenovirus vector AdS.11E4(ICP0) expresses ICP0, and AdS.10, its parent vector, does not (96). Superinfection by these vectors, followed by RT-PCR and ChIP, will be used to establish the epigenetic effects of ICP0 on reactivating quiescent genomes in the absence of other HSV-1 proteins.

In order to characterize the effects of the various functional domains of ICP0 on the chromatin structure and gene expression of reactivating quiescent d109, various mutants of ICP0 will be used to superinfect cells quiescently infected with d109. n212 expresses all of the IE genes except ICP0, and does not contain the GFP transgene (23). The RF mutant contains point mutations that inactivate the RING finger domain (146). R8507 contains point mutations in the C-terminus of ICP0 that abrogate its ability to disrupt the CoREST repressor complex (83). The wild-type (wt) strain of virus used will be KOS. Following superinfection, RT-PCR and ChIP will be performed.

These studies will give insight into the epigenetic mechanisms used by cells to suppress gene expression from incoming viral DNA, and the viral strategy used to counteract this cellular defense. If the underlying epigenetic mechanisms of HSV-1 establishment of, and reactivation from, latency can be understood, it may provide new targets for therapy and prevention of symptomatic HSV-1 infection. Additionally, this research will give greater insight into mechanisms of epigenetic transcriptional control, which has implications in many diseases, including infectious diseases and cancer (47).

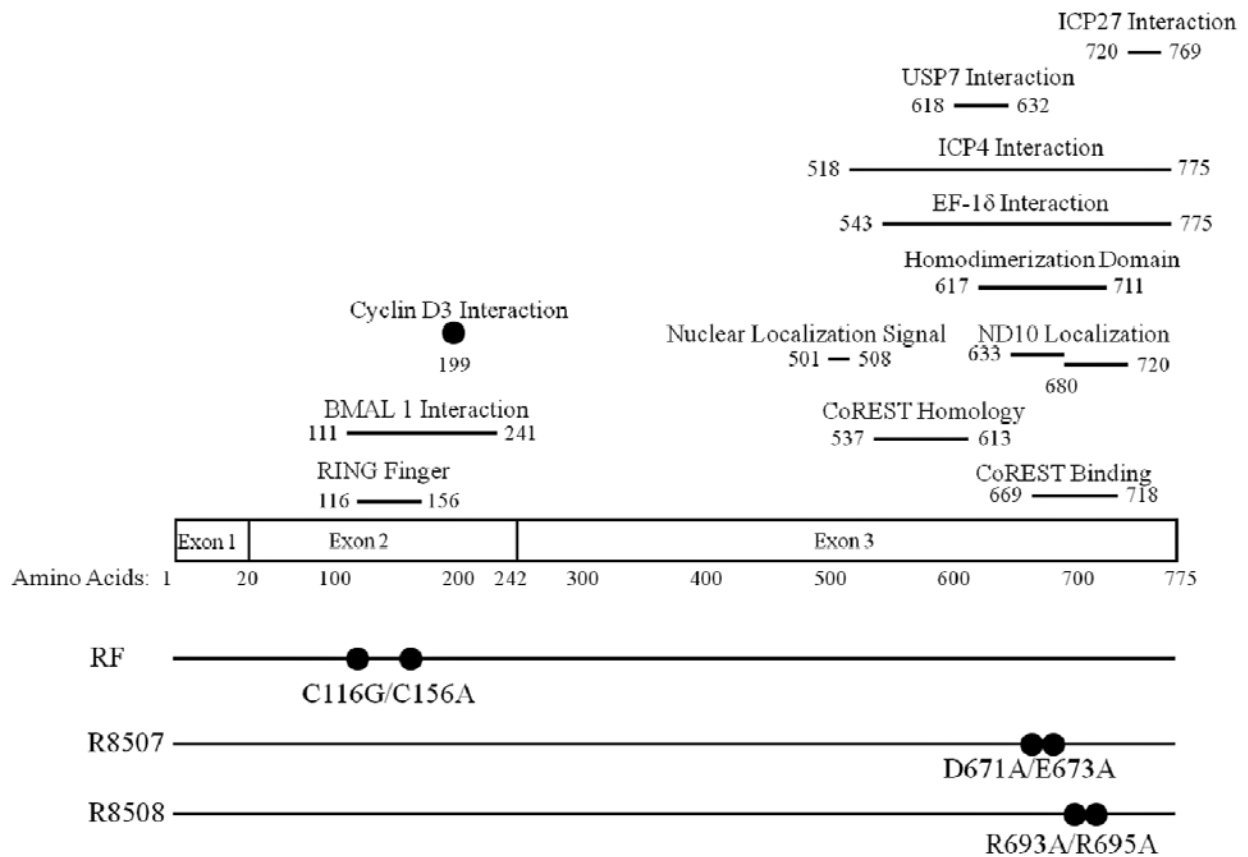


Figure 3. Functional domains attributed to ICP0, and ICP0 mutants RF, R8507, and R8508.

ICP0 is a 775 amino acid protein composed of 3 exons. Shown are the amino acids attributed to each reported function and interaction (above ICP0) and the point mutations in the ICP0 mutants RF (146), R8507 (83), and R8508 (83), used in chapter 4 (below ICP0). The studies determining each domain are as follows: RING finger (52, 68, 69), BMAL 1 interaction (115), Cyclin D3 interaction (257), CoREST homology (78) and binding (81), Nuclear Localization Sequence (173), ND10 Localization (160), Homodimerization domain (27), EF-1 δ interaction (114), ICP4 interaction (27), USP7 interaction (58), ICP27 interaction (283).

2.0 EPIGENETIC MODULATION OF GENE EXPRESSION FROM QUIESCENT HSV GENOMES

2.1 ABSTRACT

The ability of herpes simplex virus to persist in cells depends on the extent of viral gene expression, which may be controlled by epigenetic mechanisms. We used quiescent infection with the viral mutants d109 and d106 to explore the effects of cell type and the presence of the viral protein ICP0 on the expression and chromatin structure of the human cytomegalovirus (HCMV), tk, and gC promoters on the viral genome. Expression from the HCMV promoter on the d109 genome decreased with time and was considerably less in HEL cells than in Vero cells. Expression from the HCMV promoter in d106 was considerably more abundant than in d109, and this increased with time in both cell types. The same pattern of expression was seen on the tk and gC genes on the viral genomes, although the levels of tk and gC RNA were approximately 10^2 - and 10^5 -fold lower than those of wild-type virus in d106 and d109, respectively. In micrococcal nuclease digestion experiments, nucleosomes were evident on the d109 genome, and the amount of total H3 as determined by chromatin immunoprecipitation was considerably greater on d109 than d106 genomes. The acetylation of histone H3 on the d106 genomes was evident at early and late times postinfection in Vero cells, but only at late times in HEL cells. The same pattern was observed for H3 acetylated on lysine 9. Trimethylation of H3K9 on d109

genomes was evident only at late times postinfection in Vero cells, while it was observed both early and late in HEL cells. Heterochromatin protein 1 γ (HP1 γ) was generally present only on d109 genomes at late times postinfection of HEL cells. The observations of chromatin structure correlate with the expression patterns of the three analyzed genes on the quiescent genomes. Therefore, several mechanisms generally affect the expression and contribute to the silencing of persisting genomes. These are the abundance of nucleosomes, the acetylation state of the histones, and heterochromatin. The extents to which these different mechanisms contribute to repression vary in different cell types and are counteracted by the presence of ICP0.

2.2 INTRODUCTION

Early in productive infection, the herpes simplex type 1 (HSV-1) genome becomes bound with what appears to be an irregular arrangement histones, and the presence of nucleosomes has not been established (95, 96, 117, 136, 172). In contrast, nucleosomes have been found associated with latent HSV-1 genomes (110), as well as, possibly, heterochromatin (43). During latency there is little to no viral gene expression, with the predominant expressed gene being that for the latency-associated transcript, or LAT (230, 231). This suggests a general repression of transcription, probably as a result of epigenetic mechanisms. DNA methylation is probably not the major means of control of HSV-1 gene expression because latent HSV-1 DNA is not extensively methylated (19, 128). In contrast, a number of studies have implicated chromatin structure and specific histone tail modifications in the control of HSV-1 latency, reactivation, and replication (1, 20, 117, 128, 255, 259). Thus, histone association and chromatin structure

during the early stages of infection is likely to be involved in determining the extent of viral gene expression, and hence, whether productive or latent infection ensues (119).

Expression of ICP0 during this initial phase of infection may play a major role in determining which type of infection HSV-1 undergoes. ICP0 colocalizes with, and causes the disruption of, ND10 bodies, which are discrete multiprotein nuclear structures (16, 65, 79, 160). The RING finger ubiquitin ligase domain of ICP0 mediates the proteasomal degradation of the promyelocytic leukemia (PML) and Sp100 proteins, which are components of ND10 domains (79). The heterochromatin-binding protein HP1 interacts with Sp100, and can also be found at centromeres, forming a link between the disruption of ND10 bodies and chromatin (49). ICP0 also mediates the degradation of the centromere-associated proteins CENP-A (152) and CENP-C (55) in a proteasome-dependent manner. CENP-A is a histone H3-like centromere core protein thought to be involved in the assembly of heterochromatin (240). CENP-C also interacts with pro-apoptotic proteins, so degradation of CENP-C may be a viral mechanism to inhibit apoptosis, as well as to disrupt heterochromatin (191).

ICP0 also leads to the disruption of several transcriptionally repressive protein complexes. The C-terminal amino acids 537 to 613 of ICP0 share significant homology with a segment of CoREST (78). Histone deacetylases (HDACs) 1 and 2 form a complex with the REST and CoREST repressors of gene expression in nonneuronal cells. ICP0 binds the REST/CoREST/HDAC1/2 complex and causes the dissociation of HDAC1/2. CoREST and HDAC1/2 are then phosphorylated by HSV-1 proteins independently of ICP0 and translocated to the cytoplasm (78). This mechanism may provide for the specific derepression of certain cellular and viral genes. ICP0 also interacts with class II HDACs 4, 5, and 7 (153). Class II HDACs are found in multiprotein complexes with transcriptional repressors (258). HDACs 4, 5, and 7 are

involved in developmental pathways in neurons, and it has been hypothesized that ICP0 inhibits their repressive activity in order to promote neuronal survival during productive infection (153). Additionally, herpesviral homologs of ICP0 interact with HDACs (281).

HDAC inhibitors have also been shown to reactivate gene expression from quiescent genomes (97, 246). Quiescent infections of standard tissue culture cells with HSV-1 can be established using mutants defective in multiple genes that activate HSV gene expression or affect host cell metabolism (60, 96, 170, 196, 198, 211, 212). Trichostatin A (TSA) can activate the otherwise repressed expression from the human cytomegalovirus (HCMV) promoter on quiescent genomes similarly to ICP0 in Vero cells prior to 24 hours post infection (p.i.) (246). However, at 7 days p.i., reactivation induced by TSA is significantly decreased compared to ICP0-mediated reactivation. These effects were also seen in neuronal cultures, with support cells even more poorly reactivated than neurons (246). Importantly, TSA poorly activates gene expression from quiescent genomes in primary human fibroblasts, even when added at the time of infection (62), suggesting there exist repressive functions other than histone deacetylation that ICP0 can abrogate. Additionally, this higher order repression seems to be cell type dependent. Therefore, there may be multiple mechanisms by which ICP0 mediates the derepression of the viral genome.

Our laboratory has been examining the characteristics two viral mutants, d109 and d106 (211), as a model for some of the events that occur very early in infection or during latency *in vivo*. d109 is a viral mutant defective for all five immediate early (IE) genes. It expresses green fluorescent protein (GFP) under control of the HCMV IE promoter and establishes a persistent quiescent infection in several cell types, including Vero and HEL cells and primary trigeminal neurons (211). It is nontoxic to these cells and the viral genome persists in a quiescent state in

the cells for prolonged periods of time. This is similar to other quiescent systems that are based on the inactivation of multiple viral activators (60, 96, 170, 196, 198, 211, 212). d109 can be reactivated from quiescence by supplying ICP0 in *trans*. d106 expresses ICP0 and the GFP transgene, but none of the other IE proteins (211). We used this system to investigate the epigenetic state of quiescent viral genomes at three different loci as a function of time after infection, cell type, and the presence of ICP0. This was compared to the level of expression of genes at these loci. Our results suggest that the expression of the loci is generally influenced by multiple levels of epigenetic regulation that also quantitatively differ in different cell types. The expression of ICP0 resulted in the reduction of the number of histones on the genome, as well as in the extent of modifications that promote higher order chromatin structure.

2.3 MATERIALS AND METHODS

2.3.1 Cells and viruses

Experiments were performed using Vero cells (African green monkey kidney cells) or HEL (human embryonic lung) cells from the American Type Culture Collection (ATCC) and propagated as they recommended. The viruses used in this study were the wild-type (wt) HSV-1 (KOS), which was propagated on Vero cells, and IE mutants d106 and d109 (211). d106 was propagated on E11 cells and d109 on F06 cells as previously described (211).

2.3.2 ChIP

Chromatin immunoprecipitation (ChIP) analysis was carried out as previously described (213) with a few modifications. Vero or HEL cells (5×10^6) were plated in 100-mm dishes, and were infected by either d109 or d106 at a multiplicity of infection (MOI) of 10 at 4°C for 1 hour with rocking every 10 minutes. After adsorption, the inoculum was aspirated and 37°C 5% Dulbecco's modified Eagle's medium was added. This was considered 0 hours p.i. At 4 and 24 hours p.i., the cells were treated with 1% formaldehyde for 10 minutes at 37°C, washed 3 times with cold phosphate-buffered saline containing protease inhibitors (67 ng/ml aprotinin, 1 ng pepstatin, 0.16 mM TLCK [*N* α -ptosyl-L-lysine chloromethyl ketone], 1 mM phenylmethylsulfonyl fluoride [PMSF]). The cells were pelleted at 3,000 rpm for 10 minutes at 4°C and resuspended in cold PIPES [piperazine-*N,N'*-bis(2-ethanesulfonic acid) lysis buffer (100 μ l per million cells) containing protease inhibitors (5 mM PIPES, 85 mM KCl, 0.5% NP-40, 4 μ g/ml aprotinin, 2 μ g/ml pepstatin, 0.15mMTLCK, and 0.6mMPMSF), and incubated on ice for 15 min. The antibodies used were anti-histone H3 (Abcam; ab1791), anti-acetyl histone H3 (Millipore; 06-599), anti-acetyl histone H3 lysine 9 (Millipore; 07-352), anti-trimethyl histone H3 lysine 9 (Millipore; 07-442), and anti-heterochromatin protein 1 γ (Millipore; 05-690). A "no antibody control" was included for each ChIP experiment. When calculating ChIP results after quantitative PCR (qPCR), the value for the no-antibody control was subtracted from the immunoprecipitation results before the percent input of immunoprecipitation was calculated. Therefore, any values reported indicate an increase over the baseline. The baseline, or no-antibody control, was always considerably less than the results for the specific immunoprecipitations. In addition, the analysis was also performed on mock-infected cells to

control for possible external contamination. All other procedures were as described previously (213).

2.3.3 Micrococcal nuclease digestion

Vero or HEL cells (2×10^7) were infected at an MOI of 20 PFU/cell with d109 or d106. Nuclei were isolated at the indicated time points, divided into 4 aliquots, and digested with 20 units micrococcal nuclease (MN) for 2, 10, or 30 minutes. DNA was isolated by phenol chloroform extraction and ethanol precipitation and separated on a 2% agarose gel, transferred to Nytran membrane, probed with ^{32}P -labeled nick-translated HSV bacterial artificial chromosome (BAC) DNA (obtained from David Leib, Washington University), and exposed to Hybond film.

2.3.4 RNA isolation and reverse transcription

RNA was isolated with the Ambion RNaqueous -4PCR kit, following the included protocol. Briefly, 5×10^6 Vero cells or 7.5×10^6 HEL cells in 100-mm plates were infected at an MOI of 10 by d109, d106 or KOS at room temperature. RNA was harvested at the indicated time points by adding 500 μl lysis buffer, provided in the kit. The cells were scraped and vortexed. An equal volume of 67% ethanol was added, and the mixture was added to a filter, which was centrifuged at 12,500 rpm at 4°C for 1 min. The bound RNA was washed with wash buffers 1 and 2/3. RNA was eluted with 60 μl 65°C elution solution. The RNA was treated with DNase I at 37°C for 30 min to degrade any residual DNA.

Reverse transcription was performed using the Ambion reverse transcription kit and following the included instructions. Total RNA (2 μg) was reverse transcribed in a reaction

volume of 20 μ l containing RNase inhibitor, oligo(dT) primers 1 μ l Moloney murine leukemia virus reverse transcriptase (RT) and 2 μ l 10x reaction buffer. The reaction tube was incubated at 85°C for 5 minutes to remove RNA secondary structure, and the reverse transcription reaction was carried out for 1 hour at 44°C. After the reverse transcription reaction was complete, the reaction tube was incubated at 95°C for 10 minutes in order to inactivate the RT. 8 μ l of cDNA was diluted 1:6 by adding 40 μ l DNase/RNase-free H₂O for use in qPCRs. Additionally, 1 μ g RNA was diluted into a total of 60 μ l DNase/RNase-free H₂O for use as a negative control in qPCRs.

2.3.5 Real-time PCR

Reactions for ChIP or cDNA quantification were performed in triplicate using 5 μ l of DNA for each reaction as described previously (213), with a few modifications. Before the 96-well reaction plate was set up, a master mix containing 0.625 μ l of each primer (stock concentration, 1 mM), 12.5 μ l Applied Biosystems SYBR green super mix with 1.0 μ M 6-carboxy-X-rhodamine (Bio-Rad), and 6.25 μ l of water for a total of 20 μ l for each reaction was made. The final reaction volume was 25 μ l, including the DNA. The primers used for ChIP and cDNA quantification and their locations relative to the transcription start site of the gene to be analyzed are given in Table 1. d106 DNA was also included in each plate, in a standard curve of 1:10 dilutions from 500,000 to 50 copies per well, which covers the threshold cycle values for the ChIP DNA samples tested. qPCR was run on a ABI 7900HT Fast Real Time machine. The conditions for the run were as follows: stage 1, 50°C for 2 min; Stage 2, 95°C for 10 min; and stage 3, 40 cycle repeats of 95°C for 15 seconds and 60°C for 1 min. At the end of the run, a

dissociation curve was completed to determine the purity of the amplified products. Results were analyzed using the SDS 2.3 software from Applied Biosystems.

Table 1. Primers used for RT-PCR.

Primer	Sequence	Position relative to transcription start site
tkprom ^a	CAGCTGCTTCATCCCCGTGG AGATCTGCGGCACGCTGTTG	-200 to +56
tkds1 ^b	ACCCGCTTAACAGCGTCAACA CCAAAGAGGTGCGGGAGTTT	+15 to +84
gCprom ^a	CGCCGGTGTGTGATGATTT TTATACCCGGGCCCCAT	-84 to -26
gCds1 ^b	GGGTCCGTCCCCCCCAAT CGTTAGGTTGGGGGCGCT	+627 to +735
HCMVprom ^a	CATCTACGTATTAGTCATCGCTA TTACTGGAAATCCCCGTGAGTCA	-249 to -156
GFPds1 ^b	GTCGTGCTGCTTCATGTG AGTTCATCTGCACCACCG	+166 to +278

^a Promoter sequence.

^b Downstream in mRNA.

2.4 RESULTS

2.4.1 RNA expression from quiescent genomes

GFP is abundantly expressed from the HCMV promoter on the d106 genome, whereas GFP is only abundantly expressed in a subpopulation of d109-infected cells (211, 246). An aim of this study is to examine the effects of epigenetic state on the expression of viral genes. Therefore, it was of interest to determine how the physical state of chromatin on the HCMV promoter correlates with the expression of GFP. It was also of interest to examine the expression of genes

distant from the strong HCMV promoter, to determine the generality the epigenetic mechanisms. With the exception of ICP6 on d106 (211), the remaining HSV promoters on the d109 and d106 genomes are poorly expressed due to the absence of ICP4. However, transcription of early and late genes in the absence of ICP4 is detectable (212, 279). This is a consequence of cellular transcription factors functioning in the absence of viral regulators. Real time PCR was used to quantify the levels of GFP (HCMV promoter driven), tk (an early gene) and gC (a late gene) mRNAs in d109- and d106-infected Vero and HEL cells at 4 and 24 h p.i. The levels of these transcripts in wt-virus-infected cells at 2, 4, and 8 h post infection were also quantified for comparison. The abundance of GFP mRNA detected in KOS infected cells was less than 10^3 molecules/ug RNA, whereas it was as much as 2.3×10^9 molecules/ug of mRNA in d106-infected Vero cells (Figure 4). Therefore the levels of mRNA molecules measured in this experiment differed by approximately 6.5 orders of magnitude.

The amounts of GFP mRNA in d106-infected Vero cells were 2.5- and 30- fold more abundant than in d109-infected cells at 4 and 24 h, respectively. These differences were 14- and 360-fold in HEL cells at 4 and 24 h, respectively. Therefore, GFP expression in d109-infected cells decreased with time and was lower in HEL than in Vero cells. This is indicative of repression in the absence of ICP0, which becomes more restrictive over time and is possibly more pronounced in HEL cells than in Vero cells. At 4 h p.i., the levels of tk and gC RNA in cells infected with d106 and d109 were approximately 10^2 - to 10^3 - and 10^3 - to 10^4 -fold lower than in wt-virus-infected cells, respectively. In addition, depending upon the cell type and time p.i., the numbers of tk and gC mRNAs present in d106- and d109- infected cells were approximately 10^3 to 10^4 less than those of GFP mRNA. However, the same pattern of expression seen for GFP, and described above, was also seen for the tk and gC genes. Therefore,

despite the large difference in expression between the activity of HCMV IE promoter and those driving expression of the tk and gC in d109- and d106- infected cells, similar mechanisms appear to affect the expression of all three genes.

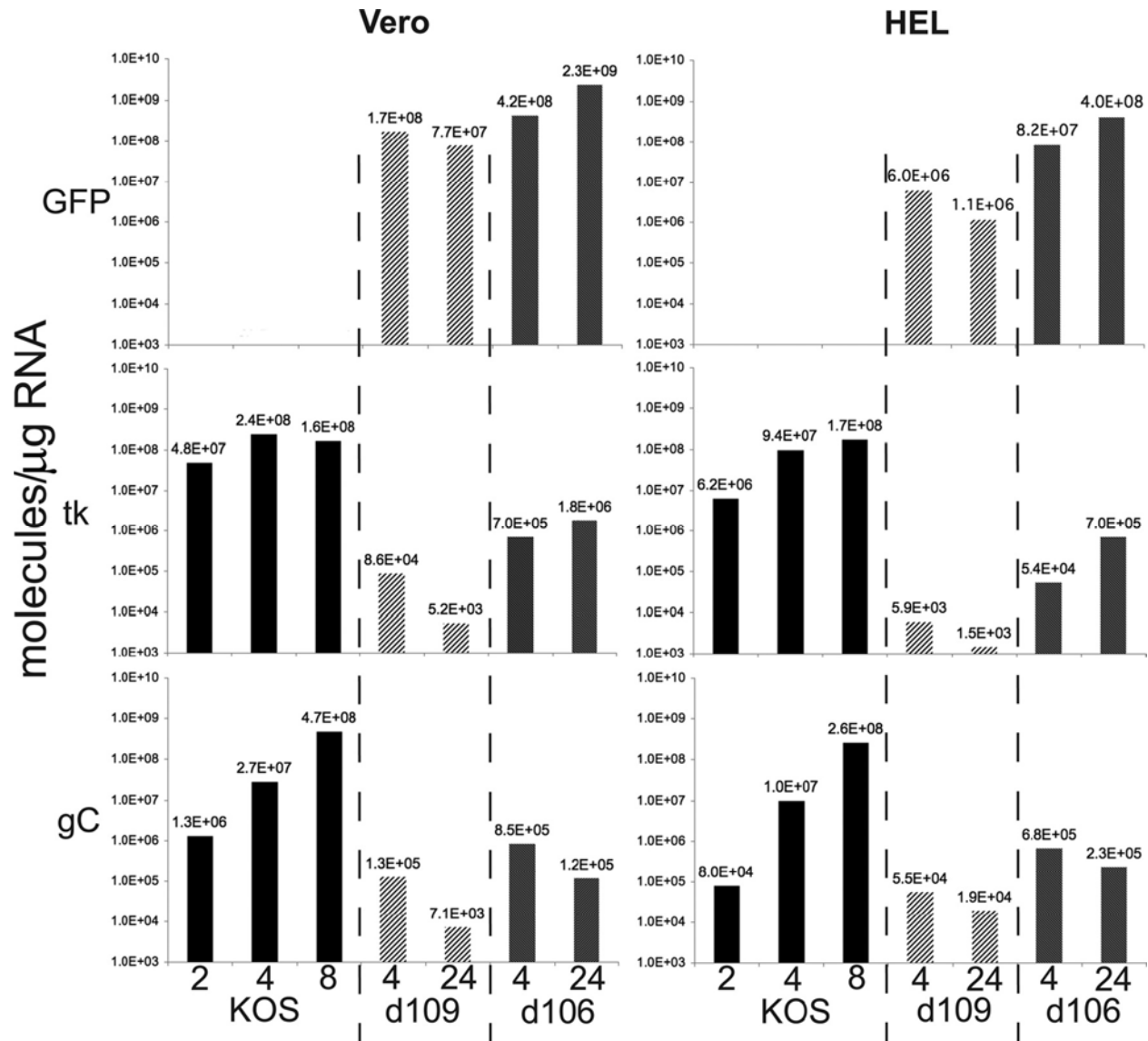


Figure 4. Abundance of GFP, tk, and gC mRNAs in KOS-, d109-, and d106-infected Vero and HEL cells.

Infections, RNA isolation, cDNA preparation, and RT-PCR with primer sets for the indicated mRNAs were performed as described in Materials and Methods. The procedure for creating standard curves for quantification using the indicated primers is also described in Materials and Methods. The graphs indicate the number of RNA molecules of each gene per μg RNA at the indicated time points (2, 4, 8, and 24 h p.i.) in Vero and HEL cells.

2.4.2 Histone deposition on the viral genome as a function of cell type and ICP0

Following entry at the plasma membrane, the nucleocapsid is transported to the nucleus, where the genome is inserted. Histones can be found on the viral genome early after infection (117, 183), and quiescent genomes are associated with histone H3 through day 6 p.i. (32). HSV-1 gene products most likely affect histone deposition on the genome. Both VP16 and VP22 have been reported to decrease histone deposition on the viral genome (95, 255). The activities of ICP0 are also consistent with effects on chromatin structure (55, 78, 80, 81, 152, 153, 195, 246). As a first step towards determining the epigenetic mechanisms that contribute to the expression profile observed in Figure 4, two approaches were employed. The first examined the nucleosomal structure of the viral genome by MN analysis of nuclear DNA. The second is to quantify the amount of total histone H3 on the viral genomes.

Vero and HEL cells were infected with d109 and d106. At 4 and 24 h p.i. nuclei were prepared and subjected to MN analysis. The nuclei were incubated with MN for increasing lengths of time. The DNA was then isolated, run on an agarose gel, blotted onto nylon and probed with ³²P-labeled HSV sequences. Figure 5 shows both the ethidium bromide (EtBr) stained gel prior to blotting and the autoradiographic images of the exposed probed blot. The nucleosomal banding pattern of the bulk cellular DNA is clearly evident in the EtBr stained gels of both cell types. The Southern blot was probed with purified ³²P-labeled HSV DNA contained in a BAC. Therefore, the observed pattern represents the sum of possibly different patterns from different regions of the genome. However, a similar pattern was seen when the HCMV IE promoter was used as a probe (unpublished observations). A reproducible nucleosomal hybridization pattern was evident, particularly in d109-infected HEL cells (Figure 5A); however, the pattern was more heterogeneous than the EtBr pattern observed for the bulk cellular DNA.

Therefore, the chromatin on the d109 genome in HEL cells may be more organized. However, there are portions or populations of d109 genomes in HEL and Vero cells that result in a heterogeneous MN pattern. Nucleosomal structure was not reproducibly observed on d106 genomes in HEL or Vero cells. The observed heterogeneous pattern might have been due to less ordered nucleosomal structure, or despite the fact that only nuclei were subjected to the analysis, some of the genomes might still have been in capsids bound to the nuclei. None of the observed hybridization pattern was due to cross-hybridization to the cellular DNA, since mock-infected cell lanes were clear.

Another approach to probe the possible association of nucleosomes with the genomes is to determine the amount of bulk histone, in this case H3, by ChIP analysis. Vero and HEL cells were infected with d109 or d106, and at 4 and 24 h p.i. were subjected to ChIP analysis using an antibody against H3 (Figure 6). The extent of sequences in the immunoprecipitate was determined by real-time PCR. In HEL cells (Figure 6B), association of histone H3 with all three promoters on d109 could be seen at 4 h p.i. and increased by 24 h p.i. In contrast, the association of histone H3 with d106 is greatly reduced and never rose above a low level. A similar pattern of histone association occurs in Vero cells, except that the histone H3 association with the tk promoter of d109 only marginally increased from 4 to 24 h p.i.

The results of the ChIP (Figure 6) and the MN (Figure 5) assays are consistent in that they suggest greater nucleosomal association with the d109 than the d106 genome. The increase in H3 on the d109 genome (Figure 6) is also consistent with the decreased expression from d109 genome at 24 h p.i. (Figure 4). The reduced amounts of H3 on the viral genome during d106 infection are consistent with the greater expression of the d106 genome (Figure 4), and possibly indicative of interference in histone deposition by ICP0.

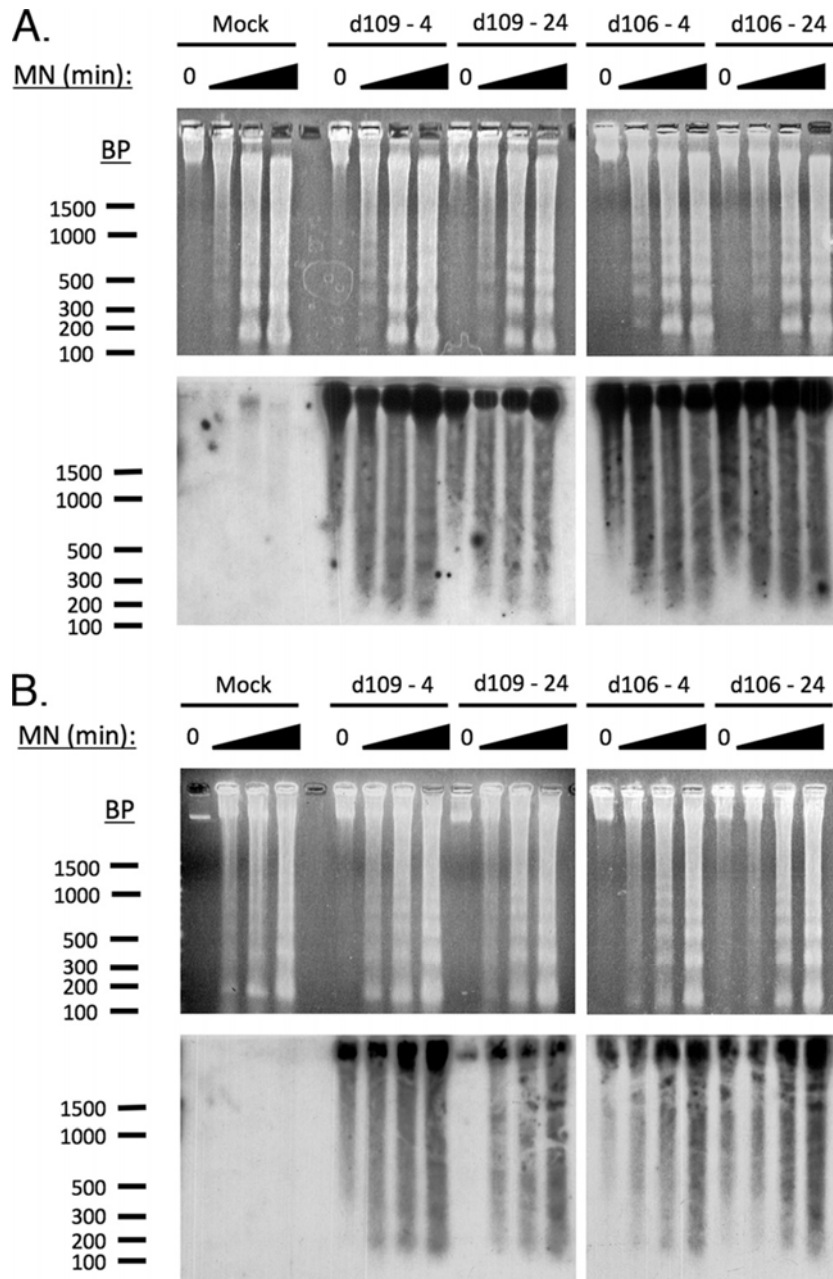


Figure 5. MN digestion of d109- and d106-infected cells.

Nuclei were isolated from d109-, d106-, or mock-infected HEL cells (A) or Vero cells (B) and digested with 20 units MN for 2, 10, or 30 min. The DNA was isolated from the nuclei at 4 and 24 h p.i., purified, and fractionated on 2.0% agarose gels. The agarose gels were stained with EtBr (top) and transferred to Nytran membranes for Southern blot hybridization as described in Materials and Methods. The Southern blots (bottom) were probed with ³²P-labeled HSV BAC DNA, washed, and exposed to X-ray film. Shown are the autoradiographic images of the probed blots (bottom).

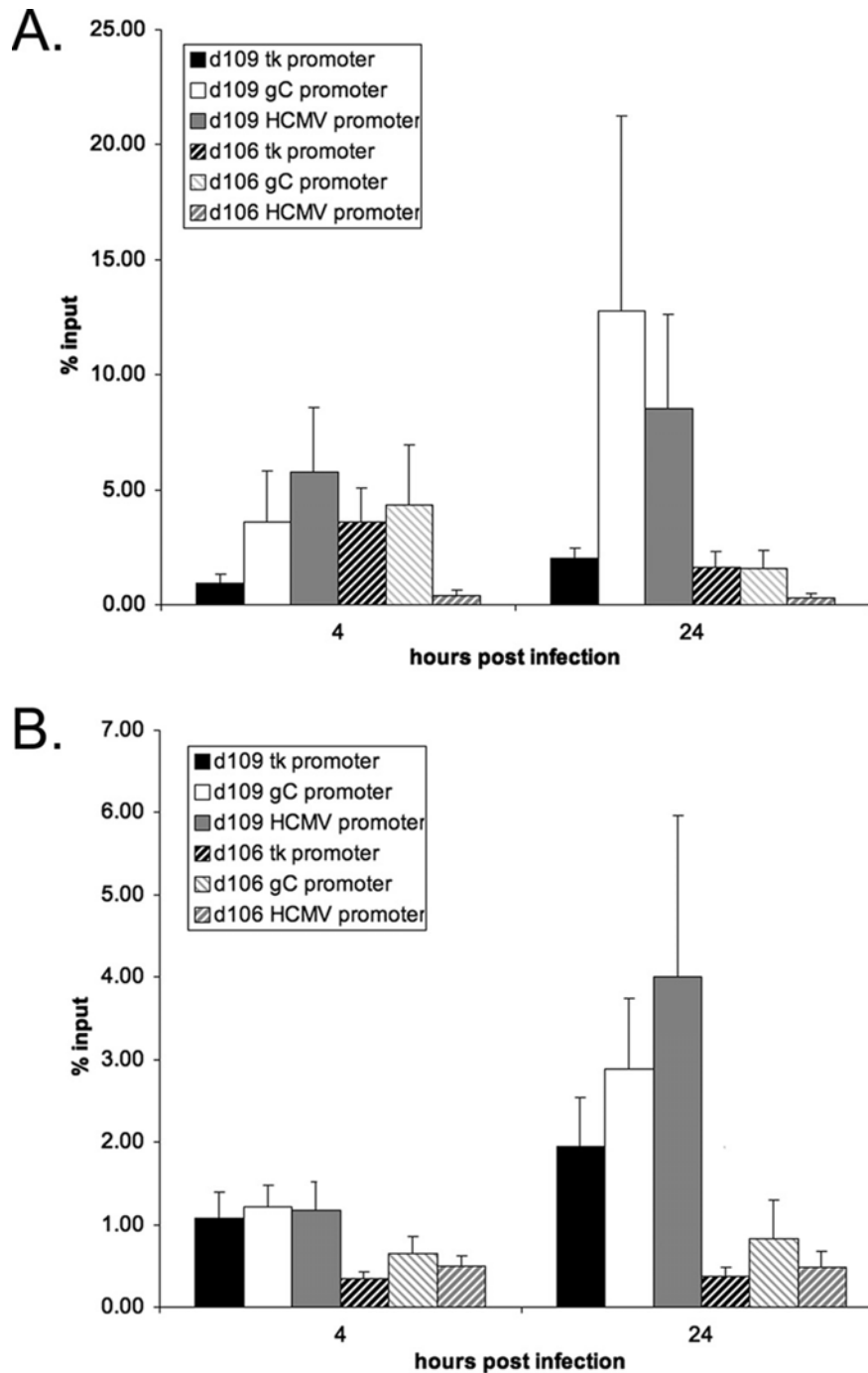


Figure 6. Binding of histone H3 to the tk, gC, and HCMV promoters of d109 and d106 in Vero and HEL cells.

ChIP with an antibody to histone H3 and RT-PCR with primer pairs corresponding to the indicated promoter regions were performed as described in Materials and Methods. The graphs show the percentages of total genomes bound at 4 and 24 h p.i. in Vero cells (A) and HEL cells (B). The error bars represent standard deviations from multiple experiments.

2.4.3 Acetylation of histone H3 on quiescent viral genomes is a function of ICP0

Histone H3 hyperacetylation (AcH3) is associated with increased transcriptional activity (221). Lytic infection has been shown to increase global cellular levels of acetylated histone H3 (117), and ICP0 has been implicated in increasing the acetylation of histones on the viral genome (29, 32). ICP0 has also been shown to inhibit repressive complexes that include HDACs (78, 82). Additionally, HDAC inhibitors, such as TSA, have been shown to increase HSV-1 expression and to derepress HSV quiescence in a manner similar to ICP0 in Vero cells (97, 246).

ChIP was used to determine the extent of AcH3 on the d109 and d106 genomes in Vero and HEL cells. In Vero cells, AcH3 was low on all the promoters on the d109 genomes, but was elevated on d106 genomes at both 4 and 24 h p.i. (Figure 7A). The extent of H3 acetylation in d106-infected cells is masked by the fact that there is less total H3 on the genomes. This is clearly seen when the amount of AcH3 is divided by the total H3 (Figure 7C). Therefore, while the amount of AcH3 on the HCMV promoter is not very much greater than in d109-infected cells, the H3 that is on the d106 genomes is more extensively acetylated. The same general pattern was observed in HEL cells (Figure 7B and D), although the amounts and fraction of AcH3 on the promoters in d106-infected cells were not as elevated relative to d109 as it was in Vero cells. This is consistent with the lower level of expression in HEL cells.

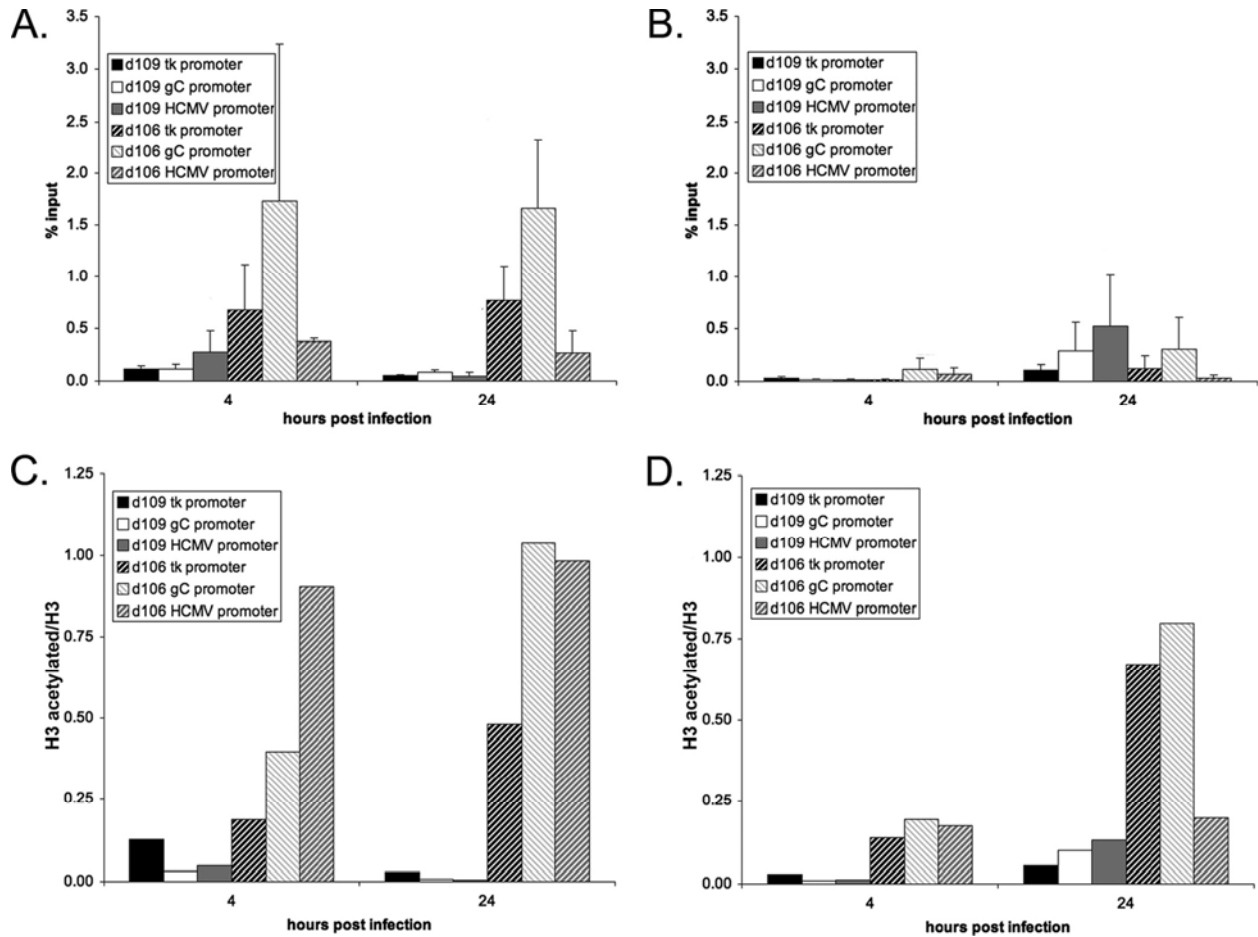


Figure 7. Binding of AcH3 to the tk, gC, and HCMV promoters of d109 and d106 in Vero and HEL cells.

ChIP with an antibody to AcH3 and RT-PCR were performed as described in the legend to Figure 6 to determine the percentages of genomes bound by AcH3 at 4 and 24 h p.i. in Vero (A) and HEL (B) cells. The error bars represent standard deviations from multiple experiments. In order to compensate for the reduced histone H3 on d106 promoters, AcH3 was normalized to the amount of histone H3 on the genome by dividing the percentage of AcH3 associated with each promoter by the percent histone H3 (Figure 6) in Vero cells (C) and HEL cells (D).

To further investigate the effects of cell type and ICP0 on the acetylation state of histones associated with quiescent genomes, we performed ChIP for acetylated histone H3 lysine 9 (H3K9Ac) (Figure 8). This specific modification has been associated with increased transcription. This may be due to the loss of the positive charge of lysine and decreased electrostatic attraction of the histone tail to the DNA backbone, and/or it may increase

transcription by preventing histone H3 lysine 9 methylation (H3K9me), which is associated with a decrease in the rate of transcription.

The amount of H3K9Ac on the promoters in d109-infected cells was relatively low (Figure 8A and B). Also as shown in Figure 7, the exception is the HCMV promoter at 4 h p.i., where the amount of H3K9Ac was elevated relative to the other promoters in both cell types. The amount of H3K9Ac on the d106 genome was readily evident at 4 h p.i. in Vero cells (Fig 8A and C), whereas it was not in HEL cells but became detectable later in infection (Figure 8B and D). Therefore, the pattern of H3K9Ac was similar to that of AcH3 on the tk, gC and HCMV promoters of d109 and d106 in both Vero and HEL cells.

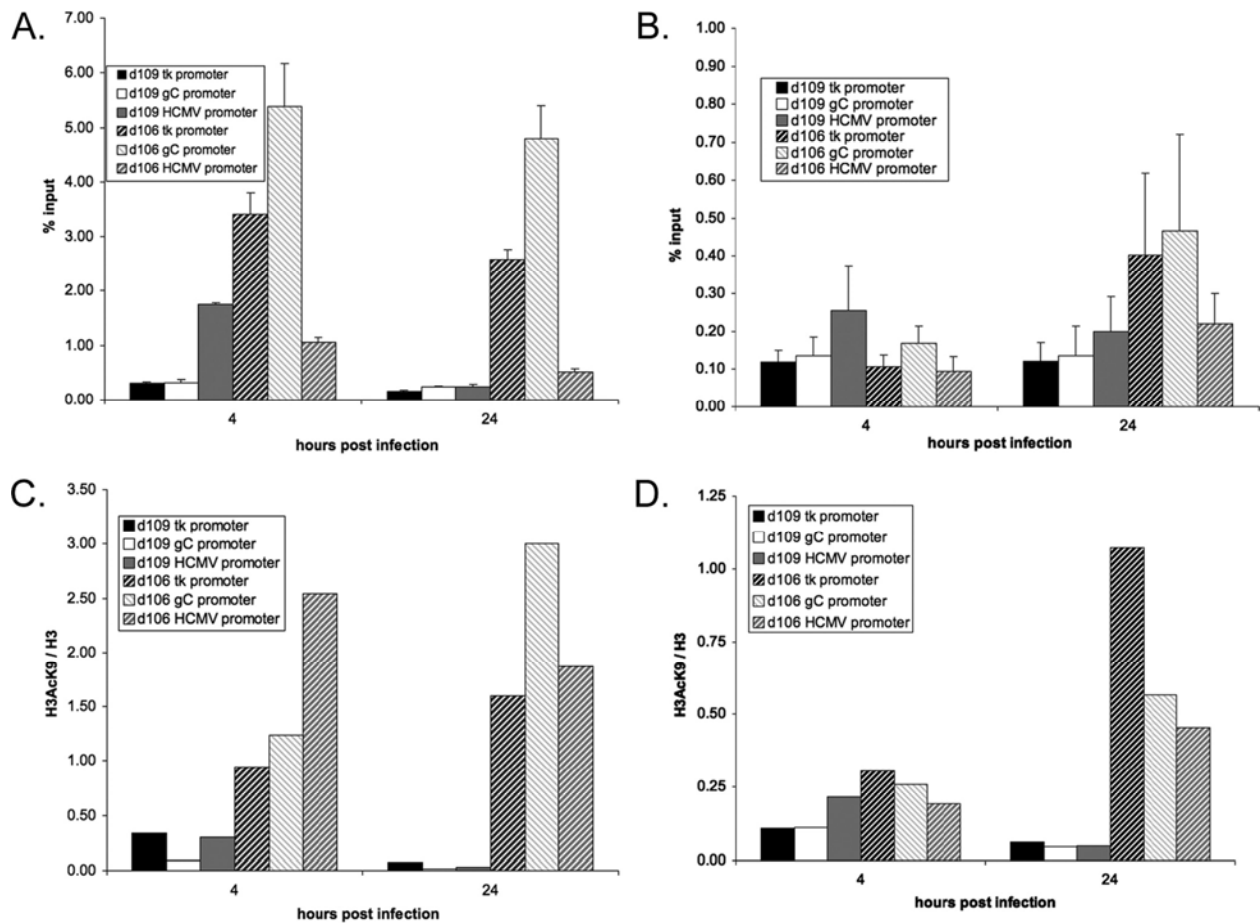


Figure 8. Binding of H3K9Ac to the tk, gC, and HCMV promoters of d109 and d106 in Vero and HEL cells.

ChIP with an antibody to H3K9Ac and RT-PCR were performed as described in the legend to Figure 6 to determine the percentage of genomes bound by H3K9Ac at 4 and 24 h p.i. in Vero (A) and HEL (B) cells. The error bars represent standard deviations from multiple experiments. In order to compensate for the reduced histone H3 on d106 promoters, Ach3 was normalized to the amount of histone H3 on the genome by dividing the percentage of Ach3 associated with each promoter by the percent histone H3 (Figure 6) in Vero cells (C) and HEL cells (D).

2.4.4 Effects of cell type and ICP0 on repressive chromatin structure

The global repression of HSV during latency is likely due to epigenetic mechanisms. Histone lysine methylation is associated with both activation and repression of transcription, depending on which residue is modified (8, 121). These modifications may recruit additional proteins that

help to either silence or activate transcription. Trimethylation of histone H3 lysine 9 (H3K9me3) is correlated with repression of expression (8). Lysine methylation does not remove a positive charge from the histone tail and also precludes acetylation. Additionally, histone lysine methylation is a very stable histone modification (202), which could help to form the basis of long-term quiescence. H3K9me3 is a binding site for heterochromatin protein 1 (HP1) (5, 131, 174), which helps to silence transcription and form higher order chromatin structure (134, 149).

We investigated the presence of H3K9me3 and HP1 γ by ChIP analysis (Figure 9). H3K9me3 was rarely found on the d109 genomes in Vero cells at 4 h p.i. or on the d106 genomes in both HEL and Vero cells (Figure 9A and B). In HEL cells, H3K9me3 was detected on all three promoters on the d109 genome at both 4 and 24 h p.i. (Fig 9B). However, H3K9me3 was detected on the gC and HCMV IE promoters only on the d109 genome in Vero cells at 24 h p.i. (Figure 9A). HP1 γ helps to form higher order chromatin structure, and binds to H3K9me3. The amounts of HP1 γ binding to the HCMV, tk, and gC promoters of d109- and d106-infected HEL and Vero cells were determined by ChIP. HP1 γ was rarely found on the d109 genomes at 4 h p.i. or on the d106 genome under any circumstances (Figure 9C and D). In d109-infected Vero cells, HP1 γ was only seen on the gC promoter at 24 h (Figure 9C), whereas it was detected on all three of the promoters in d109-infected HEL cells at 24 h (Figure 9D).

Considering d109 infection, the general pattern that arises from the data of Figure 9 is that: i. H3K9 methylation precedes HP1 γ association, ii. H3K9 methylation occurs more rapidly in HEL cells than in Vero cells, and iii. HP1 γ association is only generally seen at 24 h p.i. of HEL cells. These data are consistent with a more restrictive environment to gene expression from the d109 genome in HEL than in Vero cells (Figure 4). Reduced amounts of H3K9

methylation and HP1 γ deposition were consistently observed in d106-infected cells, suggesting a direct or indirect inhibitory effect of ICP0 on this repressive mechanism.

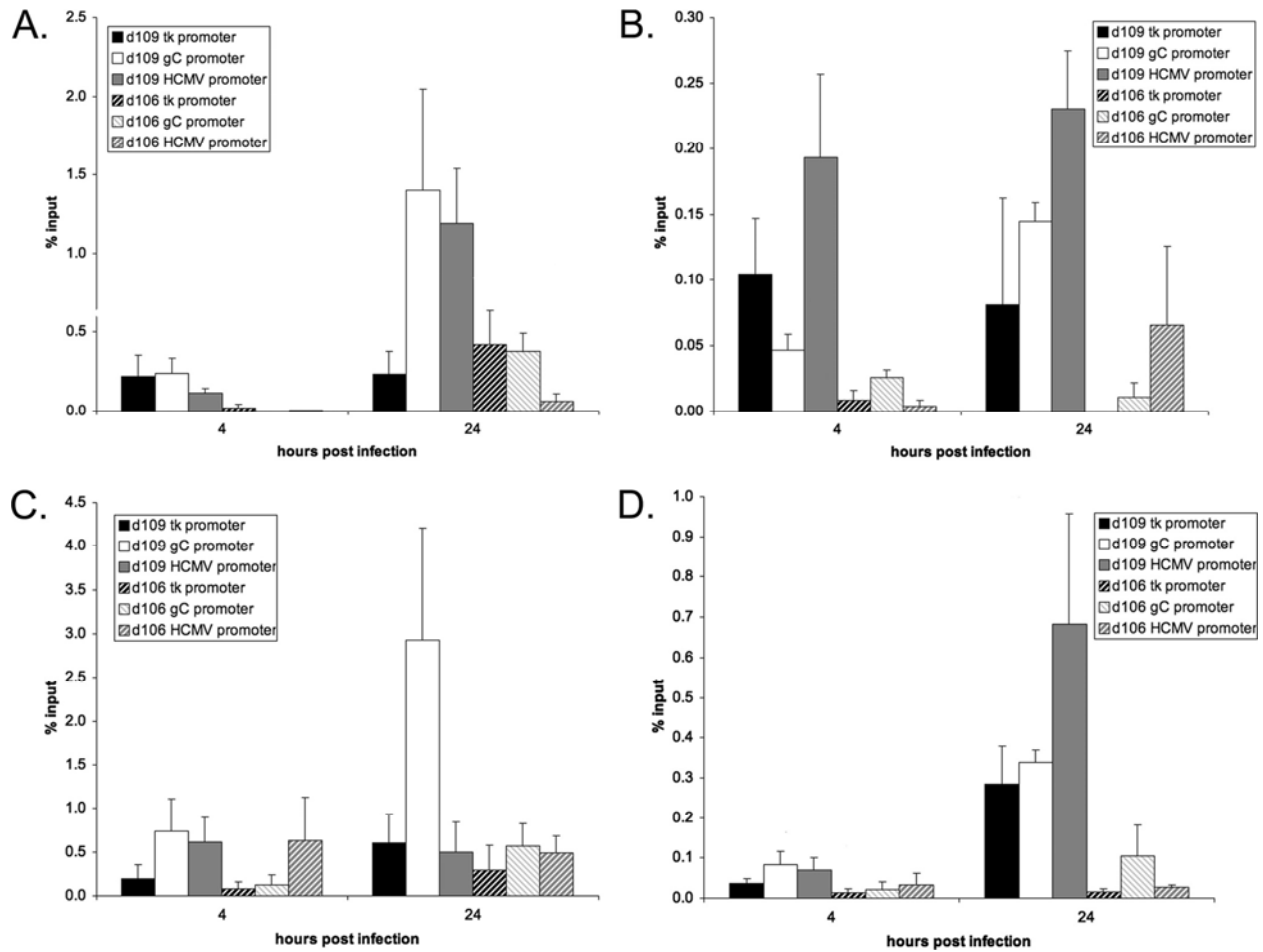


Figure 9. Repressive chromatin modifications associated with the tk, gC, and HCMV promoters of d109 and d106 in Vero and HEL cells.

ChIP with antibodies to H3K9me3 (A and B) and HP1 γ (C and D), followed by RT-PCR, was performed as described in the legend to Figure 6 to determine the percentages of genomes bound by H3K9me3 (A and B) and HP1 γ (C and D) at 4 and 24 h p.i. in Vero (A and C) and HEL (B and D) cells. The error bars represent standard deviations from multiple experiments.

2.5 DISCUSSION

The mutant virus d109 does not express HSV IE proteins and is subject to repression, where even the relatively potent HCMV IE promoter is only abundantly expressed in a subpopulation of infected cells. d109 genomes persist in a quiescent state in most cell types. Thus, aspects of the cellular mechanisms influencing quiescent genomes in culture may reflect HSV latency in animal models (43, 259). In this study, ChIP was used to examine the states of chromatinization of three promoters with different relative activities and locations on quiescent viral genomes and to observe how this state may be affected by the expression of ICP0, and possibly differ in different cell types. We examined the deposition of nucleosomes on the genomes, and focused on histone H3 with respect to its abundance on the genomes, acetylation (total and lysine 9) and methylation (lysine 9) states, and the presence of the heterochromatin protein, HP1 γ . The chromatinization state was correlated with the level of expression at the three analyzed loci.

2.5.1 Gene expression as a function of IE proteins

In the absence of the IE proteins ICP4, -27 and -22 (d106-infected cells), expression levels of the tk and gC loci were dramatically reduced relative to that seen in KOS-infected cells (Figure 4), largely due to the absence of ICP4, which is the major activator of early and late genes. Unlike tk and gC, expression from the HCMV IE promoter was abundant in d106-infected cells. This is presumably due to the presence of the strong enhancer in the HCMV IE promoter (235, 236, 249). The additional lack of ICP0 expression (d109) further lowered the expression of the HCMV IE, tk and gC promoters. This was more pronounced at 24 h than at 4 h p.i., suggesting either an activation of expression in the presence of ICP0 or the active inhibition of transcription

in the absence of ICP0. Expression was generally lower in HEL cells than in Vero cells. In addition, the difference in the expression in the presence of ICP0 relative to expression in its absence was greater in HEL cells than in Vero cells. This is consistent with a greater involvement of repression mechanisms functioning on the genome in HEL cells.

2.5.2 Deposition of nucleosomes and histone H3 as a function of ICP0

Nucleosomal structure as visualized by MN analysis was evident on d109 genomes, particularly in HEL cells (Figure 5). It was less evident for d106 genomes. However in both d106 and d109, there was a background of nuclease digestion products that was not consistent with an ordered nucleosomal structure. Previous studies of wt HSV suggested that during productive infection there is little nucleosomal structure and that the genome may be more sensitive to MN digestion (136, 137). The more heterogeneous component in the MN analysis in our studies may be similar to that observed in these previous studies. However it is not entirely appropriate to compare wt infections to those analyzed in this study. Unlike that of wt virus, the genomes of d106 and d109 are not replicating and are not being packaged. In wt virus infections, these processes typically begin at 4 and 6 h, respectively, and undoubtedly influence the MN analysis. A more appropriate comparison is a previous study by Jamieson et al. (110), which did not find an ordered nucleosomal structure on the tk promoter in cells infected with a mutant defective in VP16 and with restricted expression of ICP0 in the presence of alpha interferon. The difference between our results and these may be the extent of IE gene inactivation in the two systems. Alternatively, there may be little difference at all. In both studies, the analysis was complicated by the fact that not all infecting genomes are exposed to the cellular machinery in the nucleus. The previous study hypothesized that many of the

genomes did not uncoat, for example. In addition, while the entire HSV-1 genome was used as a probe in Figure 5, the use of promoter-specific probes revealed little difference from the results in Figure 5 (unpublished observations).

As an alternative approach to examining possible nucleosomal deposition on quiescent genomes, the abundance of bulk histone H3 was determined by ChIP analysis (Figure 6). The expression of ICP0 resulted in the decreased association of H3 at all three promoter loci in both HEL and Vero cells (Figure 6). Therefore, the presence of ICP0 somehow prevents the association of histone H3 with the genome. The reduced association of H3 in the presence of ICP0 is probably not a function of transcription, since the amount of H3 on the tk and gC promoters is comparable to that on the HCMV IE promoter in d106-infected HEL cells, despite the observation that the tk and gC promoters are 2 to 3 orders of magnitude less transcriptionally active than the HCMV IE promoters (Figure 4).

A recent study by Coleman, et al. (32) investigated H3 association with quiescent genomes upon reactivation from quiescence, and found that although hyperacetylation of the histones bound to the viral genome occurred upon the expression of ICP0, the total amount of bound histone H3 remained constant upon reactivation. This indicates that ICP0 does not facilitate the removal of histones from the viral genome. Our study, in which ICP0 is expressed from the outset of infection, suggests that it is able to prevent the deposition of histone H3 onto all three types of viral promoters. This is consistent with a study showing that ICP0 prevented the binding of H3 to the genome during productive infection (29). This may occur by relocalization or degradation of histones or histone chaperones, which subsequently leads to a more open viral genome configuration in which the availability of transcription factors can control expression, unimpeded by epigenetic structure.

ICP0 causes increased acetylation of histone H3 bound to the viral genome (32). ICP0 interacts with and causes the relocalization of class II HDACs (153). It is also known to disrupt the REST-CoREST-HDAC complex (78, 82), which is able to inhibit ICP4 expression in transient transfection assays (190). This inhibition is counteracted by the addition of TSA, an HDAC inhibitor. TSA can also partially substitute for ICP0 in the reactivation of gene expression from quiescent HSV genomes (246), and the effects of d106 on cellular gene expression are similar to those induced by the addition of TSA (97). In our study it was difficult to assess the hyperacetylation of histone H3 on the viral promoters simply by quantifying the abundance of AcH3. The total amount of hyperacetylated histone H3 associated with the viral promoters was not uniformly increased in d106 infection over d109 infection (Figure 7). This was most pronounced in HEL cells (Figure 7B). This is because the amount of total H3 on the genome is greatly reduced (Figure 6). When the amount of AcH3 was normalized to the total amount of H3, there was a significant increase in acetylation of the histones associated with d106. Thus, the small number of histones that become associated with the viral genome are generally found in an acetylated state. The histones bound to the d106 HCMV, tk, and gC promoters are hyperacetylated in comparison to those on the d109 viral promoters in both HEL and Vero cells (Figure 7). This is consistent with the 1 to 3 order of magnitude increase in gene expression from d106 relative to d109. This hyperacetylation of histone H3 may be due to ICP0-mediated reduction of HDAC activity. A number of studies suggest that this is mechanistically connected to the disruption of ND10 through the ubiquitin ligase activity of ICP0 and/or the ability of ICP0 to disrupt REST-CoREST HDAC complexes (78-81, 83).

ICP0 expression also resulted in the specific hyperacetylation of histone H3 lysine 9 (Figure 8). Although histone acetyltransferase (HAT) activity is somewhat generalized, specific

residues of histone tails are generally acetylated by specific HATs. H3K9 acetylation has been linked to the HATs GCN5 and PCAF (75, 125). ICP0 may be increasing the activity of these HATs, as well as others. ICP0 colocalizes with the HATs CBP and p300, and can be coimmunoprecipitated with p300 (166). Thus, ICP0 may have an effect on HAT activity, concurrent with its decrease of HDAC activity, leading to the hyperacetylation of histones bound to the viral genome, and a subsequent increase in transcription.

AcH3 and H3K9Ac were observed on the d106 genome at 4 h p.i. in Vero cells (Figure 7A, C and 8A, C). They were not observed on the d106 genome in HEL cells at that time (Figure 7B, D and 8B, D). This may be because positive effects of ICP0 are competing with the cellular repression mechanisms, which may be more potent in HEL than in Vero cells. The repression of viral genomes is considered below.

2.5.3 The formation of repressive chromatin

H3K9me3 occurs exclusively of H3K9Ac and vice versa. It is a binding site for HP1 γ , which is a component of heterochromatin, a repressive chromatin structure. H3K9me3 was seen very early in infection of HEL cells (Figure 9B), whereas it was only detected at the 24 h point in Vero cells (Figure 9B). The formation of heterochromatin, as seen by the binding of HP1 γ , occurs only after the trimethylation of histone H3. This is consistent with the observation that HP1 γ binding follows H3K9me3 presence on the d109 genomes in HEL cells (Figure 9B and D). HP1 γ was detected in Vero cells only on the gC promoter in the d109 genome at 24h p.i. Interestingly, gC is the only gene expressed by d109 at a higher level in HEL than in Vero cells at 24 h p.i. This exception aside, the lack of heterochromatin formation in Vero cells is consistent with the greater transcriptional activity of the d109 genome in Vero than in HEL cells.

This observation also explains the greater ease with which expression can be reactivated with HDAC inhibitors, such as TSA, from quiescent genomes in Vero cells as opposed to HEL cells.

Heterochromatin formation appears to be a process that is inhibited by ICP0. ICP0 may actively prevent the methylation of histones by inhibiting the activity of a histone methyltransferase or increasing the activity of a histone demethylase. However, it is more likely that the decreased H3K9me3 and HP1 γ binding on the d106 genome is a downstream effect due to the decrease in H3 binding and an increase in H3K9 acetylation, with the latter precluding K9 methylation. This would not explain the reported decrease in H3K9me following reactivation with ICP0, without a decrease in H3 binding (32). This is remarkable considering that methylation of histones is considered a long-lived modification (202), which until recently was thought to remain until the histone is replaced or the tail removed (224). It is possible that the reversal of heterochromatin formation upon ICP0-mediated reactivation may be different from the mechanism by which it prevents heterochromatin formation.

The results of these studies indicate that a complex, multistep process occurs in the formation of a silenced and heterochromatic state of the HSV genome. Multiple levels of chromatin structure can be observed in the quiescent genome system, and these levels of chromatin structure correlate with gene expression levels. The observations that we made under any given condition probably represent the sum of a number of chromatin states. A subpopulation of d109-infected Vero (~10%) and HEL (~0.1%) cells abundantly express GFP from HCMV IE promoter (246), indicative of multiple populations of genome states. Heterochromatin has been observed in latently infected mouse ganglia (259). However, it is possible that the multiple states of repression observed in this study exist in latency, as well. Primary trigeminal neurons are more permissive for gene expression from the d109 genome than

support cells (246). Moreover, quiescent genomes in primary neurons are more readily activated by TSA (4, 246). Reactivation of latently infected ganglia by HDAC inhibitor sodium butyrate has also been observed (176). These observations suggest that genomes persisting in latency are not necessarily repressed by heterochromatin. The more relaxed repression may allow for more readily reactivated genomes leading to some viral gene expression, which could lead to abortive or productive reactivation events.

3.0 REVERSAL OF HETEROCHROMATIC SILENCING OF QUIESCENT HSV-1 BY ICP0

3.1 ABSTRACT

Persisting latent herpes simplex virus genomes are to some degree found in a heterochromatic state, and this contributes to reduced gene expression resulting in quiescence. We used a relatively long-term quiescent infection model in human fibroblasts, followed by provision of ICP0 *in trans*, to determine the effects of ICP0 on the viral chromatin state as gene expression is reactivated. Expression of ICP0, even at low levels, results in a reduction of higher order chromatin structure and heterochromatin on quiescent viral genomes, and this effect precedes an increase in transcription. Concurrent with transcriptional activation, high levels of ICP0 expression result in the reduction of the heterochromatin mark trimethylated H3K9, removal of histones H3 and H4 from the quiescent genome, and hyperacetylation of the remaining histones. In contrast, low levels of ICP0 do not appreciably change histone levels. These results indicate that ICP0 has the ability to alter the chromatin structure of quiescent genomes at multiple levels, including higher order chromatin structure, histone modifications, and histone association. Additionally, the level of ICP0 expression affected its ability to change chromatin structure, but not to reactivate gene expression. Thus, it is likely that ICP0 exerts its effects through multiple mechanisms.

3.2 INTRODUCTION

Herpes Simplex Virus Type 1 (HSV-1) latency is characterized by significantly reduced transcription of the viral genome relative to productive infection. One gene that appears to be selectively transcribed is that for the latency associated transcript (LAT) (229, 234). This general repression of gene expression suggests that latent gene expression is controlled by epigenetic mechanisms. Since viral DNA is not extensively methylated (128) expression is probably repressed by chromatin structure on the viral genome. During latency, the viral genome is found in an endless, possibly circular, episomal structure, bound by nucleosomes (43, 110) and heterochromatin (43).

Periodically *in vivo*, HSV-1 reactivates, replicates, and can cause recurrent disease. Cellular stress (36, 38, 148, 197, 274) and decrease in immune function can both contribute to reactivation (67). Upon reactivation, the full repertoire of viral genes is eventually expressed. The exact order of gene expression upon reactivation is unclear, but latently infected explanted mouse TG were shown to express genes in a different temporal pattern to that seen in productive infection (242), while there is also a decrease in LAT prior to, or concurrent with, lytic gene expression (231, 274). The relative contributions of viral activators of gene expression to different aspects of the reactivation process are unclear. However one activator, the immediate early protein ICP0, is required for efficient reactivation from latency *in vivo* (21-23, 85, 86, 113).

ICP0 is a promiscuous activator of gene expression at the level of RNA synthesis (51, 72, 113, 180, 200). Since it does not directly bind DNA, it has been postulated that ICP0 may exert its effects indirectly by interaction with proteins controlling transcription or by influencing some general step prior to the assembly of transcription complexes on the viral genome. ICP0 contains an E3 ubiquitin ligase RING finger domain (17, 48), and expression of ICP0 leads to the

degradation of a number of proteins, including the centromeric histone variants CENP-A (152), -B (151), and -C (55), as well as constituents of the PML nuclear bodies (57, 79), which are thought to be part of the innate antiviral defense (50, 244). ICP0 also interacts with, and redistributes, class II HDACs (153) and the C-terminus of ICP0 has also been shown to interact with and disrupt the repressive histone deacetylase (HDAC)-containing complex of HDAC1/HDAC2/REST/CoREST/LSD1 (78, 80, 81, 83), which has been implicated in increased viral gene expression. Additionally, ICP0 may also interact with the histone acetyltransferase (HAT) PCAF (139).

These observations suggest that ICP0 may mediate its transactivation function through manipulation of epigenetic control of gene expression by chromatin. Few studies have investigated the changes to viral chromatin upon reactivation of quiescent or latent virus. A study by Coleman, et al. examined ICP0-mediated derepression in a fibroblast model of quiescence utilizing replication-deficient HSV mutants (32). After establishment of quiescence, followed by superinfection with an adenovirus providing ICP0, an increase in AcH3 was found on the ICP0, ICP4, ICP27, VP16, gC and LAT promoters, and a decrease in the repressive modification of histone H3 lysine 9 trimethylation (H3K9me3) was found on the ICP0, ICP27, VP16, and gC promoters. These results demonstrated that derepression of quiescent genomes by ICP0 induces a global change in chromatin structure, specifically, acetylation of histones associated with quiescent viral genomes.

In the current study, we explored the effects of ICP0 on gene expression and epigenetic structure of quiescent HSV genomes using a cell culture model of HSV quiescence in HEL cells. The results suggest that there may be multiple mechanisms through which ICP0 exerts its effects, and that these mechanisms may depend on the abundance of ICP0. In addition to its previously

demonstrated effects on the acetylation and methylation of histones associated with quiescent genomes, ICP0 is able to work at an additional level of chromatin repression, by facilitating the removal of preformed nucleosomes from quiescent genomes.

3.3 MATERIALS AND METHODS

3.3.1 Cells and viruses

Experiments were performed using MRC-5 (human embryonic lung) cells obtained from, and propagated as recommended by, American Type Culture Collection (ATCC). The viruses used in this study were the HSV-1 IE mutants d105 (96, 211) and d109 (211), as well as the adenoviruses Ad.S11D and Ad.S11E4(ICP0) (96). d105 was propagated on E11 cells and d109 on F06 cells as previously described (211).

3.3.2 ChIP

ChIP was carried out as previously described (66, 213) with a few modifications. 5×10^6 MRC-5 cells were plated in 100mm dishes, and were infected by d109 at an MOI of 10 at room temperature for 1 hour. After adsorption, the inoculum was removed and 37°C 5% DMEM was added. Infected cells were maintained at 37°C for 24 hours. At 24 hpi, the media was replaced with fresh media, and infected cells were maintained at 34°C. On day 4 post infection, media was again replaced with fresh media. At day 7 post infection, d109-infected cells were either mock superinfected, superinfected with d105 at an MOI of 10, or superinfected with Ad.S11D

and Ad.S11E4(ICP0) at 200 focus forming units (FFU) per cell for 1 hour at room temperature. After adsorption, the inoculum was aspirated and the conditioned media (which was saved and maintained at 37°C) was replaced. This was considered time 0 post superinfection. At the indicated times post infection, cells were treated with 1% formaldehyde for 10 minutes at 37°C, washed 3 times with cold phosphate-buffered saline (PBS) containing protease inhibitors (67 ng/ml aprotinin, 1 ng pepstatin, 0.16 mM TLCK [*N* α -ptosyl-L-lysine chloromethyl ketone], 1 mM phenylmethylsulfonyl fluoride [PMSF]), and scraped into PBS containing protease inhibitors. The cells were pelleted at 3,000 rpm for 10 minutes at 4°C and resuspended in cold SDS lysis buffer (100 μ l per million cells) containing protease inhibitors (1% SDS, 10mM EDTA, 50mM Tris-HCl [pH8.1], 4 μ g/ml aprotinin, 2 μ g/ml pepstatin, 0.15mM TLCK, and 0.6mM PMSF), and incubated on ice for 30 minutes. All other procedures were as described. The antibodies used were anti-histone H3 (Abcam, ab1791), anti-histone H4 (Millipore, 05-858), anti-acetyl histone H3 (Millipore, 06-599), anti-acetyl histone H4 (Millipore, 06-866), anti-trimethyl histone H3 lysine 9 (Millipore, 07-422), and anti-heterochromatin protein 1 γ (Millipore, 05-690). A “no-antibody control” was included for each ChIP experiment. When calculating ChIP results after quantitative PCR (qPCR), the value for the no-antibody control was subtracted from the immunoprecipitation results before the percent input of immunoprecipitation was calculated. Therefore, any values reported indicate an increase over the baseline. The baseline, or no-antibody control, was always considerably less than the results for the specific immunoprecipitations.

3.3.3 Micrococcal nuclease digestion

7.5×10^6 MRC-5 cells were plated per 100mm dish in 12 dishes. 4 dishes were mock infected, and 8 were infected with d109 at an MOI of 20 for 1 hour with rocking every ten minutes at room temperature. After adsorption, the inoculum was removed and 37°C 5% DMEM was added. Infected cells were maintained at 37°C for 24 hours. At 24 hpi, the media was replaced with fresh media, and infected cells were maintained at 34°C. On day 4 post infection, media was again replaced with fresh media. At day 7 post infection, 4 d109-infected dishes and 4 mock-infected dishes were superinfected with d105 at an MOI of 10, while the remaining 4 d109-infected dishes were mock superinfected at room temperature for 1 hour. After adsorption, the inoculum was removed and the conditioned media, which had been saved at 37°C, was replaced. This was considered time 0 post infection. 8 hours post superinfection, nucleoprotein complexes were digested by *in situ* micrococcal nuclease digestion (280) (protocol 1). Briefly, cells were permeabilized with lysolecithin (0.5mg/mL) in permeabilization solution 1 (150mM sucrose, 80mM KCl, 35mM HEPES, pH 7.4, 5mM K₂HPO₄, 5mM MgCl₂, 0.5 mM CaCl₂) for 1 minute at 37°C. Chromatin from each of the three groups of 4 infections was then digested with 2.5 mL permeabilization solution 2 (150 mM sucrose, 50 mM Tris-Cl, pH 7.5, 50 mM NaCl, 2 mM CaCl₂) with 0, 300, 1000, or 3000 gel units micrococcal nuclease (NEB, M0247S) for 5 minutes at room temperature. Cells were scraped into 500µl NDPK buffer (20mM Tris-Cl, pH 7.4, 0.2M NaCl, 3mM EDTA, 1% SDS, 0.2 mg/ml proteinase K) and digested at 37°C overnight. DNA was isolated by phenol chloroform extraction and ethanol precipitation, RNase A treated, separated on a 2% agarose gel, transferred to a Nytran membrane, probed with 2µg ³²P-labeled nick-translated GFP fragment of pEGFP-C1 digested with AseI and BglII (New England Biolabs), and exposed to Hybond film.

3.3.4 RNA isolation and reverse transcription

RNA was isolated with the Ambion RNaqueous -4PCR kit, following the included protocol. Briefly, 5×10^6 MRC-5 cells in 100mm plates were infected at an MOI of 10 by d109 for one week and superinfected as in the CHIP experiments. RNA was harvested at the indicated time points by adding 500 μ l Lysis/Binding Buffer. Cells were scraped and vortexed. An equal volume of 67% ethanol was added, and the solution was added to a filter, which was centrifuged at 12,500 RPM at 4°C for 1 minute. The bound RNA was washed with wash buffers 1 and 2/3. RNA was eluted with 60 μ l 65°C Elution Solution. The RNA was treated with DNase I at 37°C for 30 minutes to degrade any residual DNA.

Reverse transcription was performed using the Ambion reverse transcription kit and following the included instructions. 2 μ g total RNA was reverse transcribed in a reaction volume of 20 μ l containing RNase inhibitor, oligo(dT) primers, 1 μ l MMLV-RT and 2 μ l 10x reaction buffer. The reaction tube was incubated at 85°C for 3 minutes to remove RNA secondary structure, and the reverse transcription reaction was carried out for 1 hour at 44°C. After the reverse transcription reaction was complete, the reaction tube was incubated at 95°C for 10 minutes in order to inactivate the reverse transcriptase. 8 μ l of cDNA was diluted 1:8 by adding 40 μ l DNase/RNase free H₂O for use in qPCR reactions. Additionally, 1 μ g RNA was diluted into a total of 60 μ l DNase/RNase free H₂O for use as a negative control in qPCR reactions.

3.3.5 qPCR

Reactions for CHIP or cDNA quantification were performed in triplicate using 2.5 μ l of DNA for each reaction as described (213), with a few modifications. Before setting up the 96-well

reaction plate, a master mix containing 0.3125 μ l of each primer (stock concentration, 1 mM), 6.25 μ l Applied Biosystems SYBR green super mix with 1.0 μ M 6-carboxy-X-rhodamine (Bio-Rad), and 3.125 μ l of water for a total of 10 μ l for each reaction was made. The final reaction volume was 12.5 μ l, including the DNA. The primers used for ChIP and cDNA quantification and their locations relative to the transcription start site of the gene to be analyzed are as previously published (66). d106 DNA was also included in each plate, in a standard curve of 1:10 dilutions from 250,000 to 25 copies per well, which covers the threshold cycle values for the ChIP DNA samples tested. qPCR was run on a StepOne Plus Real Time PCR machine. The conditions for the run were as follows: stage 1, 95°C for 10 min; and stage 2, 40 cycle repeats of 95°C for 15 seconds and 60°C for 1 min. At the end of the run, a dissociation curve was completed to determine the purity of the amplified products. Results were analyzed using the StepOne v2.1 software from Applied Biosystems.

3.4 RESULTS

3.4.1 RNA expression from quiescent genomes upon reactivation by ICP0

Immediate early gene expression does not occur during infection with d109. As a consequence, viral gene expression is repressed and the viral genome persists in cells (211). The virus contains a model transgene consisting of the EGFP gene driven by the HCMV IE promoter. GFP expression is reduced over time in d109-infected cells, with the greatest level of repression in fibroblasts (66, 96, 211, 246). This repression of GFP expression can be reversed in fibroblasts at 7dpi by provision of ICP0 (96, 246). In order to characterize the effects of

epigenetic changes on the quiescent HSV genome induced by ICP0, it was important to measure the kinetics of GFP RNA expression upon reactivation. It was also of interest to examine the induction of other viral promoters, to determine whether the effects of ICP0 were specific for the HCMV promoter, or are more generally targeted to the HSV-1 genome.

After quiescent infection was established with d109 for 7 days, MRC-5 cells were superinfected with d105 or adenovirus vector, and RNA levels were determined at various time points by RT-PCR (Figure 10A). The steady state level of GFP expression driven by the HCMV promoter of d109 was approximately 5×10^5 copies per μg of total RNA, or approximately an average of 10 molecules per cell. This level of expression was reached by approximately 24 hpi (66), and can be found after 7 dpi. Induction of GFP expression by superinfection with d105 was seen by 2 hpi, at which time GFP expression was increased 10-fold. There was a continuous increase in expression over time after 2 hpi, and by 24 hpi with d105, quiescent genomes were induced 1000-fold.

The same pattern of transcriptional induction was seen when ICP0 was provided by an adenovirus vector (Figure 10B). By 24 hpi, GFP expression increased 1000-fold. Levels of tk and gC RNA, which were undetectable in AdS.11D-superinfected cells, increased by greater than four orders of magnitude upon infection with AdS.11E4(ICP0). Additionally, the level of transcriptional activation was proportional to the relative strength of each promoter. These data indicate that the effects of ICP0 are general across the entire viral genome, and that transcriptional activation depends on the strength of the promoter, once repression is removed by ICP0.

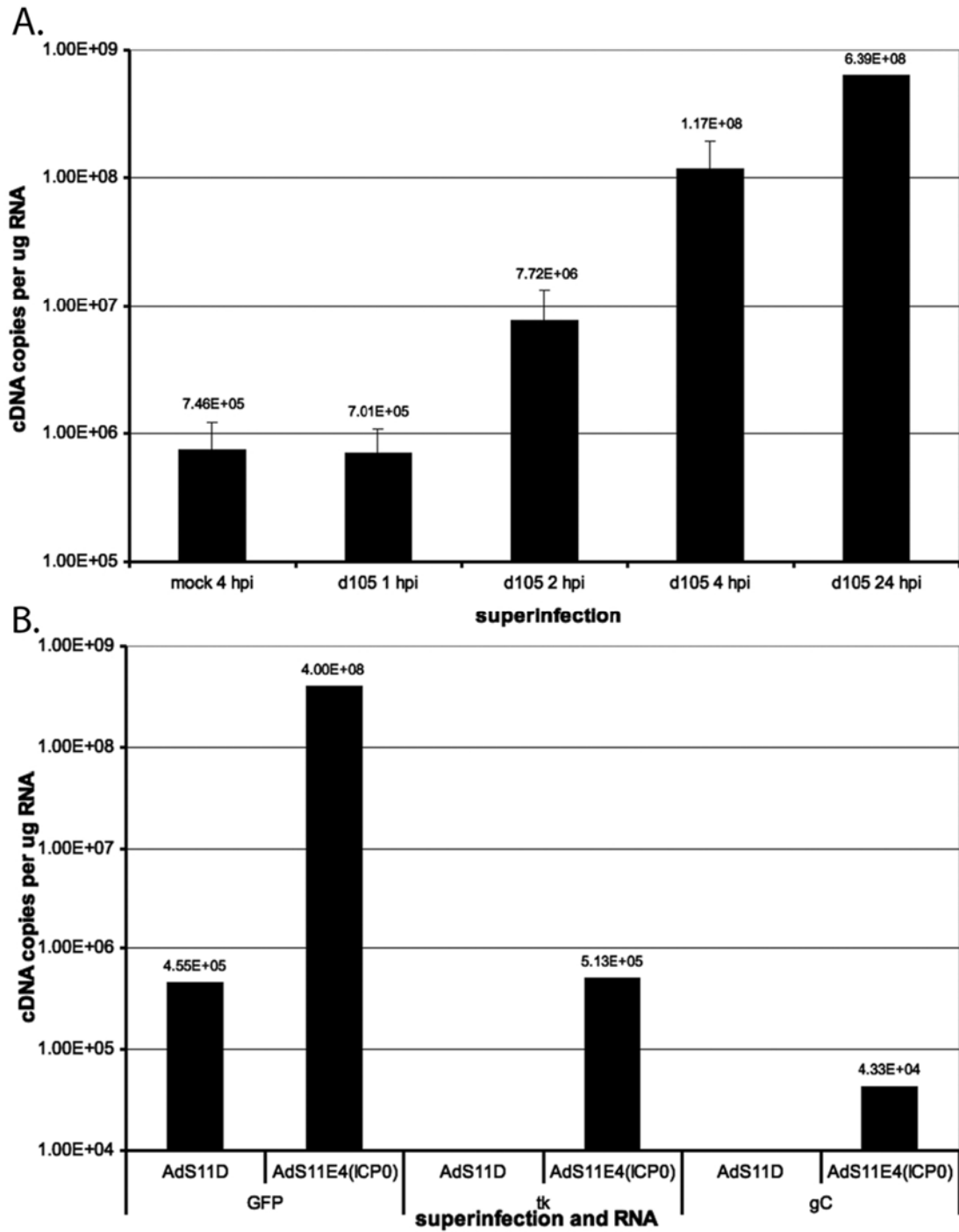


Figure 10. Abundance of GFP, tk, or gC mRNA in d109-infected MRC-5 cells after superinfection.

Infections, RNA isolation, cDNA preparation, and RT-PCR were performed as described in Materials and Methods. Quiescent infection by d109 was established for 1 week. The graphs indicate the number of RNA molecules of GFP per μg RNA at the indicated time points after superinfection by d105 (A), or at 24 hpi after the indicated adenovirus infection (B).

3.4.2 Removal of higher order chromatin structure and repressive epigenetic marks upon expression of ICP0

It has been previously shown that expression of ICP0 prevents the accumulation of heterochromatin on the viral genome at representative promoters (29). Specifically, expression of ICP0 prevented accumulation of the heterochromatin mark H3K9me₃, as well as deposition of HP1 γ at the tk, gC, and HCMV promoters, and that these effects were correlated with transcriptional activation (66). We wished to test whether ICP0 could also remove heterochromatin marks from repressed, quiescent genomes, once a highly repressed state was established. ChIP assays were performed following d105- and AdS.11E4(ICP0)-superinfection reactivation.

ChIP assays for HP1 γ and H3K9me₃ on the HCMV promoter were performed on d109 infected cells that were superinfected for different lengths of time with d105 (Figure 11A and B). Expression of ICP0 from d105 caused the removal of HP1 γ beginning at 1 hour post-superinfection (Figure 11A), which preceded a detectable increase in GFP RNA (Figure 10). HP1 γ levels continued to decrease over time, and by 24 hours post infection, were approximately one-fifth the level of mock-superinfected cells. H3K9me₃ levels did not decrease until 2 hours post-superinfection with d105 (Figure 11B). This is presumably because access to histone modifications is limited when they are found in higher-order heterochromatin structures, and binding proteins such as HP1 γ must first be removed. H3K9me₃ was reduced by 2 hours post-superinfection, and also continued to decrease over time. The ICP0-mediated reduction in heterochromatin on the d109 HCMV promoter was concurrent with reactivation of gene expression.

In order to investigate whether the removal of heterochromatin was a general effect, or limited to the HCMV promoter, we tested the effects of superinfection with adenovirus-provided ICP0 on the quiescent d109 genome. After d109 quiescence was established for 7 days, cells were superinfected with either AdS.11D or AdS.11E4(ICP0). 24 hpi, ChIP was performed, and the levels of heterochromatin marks on the tk and gC promoters were determined. Additionally, the EGFP coding sequence was assayed. This was necessary, because AdS.11D and AdS.11E4(ICP0) contain the secretory alkaline phosphatase reporter gene under control of the HCMV promoter (96).

Expression of ICP0 from the adenovirus vector caused a reduction in HP1 γ on all three classes of viral promoter, with the greatest decrease on the tk promoter (Figure 11C). Additionally, H3K9me3 was reduced on all three promoters (Figure 11D). These results demonstrate that ICP0 expression results in a decrease in heterochromatin on quiescent genomes, that this reduction is not dependent on the viral context in which ICP0 is provided, and that the reduction of heterochromatin is general across the quiescent viral genome.

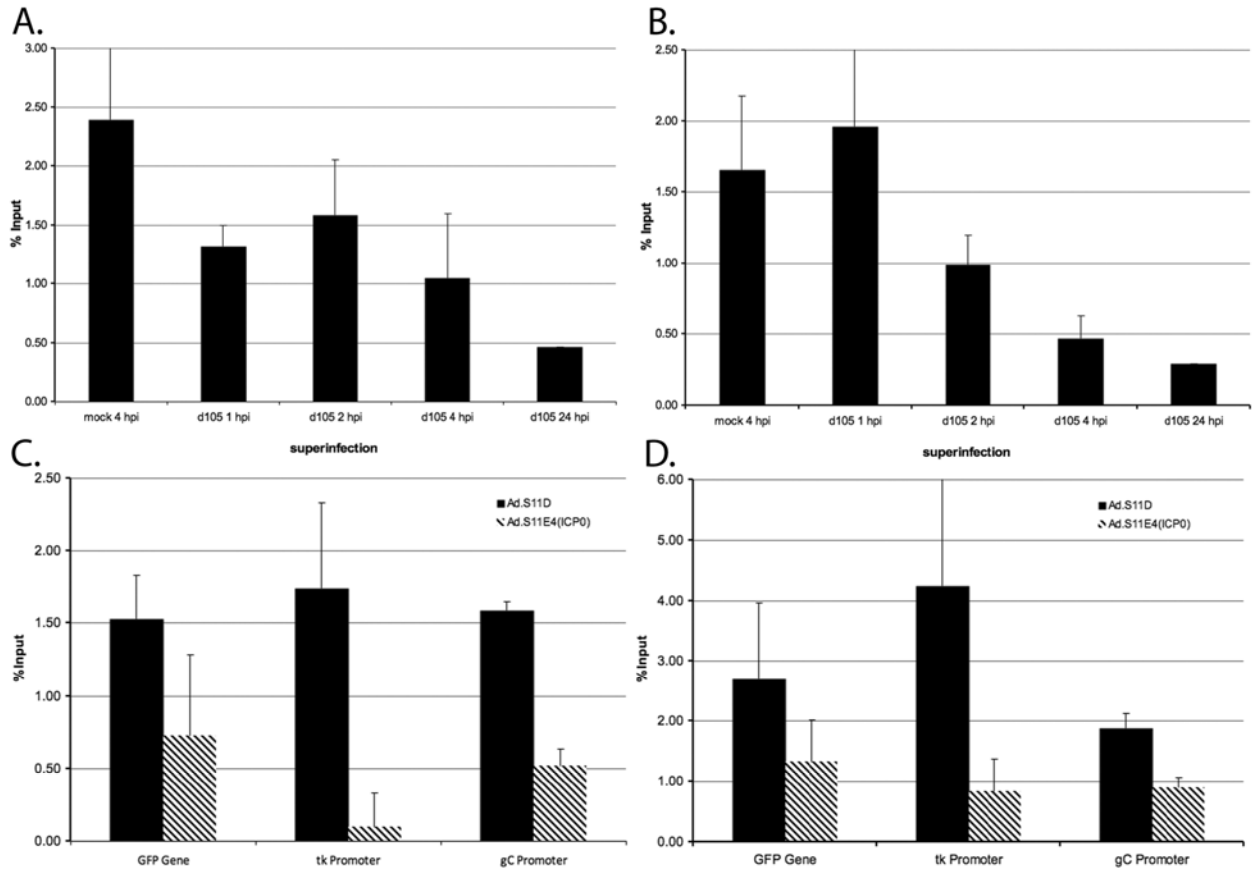


Figure 11. Repressive chromatin modifications associated with the tk, gC and HCMV promoters, and GFP 5' region of d109 in MRC-5 cells after superinfection.

Chromatin Immunoprecipitation (ChIP) with antibodies to HP1 γ (A and C) and H3K9me3 (B and D), and followed by RT-PCR with primer pairs corresponding to the indicated promoter regions were performed as described in the Materials and Methods. Graphs show the percentages of total genomes bound after superinfection with d105 at the indicated time points (A and B), or after superinfection with the indicated adenovirus at 24 hpi (C and D). Error bars represent standard error of the mean from multiple experiments.

3.4.3 Removal of histones upon expression of ICP0

The basic unit of chromatin structure is the nucleosome, which is an octamer of 4 histone proteins, H2A, H2B, H3 and H4, around which approximately 150 base pairs of DNA are wrapped (154). Nucleosomes are associated with quiescent HSV DNA (110), while transcriptionally active HSV DNA is most likely not bound by stable classical nucleosomes (117,

130, 136). Previously, it was demonstrated that expression of ICP0 during productive infection prevents the accumulation of histone H3 on the viral genome (29), and that this effect is also seen during the establishment of quiescence (66). In order to determine whether histones are removed during ICP0-mediated reactivation, ChIP was performed for histones H3 and H4 upon ICP0-mediated reactivation of quiescent d109.

As in previous experiments, quiescence of d109 was established for one week in MRC-5 cells, and cells were superinfected with d105 for 1, 2, 4, or 24 hours (Figure 12). Histone H3 and H4 occupancy of the d109 HCMV promoter was reduced upon expression of ICP0 (Figure 12). This reduction in histone occupancy is coincident with RNA expression (Figure 10).

In order to extend these results and further probe the nucleosomal structure of quiescent genomes, and the changes induced upon ICP0 expression, *in situ* micrococcal nuclease digestion was performed. Quiescent infection with d109 was established for one week, and cells were either superinfected with d105, or mock superinfected. 8 hours post superinfection, the cells were permeabilized, and increasing concentrations of micrococcal nuclease were added. Total cell-associated DNA was isolated, size-fractionated on an agarose gel, and stained with ethidium bromide to visualize bulk cellular DNA. The DNA was transferred onto a nylon membrane, and probed with a ³²P-labelled GFP DNA probe. Therefore, the observed MN patterns represent the chromatin structure of the gene unique to the quiescent genomes. The ethidium bromide stained gel showed the standard nucleosomal pattern of the bulk cellular DNA (Figure 13). The hybridization signals revealed that the quiescent d109 genomes were more resistant to MN digestion than bulk cellular DNA (Figure 13), implying that these genomes are packaged in a higher order structure. If quiescent genomes are packaged in regular nucleosomes, additional structure masks this by preventing access by micrococcal nuclease. Provision of ICP0 by d105

resulted in a chromatin configuration that was degraded by low concentrations of micrococcal nuclease. The GFP gene of ICP0-reactivated d109 is at least as sensitive to MN digestion as bulk cellular DNA. These results are consistent with the ChIP data demonstrating removal of both heterochromatin and histones from quiescent d109 upon ICP0 expression.

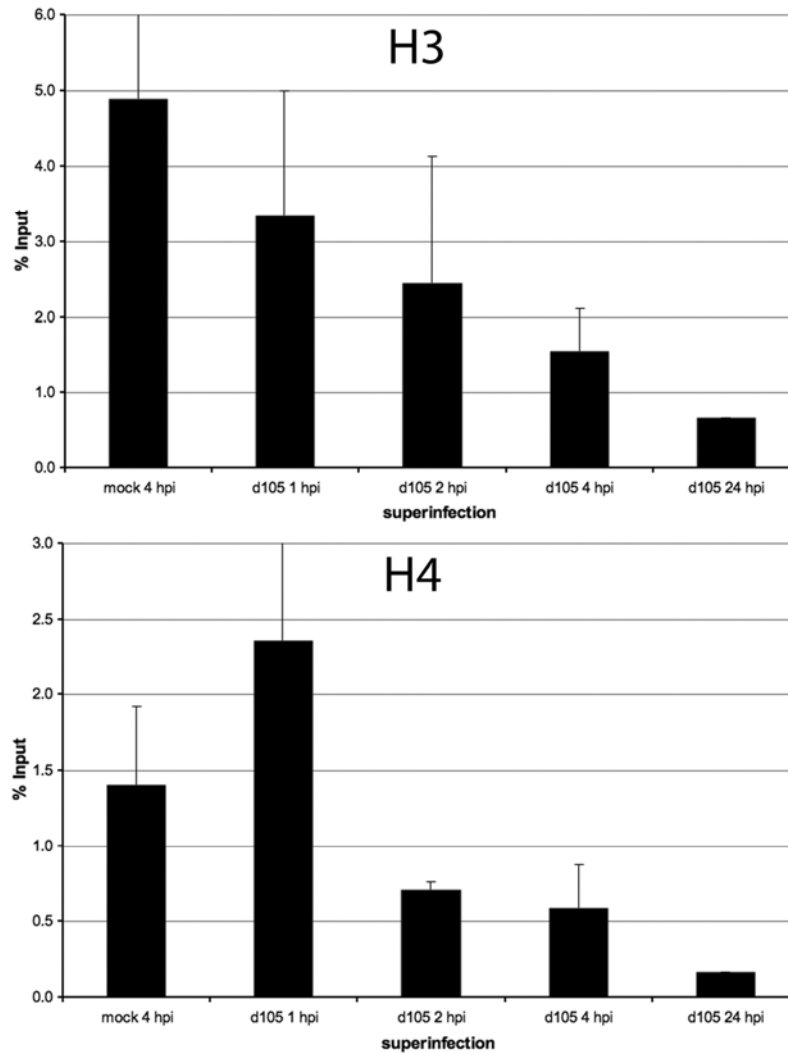


Figure 12. Binding of histones H3 and H4 to the HCMV promoter of d109 in MRC-5 cells after superinfection with d105.

ChIP with antibodies to histones H3 and H4, and RT-PCR were performed as described in the legend to Figure 11 to determine the percentages of genomes bound by histones H3 (A) and H4 (B). Graphs show the percent of total genomes bound at the indicated times post infection with d105. Error bars represent standard error of the mean from multiple experiments.

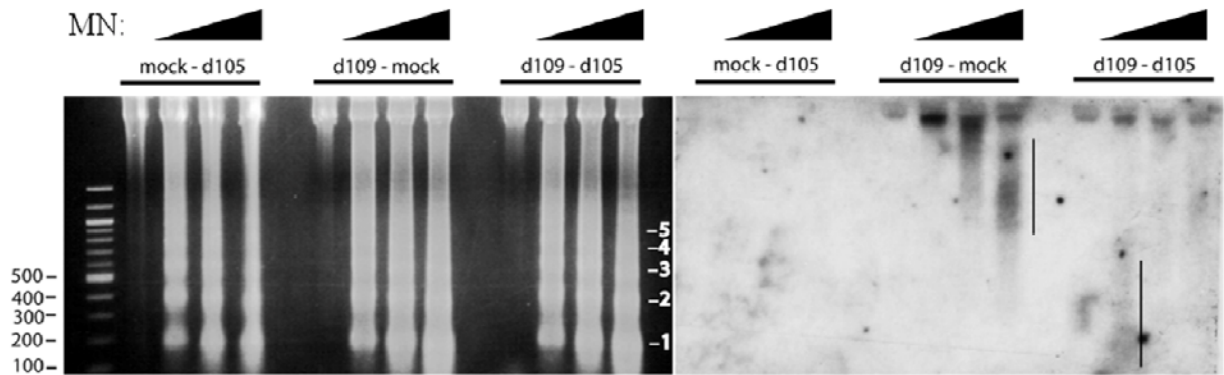


Figure 13. Micrococcal nuclease digestion of d109-infected MRC-5 cells after superinfection.

MRC-5 cells were mock- or d109-infected for one week, followed by superinfection with the indicated virus. Cells were permeabilized and digested for 5 minutes with 0, 200, 1000, or 300 units micrococcal nuclease. The DNA was isolated from the nuclei at 8 h post infection, purified, and fractionated on 2.0% agarose gels. The agarose gels were stained with ethidium bromide (left) and transferred to NYTRAN membranes for Southern Blot hybridization as described in the Material and Methods section. The Southern Blots (right) were probed with ^{32}P -labeled GFP DNA, washed and exposed to X-ray film. Shown are the autoradiographic images of the probed blots (right).

In a study by Coleman, et al., ICP0 provided by a superinfecting adenovirus failed to cause the removal of histones from quiescent HSV genomes during reactivation, which contrasts with the effects seen when ICP0 was expressed by d105. We therefore tested whether ICP0 expressed from AdS.11E4(ICP0) caused the reduction of histone occupancy on the quiescent d109 genome. Using ChIP analysis, it was seen that ICP0 expression from AdS.11E4(ICP0) did not cause appreciable reduction of histone H3 on either the tk or gC promoter, or EGFP gene, when compared to the empty adenoviral vector (Figure 14). Histone H4 occupancy was reduced a minimal amount on all three regions tested (Figure 14). Despite the lack of histone removal from quiescent genomes during AdS.11E4(ICP0) superinfection (Figure 14), GFP expression was activated to the same extent as in d105 superinfection (Figure 10). This implies that the removal of histones from quiescent genomes is not required for significant ICP0-mediated reactivation.

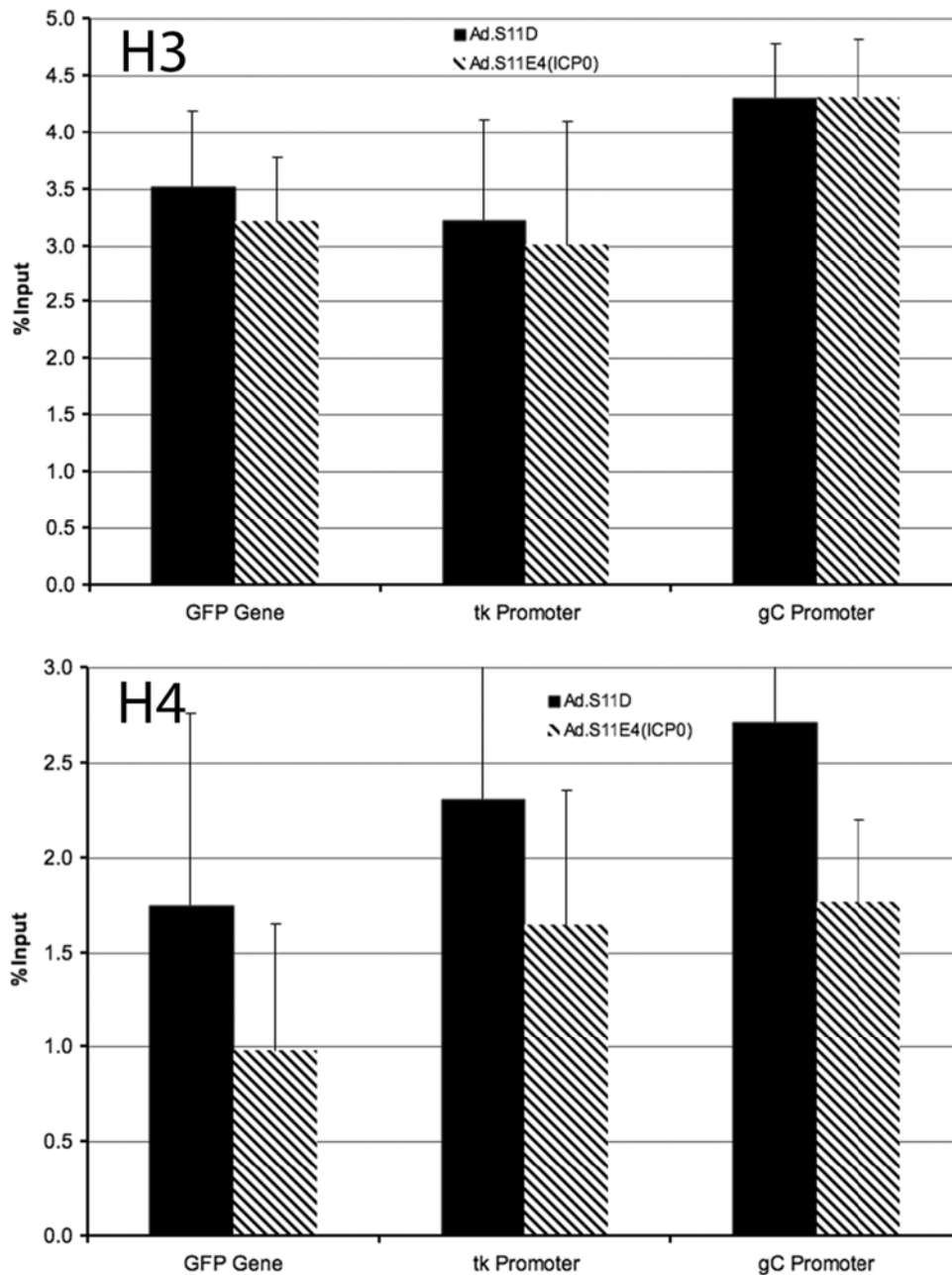


Figure 14. Binding of histones H3 and H4 to the tk and gC promoters and GFP 5' region of d109 in MRC-5 cells after superinfection with adenovirus.

ChIP with antibodies to histones H3 and H4, and RT-PCR were performed as described in the legend to Figure 11 to determine the percentages of d109 genomes bound by histones H3 (A) and H4 (B). Graphs show the percent of total genomes bound at 24 hpi with the indicated adenovirus. Error bars represent standard error of the mean from multiple experiments.

3.4.4 Hyperacetylation of histones is a result of ICP0 expression

It has been shown in a number of studies that infection with HSV results in global hyperacetylation of histones (117), and that ICP0 expression causes hyperacetylation of histones bound to the HSV genome (29, 32, 66). ICP0 has also been shown to cause the disruption of the repressive complex HDAC1/HDAC2/REST/CoREST/LSD1 (78, 80, 81, 83). The effects of ICP0 expression also seem to share some similarities to HDAC inhibitors such as trichostatin A (97).

In order to determine the effects of ICP0 on histone acetylation during activation of quiescent HSV, we performed ChIP on a time course following d105 superinfection and compared it with expression data at the same time points. In order to account for the reduction of histones on the quiescent genome upon reactivation, AcH3 and AcH4 levels were normalized to the bulk amount of histones H3 and H4 (Figure 12). As has been seen previously, ICP0 expression by d105 caused hyperacetylation of the histones that were bound to d109 HCMV promoter (Figure 15). However, the activation of transcription under these conditions (Figure 10A) preceded the appearance of acetylated histones. This may indicate that hyperacetylation of the histones bound to the reactivating quiescent genome is not an event required for the initiation of transcriptional reactivation. This hyperacetylation could be significant in that it may act to prevent reestablishment of repression and allow for continuous access to the genome by the transcriptional apparatus.

ChIP experiments performed after adenovirus superinfection demonstrated that expression of ICP0 from AdS.11E4(ICP0) caused an increase in acetylation of histone H3 and H4 on all three genes tested (Figure 16). The percent of H3 acetylated on viral promoters is most significantly increased on the gC promoter, while it is only slightly increased on the GFP gene

and tk promoter, whereas the fraction of hyperacetylated H4 is increased to a small extent on the tk and gC promoters, and is greatly increase on the HCMV promoter. These results indicate that expression of ICP0 causes hyperacetylation of histones across the viral genome, which has also been seen previously (32). Hyperacetylation of viral-bound histones is seen both when histones are removed from the viral genome, and when they remain, showing that these effects are not necessarily tied together by the same mechanism. Therefore, the effects of ICP0 on the acetylation and higher order chromatin structure of quiescent HSV genomes may be mediated through different mechanisms.

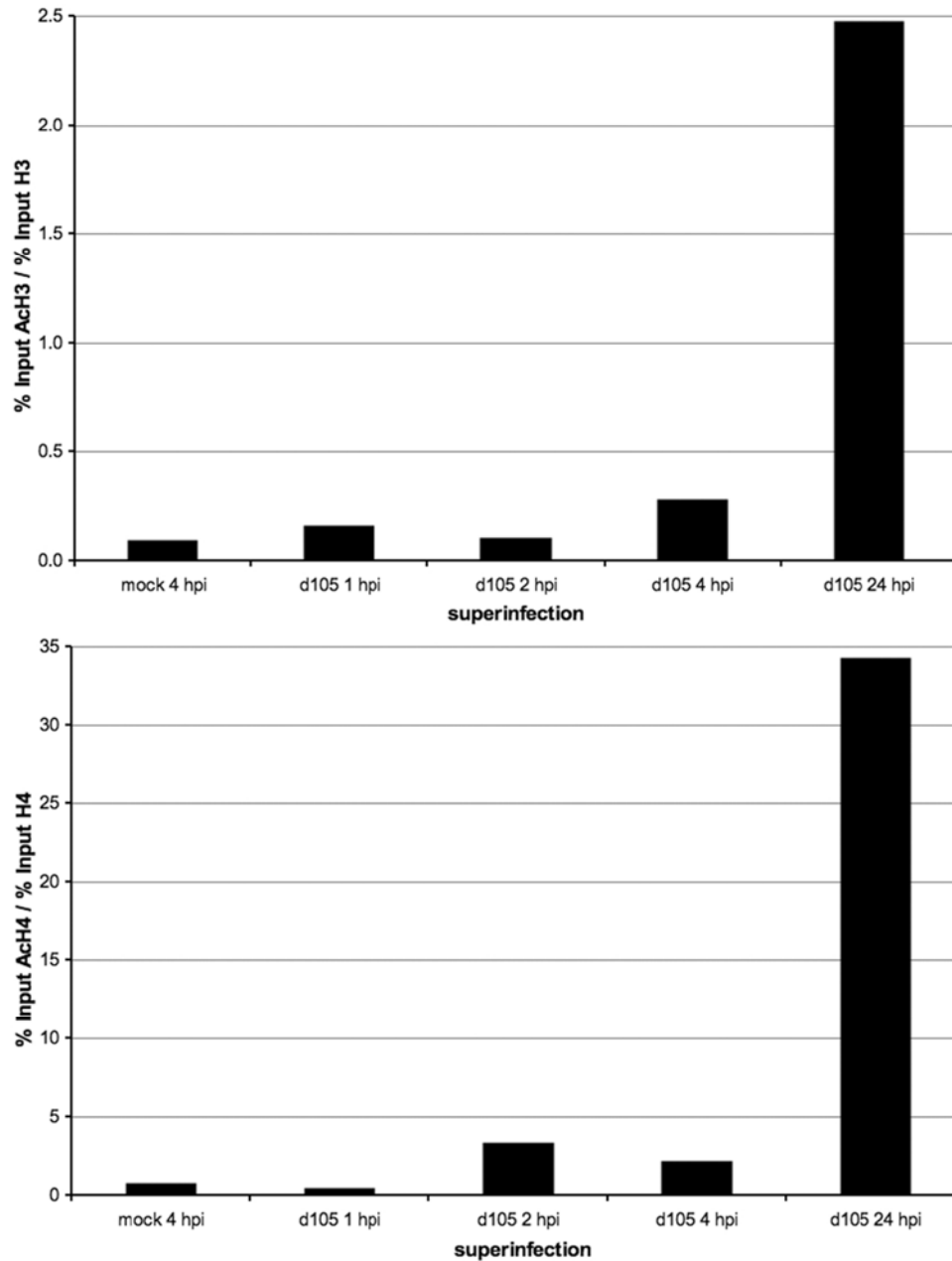


Figure 15. Binding of hyperacetylated histone H3 and hyperacetylated H4 to the HCMV promoter of d109 in MRC-5 cells after superinfection with d105.

ChIP with an antibody to AcH3 and AcH4 and RT-PCR were performed as described in Figure 11 to determine the percentage of d109 genomes bound by AcH3 or AcH4 at the indicated times post infection with d105. In order to compensate for the changing amounts of total histone H3 and H4, AcH3 was normalized to the amount of histone H3 (A) and AcH4 was normalized to the amount of histone H4 (B) on the genome by dividing the percent of acetylated histone by the percent of total histone (Fig. 3). Error bars represent standard deviations from multiple experiments.

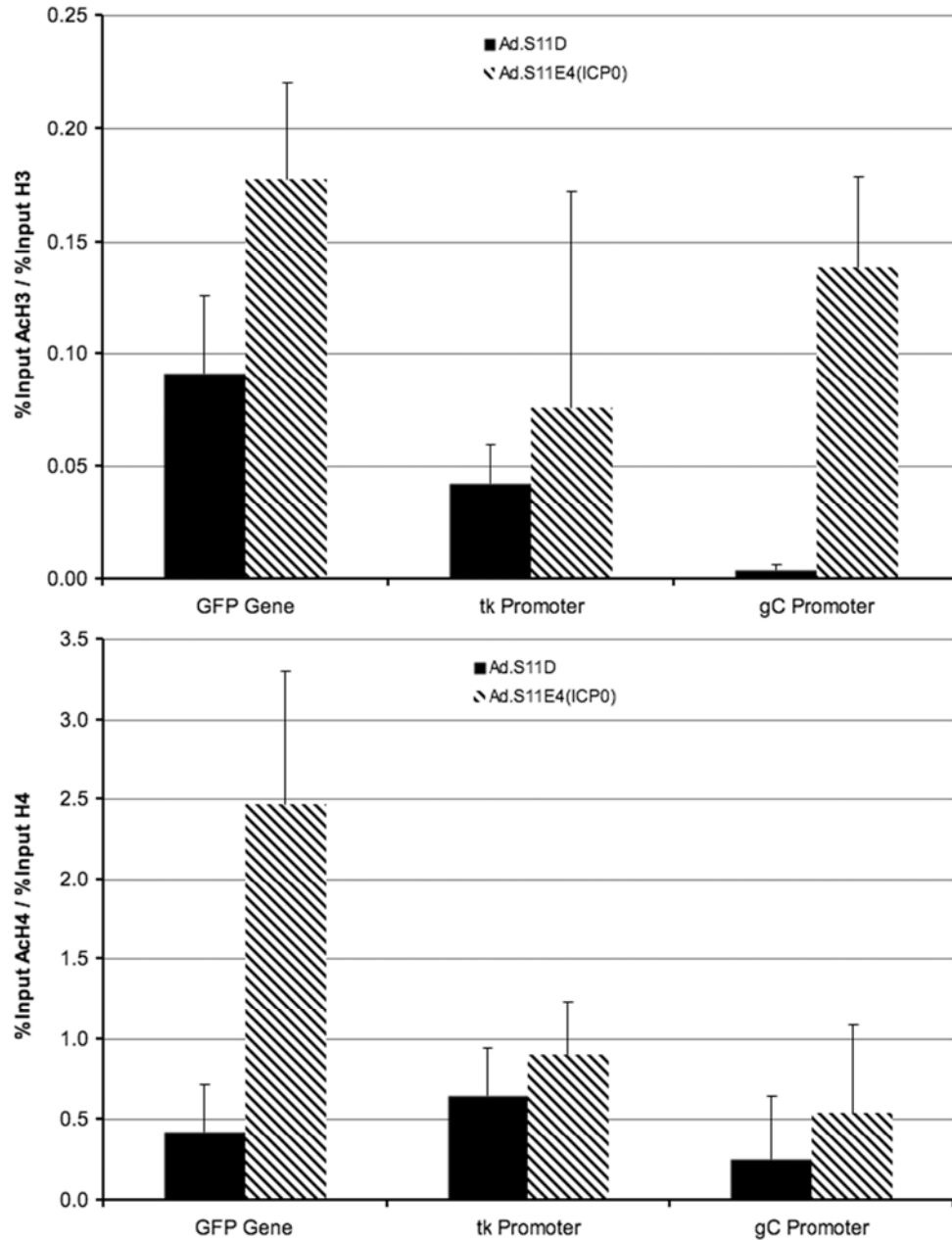


Figure 16. Binding of hyperacetylated histone H3 and hyperacetylated H4 to the tk and gC promoters and GFP 5' region of d109 in MRC-5 cells after superinfection with adenovirus.

ChIP with an antibody to AcH3 and AcH4 and RT-PCR were performed as described in Figure 11 to determine the percentage of d109 genomes bound by AcH3 or AcH4 at the indicated times post infection with d105. In order to compensate for the changing amounts of total histone H3 and H4, AcH3 was normalized to the amount of histone H3 (A) and AcH4 was normalized to the amount of histone H4 (B) on the indicated regions of the genome by dividing the percent of acetylated histone by the percent of total histone (Fig. 3). Error bars represent standard deviations from multiple experiments.

3.5 DISCUSSION

ICP0 is a promiscuous transactivator of gene expression, and is one of several viral proteins that can reactivate gene expression from quiescent genomes. Some of the effects of ICP0 are similar to those of the HDAC inhibitor trichostatin A (97, 246), but as quiescence is established, inhibiting histone deacetylases is not sufficient to activate gene expression (246). However, ICP0 maintains the ability to reactivate the quiescent virus (246). Additionally, replicating HSV lacking ICP0 cannot participate in recombination with quiescent HSV-1 (168, 246), implying that quiescent genomes are inaccessible to viral proteins and the recombination machinery in the absence of ICP0. Therefore, it appears that ICP0 is involved in the removal of a repressive mechanism, and this mechanism involves perturbation of a higher order chromatin structure. In this study, quiescence was established with the HSV mutant d109, which expresses no IE proteins and cannot replicate in noncomplementing cells. After one week, d109 was reactivated by providing ICP0 *in trans*, either by the HSV-1 mutant d105, or by an adenovirus vector. RNA expression was quantified, and ChIP was used to determine the relationship of chromatin structure to gene expression patterns upon reactivation of viral gene expression. We determined the presence of heterochromatin on the quiescent genomes, whether histones were removed, and whether remaining histones were acetylated, and correlated the chromatin structure temporally with gene expression, both from the HCMV IE promoter, and from representative E and L genes.

3.5.1 Gene expression upon ICP0 induced reactivation

The steady state level of GFP expression from quiescent d109 in MRC-5 cells was approximately 10 mRNA copies per cell. The majority of this expression likely occurs in the

few (less than 0.1%) of cells which do not become repressed (246). Upon provision of ICP0 by d105 superinfection, expression of GFP mRNA increased, 10-fold by 2 hours, 150-fold by 4 hours, and approximately 1000-fold by 24 hours post superinfection (Figure 10).

Due to the absence of ICP4, ICP0 is over expressed in the d105 background. In contrast, the amount of ICP0 expressed in AdS.11E4(ICP0) infected cells at 24 h post infection is less than 1000 times that expressed in d105 infected cells, and approximately equal to that seen in the first hour of infection by wt virus (96). Therefore, we also measured the ability of ICP0 expressed from AdS.11E4(ICP0) to reactivate gene expression. As seen in Figure 10, the level of mRNA GFP accumulating at 24 hpi was equivalent in d105 and AdS.11E4(ICP0) superinfection. As we have previously shown (96), this result reinforces the finding that even small amounts of ICP0 can alleviate repression to an extent that allows for full transcriptional activation. Additionally, superinfection with AdS.11E4(ICP0) allowed the measurement of detectable levels of the E and L representative genes, tk and gC. The level of activation of these genes varied with their relative promoter strength, as previously reported (66).

3.5.2 Removal of heterochromatin as a function of ICP0

It has been shown that ICP0 prevents the association of HP1 γ with incoming viral genomes as quiescence is established (66). In this study, it was determined that ICP0 expression in *trans* can cause the removal of HP1 γ from highly heterochromatic quiescent genomes. This effect was seen both in d105 and AdS.11E4(ICP0) superinfection, indicating that even small amounts of ICP0 can facilitate the removal of HP1 γ . Additionally, during AdS.11E4(ICP0) superinfection, all three promoter classes tested showed a reduction in HP1 γ , indicating that this is a general effect across the genome. The removal of HP1 γ occurred by 1 hpi, which precedes a measurable

increase of RNA levels. This is presumably because higher order chromatin structure must be removed before the transcriptional machinery can access the DNA.

A previous report (32) determined that HP1 α was enriched at viral promoters after superinfection with HSV-2, while no large change in HP1 α levels was observed after ICP0 expression by an adenovirus. The differences between these observations and our results can be explained by several possibilities. First and most obvious, is that although the three isoforms of HP1 share homology and similar roles in gene silencing, they have different localization characteristics and may have different interaction partners (149, 157). Thus HP1 α localizes exclusively to heterochromatin, while HP1 γ has been shown to localize to both heterochromatin and silenced euchromatic regions. This suggests that the HP1 isoforms play different roles in HSV-1 silencing during quiescence. Additionally, the previous study employed phosphonoacetic acid to prevent replication in HSV-2 superinfection, and doxycycline to drive expression during adenovirus superinfection. These chemicals may have altered the chromatin dynamics on quiescent virus, as we have seen that even replacing conditioned media with fresh media can drastically change histone occupancy levels on quiescent viral genomes (data not shown).

Trimethylation of histone H3 lysine 9 is associated with repression of transcription (8), and recruits HP1 (5). After superinfection with d105, a reduction of H3K9me3 on the HCMV promoter was seen by 2 hpi, concurrent with a detectable rise in GFP RNA levels. As would be expected, the change in H3K9me3 levels followed a reduction in HP1 γ association with the quiescent genome. The reduction of H3K9me3 was also found on gC and tk promoters after AdS.11E4(ICP0) superinfection, showing that the reduction of heterochromatin is a general effect across the quiescent genome. The temporal order of heterochromatin removal suggests

that HP1 γ removal is required before changes to histone modifications can occur, and before transcriptional activation can be induced.

3.5.3 The abundance of ICP0 may affect the removal and acetylation of histones from quiescent genomes

Previously, it has been seen that superinfection with an adenovirus expressing ICP0 does not result in the removal of histone H3 from quiescent HSV-1 (32), while the presence of ICP0 prevents the accumulation of histone H3 and quiescence (66). These results taken together suggest that ICP0 expression can prevent histone deposition on incoming viral genomes, but that it cannot cause the removal of histones from previously chromatinized quiescent genomes. Further analysis, however, reveals a more complex picture of ICP0 function.

When ICP0 was overexpressed in *trans* from d105, histones H3 and H4 were removed from the HCMV promoter of the quiescent d109 genome, concurrent with gene expression, as well as with the decrease of H3K9me3. Micrococcal nuclease analysis of the GFP gene revealed that d105 infection resulted in greater susceptibility to micrococcal nuclease than even cellular DNA, and no detectable banding pattern, indicating that both higher order chromatin structure, as well as nucleosomes were removed from the d109 GFP gene upon ICP0 expression. However, when ICP0 is expressed at low levels, which more closely mimics wild-type levels, from AdS.11E4(ICP0), histone H3 was not removed from the HCMV, tk, or gC promoters of d109, while there was a slight reduction in histone H4 occupancy at these promoters.

While the removal of histones may vary with the amount of ICP0 expressed, transcriptional activity remains approximately equal after ICP0-induced reactivation. This indicates that full histone removal is not essential for transcription from quiescent genomes to

occur. Additionally, it has been shown previously that expression of small amounts of ICP0 from AdS.11E4(ICP0) can activate gene expression from quiescent d109 without perturbing cellular gene expression, whereas expression of large amounts of ICP0 from d106 (from which d105 was derived) results in significant changes to the cellular expression pattern (96).

A possible explanation for this phenomenon lies in the multifunctional nature of ICP0, which has at least two distinct regions that are required for its full transcriptional activation function. The RING finger region is an E3 ubiquitin ligase, and is responsible for the degradation of multiple proteins, many of which are involved in the cellular antiviral response, as well as heterochromatin maintenance (25, 55, 151, 152) and the DNA damage response (133, 143, 188). When the RING finger is disrupted, this activity is lost. Thus, the enzymatic activity of the RING finger is essential for ICP0 function. However, a number of studies (21-23, 282), have shown that regions of the C-terminus of ICP0 are required for full activation of gene expression. When the C-terminus is truncated, the RING finger portion of ICP0 has a reduced ability to activate gene expression.

This phenotype may be explained, in part, by recent work demonstrating a region of the C-terminus of ICP0 responsible for disrupting the repressive complex formed by HDAC1/HDAC2/REST/CoREST/LSD1 (78, 80, 81, 83, 205). A region of ICP0 with homology to CoREST has the ability to physically disrupt and cause the translocation of the CoREST repressive complex. The ability of ICP0 to disrupt this complex may require relatively large amounts of ICP0 compared to its enzymatic function, and may explain the differences seen in removal of histones from quiescent genomes.

Abundant expression of ICP0 was also required for full hyperacetylation of histones H3 and H4. Upon d105 superinfection, the histones H3 and H4 remaining on the quiescent genome

were hyperacetylated. When ICP0 was provided by superinfection with AdS.11E4(ICP0), however, only the gC promoter shows a large increase in the hyperacetylation of remaining histone H3. Hyperacetylation of histone H4 was only prominent on the GFP gene after AdS.11E4(ICP0) superinfection. Taken together with the lack of significant histone removal when ICP0 is expressed at low levels, this lack of full hyperacetylation of histones supports the hypothesis that the physical disruption of the CoREST complex may require more abundant levels of ICP0, while the enzymatic functions of ICP0 occur even at low expression levels.

The results of these studies indicate that ICP0 expression is able to cause the disruption heterochromatin on quiescent HSV-1 genomes. The loss of HP1 γ and a higher order chromatin structure precedes reactivation of gene expression, while the decrease in the heterochromatin mark H3K9me3 occurs concurrently with detectable transcriptional activation. Additionally, large amounts of ICP0 were able to facilitate the removal of histones from quiescent virus, while small amounts were not, suggesting that ICP0 may exert its function through multiple mechanisms. It also demonstrates that full transcriptional activation does not require full histone removal. Lastly, hyperacetylation of histones temporally followed derepression of gene expression, suggesting that this is either a bystander effect of the other functions of ICP0, or acetylation of histones is a means by which the virus maintains a euchromatic state during reactivation.

4.0 FUNCTIONAL DOMAINS OF ICP0 INVOLVED IN REVERSAL OF EPIGENETIC SILENCING OF QUIESCENT HSV-1

4.1 ABSTRACT

ICP0 is a multifunctional transcriptional activating protein required for the efficient reactivation of latent HSV-1. Multiple regions of ICP0 play a role in its activity, the most prominent of which appears to be a RING finger motif, an E3 ubiquitin ligase domain responsible for the degradation of numerous proteins. Additional regions of ICP0 have been implicated in other functions, including the disruption of a cellular repressor complex with histone deacetylase and methylase activity (REST/CoREST/HDAC1/2/LSD1). We used quiescent infection of MRC-5 cells, followed by superinfection with various viral mutants of ICP0 to quantify the contributions of the RING finger (RF) and other activities to alter the chromatin structure and reactivate gene expression from quiescent d109. Superinfection of quiescently infected MRC5 cells with wild-type virus resulted in a 1000-fold increase in transcription from the HCMV promoter of d109, the removal of heterochromatin and histones, and an increase in histone marks associated with activated transcription (acetylation of histones and methylation of H3K4). An RF mutant was unable to reactivate transcription or remove heterochromatin from d109, while a mutant previously shown to be unable to interact with CoREST (R8507) was able to reactivate gene expression 100-fold from quiescent d109, and partially remove heterochromatin. However,

R8507 expression did not result in the acetylation of histones H3 and H4 or the methylation of histone H3K4. Additionally, the RF mutant and R8507 were unable to functionally complement one another, demonstrating that both regions must be on the same molecule for full ICP0 function. These results indicate that the RF is necessary and sufficient to reactivate transcription, but other activities, possibly the disruption of the CoREST repressor complex, is required for full reactivation of gene expression. This implies that ICP0 derepresses quiescent genomes and reactivates gene expression through interference with multiple cellular repression mechanisms.

4.2 INTRODUCTION

Lytic replication of herpes simplex type 1 (HSV-1) occurs in the epithelial cells, followed by viral infection of the sensory neurons enervating the site of initial infection. The viral capsid travels via retrograde transport to the nucleus, where the DNA becomes latent. Latency is characterized by circularization of the genome and an almost complete lack of gene expression, with the exception of the latency associated transcript. This global shutdown of transcription suggested that an epigenetic mechanism was involved in the silencing of HSV-1 during latency.

Since HSV-1 DNA is not extensively methylated (128), it is likely that chromatin structure helps to control transcriptional repression. Chromatin can epigenetically modulate gene expression on a number of levels. Histones can physically impede access of the transcriptional machinery to the DNA. Certain modifications of the histone tails can recruit repressive or a transcriptionally activating proteins to promoters. For example, the repressive chromatin mark trimethylation of histone H3 lysine 9 (H3K9me3) has been shown to form a binding site for, and recruit, heterochromatin protein 1 γ (HP1 γ).

Latent viral DNA was shown to be in a chromatin structure in mice (43) and in cell culture (110), and it has been previously seen in a cell culture model of quiescence that incoming viral DNA is chromatinized in the absence of viral immediate early (IE) genes (66). Specifically, it was seen that, in HEL cells, by four hours post infection (hpi), histones are deposited on the incoming genome, and these histones begin to acquire trimethylation of histone H3K9. By 24 hpi, HP1 γ becomes associated with viral promoters. This accumulation of heterochromatin is coincident with a decrease in gene expression, and helps to explain the global lack of gene expression during viral latency and quiescence.

Periodically, latent viral DNA can reactivate and cause recurrent disease at the initial site of infection. Reactivation stimuli include various forms of cellular stress (36, 38, 148, 197, 274) and diminished immune function (67). The immediate early protein ICP0 is required for efficient reactivation from latency *in vivo* (21-23, 85, 86, 113). ICP0 is a promiscuous transactivator of gene expression. ICP0 does not bind DNA, but mediates its functions through interactions with a large number of cellular proteins, including those involved in cell cycle regulation (44, 257), transcription (44, 115), the double-stranded break repair mechanism (108, 188), and the interferon response (41, 169)

Many of ICP0's functions are the result of degradation of cellular proteins through its RING finger domain (17, 48). The RING finger is a C3HC4 zinc binding region that coordinates two zinc ions and functions as an E3 ubiquitin ligase (7, 48, 52, 61). One of the major degradation targets of the RING finger domain are constituents of the ND10, or PML, bodies (25, 57). Incoming viral genomes localize next to ND10 bodies, which are upregulated by interferon (54, 245), and are thought to play a role in the intrinsic cellular antiviral response (50). ICP0 colocalizes with, and causes the degradation of, the major ND10 components promyelitic

leukemia (PML) and Sp100 proteins (79). The RING finger is also responsible for the degradation of the centromeric proteins CENP-A (152), CENP-B (151), and CENP-C (55). RING finger mutations that disrupt zinc binding eliminate the ability of ICP0 to degrade components of ND10 bodies, as well as other proteins, and eliminate the transcriptional activation function of ICP0.

ICP0 has also been shown to interact with histone deacetylases in a RING finger-independent manner. ICP0 interacts with, and causes the relocalization of, class II HDACs (153), and consequently inhibits their HDAC activity. The C-terminal amino acids 537-613 of ICP0 have homology to CoREST, and amino acids 669-718 are involved in binding to CoREST. This allows ICP0 to interact with and disrupt the REST/CoREST/HDAC1/2/ LSD1 repressor complex (78, 80, 81, 83), leading to the relocalization of components of the complex. When this region of ICP0 is mutated to abrogate CoREST binding, viral replication and degradation of PML is delayed, but not completely eliminated (83). Truncation mutants of ICP0 show similarly intermediate phenotypes, with truncation before or in the CoREST homology region showing partial loss of activation function and a loss of full ability to reactivate in explanted mouse ganglia (21).

Previously, we have shown that ICP0 expression is able to prevent the accumulation of histones, repressive histone modifications, and higher-order chromatin structure on the incoming viral genome, as well as cause the hyperacetylation of the few histones that do bind (66). In the current study, we have examined the ability of mutants in the RING finger and CoREST regions of ICP0 to reactivate gene expression from quiescent HSV-1. The chromatin structure of highly repressed, quiescent genomes before and after ICP0-mediated reactivation was characterized, and agrees with the previously published observations of ICP0 mutants. It was found that

disruption of the RING finger prevents ICP0's ability to remove heterochromatin from quiescent genomes, or to activate gene expression from genomes which have undergone various levels of repression. Disruption of CoREST binding resulted in a phenotype that was intermediate between ICP0-null viruses and wild-type ICP0. Thus partial transcriptional activation occurred, and heterochromatin was partially removed from the quiescent viral genomes upon provision of mutant ICP0 *in trans*. These results indicate that while the RING finger is absolutely necessary for ICP0 to cause the removal of heterochromatin and reactivation of transcription from epigenetically repressed quiescent genomes, the C-terminus is necessary for ICP0's full activity.

4.3 MATERIALS AND METHODS

4.3.1 Cells and viruses

Experiments were performed using MRC-5 (human embryonic lung) cells, Vero (African Green Monkey Kidney) cells, and U2OS (human osteosarcoma) cells, obtained from, and propagated as recommended by, American Type Culture Collection (ATCC). F11 cells were maintained as previously described (211). The viruses used in this study were the IE mutant d109 (211), wild-type HSV-1 (KOS), the ICP0-negative mutant n212 (23), the ICP0 RING finger point mutant (referred to as RF) (146), and the CoREST binding mutant R8507 (83) and control mutant R8508 (83). The RF virus (originally created by Saul Silverstein), the R8507, and R8508 viruses were a kind gift of Bernard Roizman. d109 was propagated on F06 cells as described (211), and all other viruses were propagated on U2OS cells to minimize differences between the viral stocks.

4.3.2 ChIP

ChIP was carried out as previously described (66, 213) with a few modifications. 5×10^6 MRC-5 cells were seeded in 100mm dishes, and were infected by d109 at an MOI of 10 at room temperature for 1 hour. After adsorption, the inoculum was removed and 37°C 5% DMEM was added. Infected cells were maintained at 37°C for 24 hours. At 24 hpi, the media was replaced with fresh media, and infected cells were maintained at 34°C. On day 4 post infection, media was again replaced with fresh media. At day 7 post infection, d109-infected cells were either mock superinfected, or superinfected with various mutants at an MOI of 10 PFU per cell for 1 hour at room temperature. After adsorption, the inoculum was aspirated and the conditioned media (which was saved and maintained at 37°C) was replaced. This was considered time 0 post superinfection. At 4 hpi, cells were treated with 1% formaldehyde for 10 minutes at 37°C, washed 3 times with cold phosphate-buffered saline (PBS) containing protease inhibitors (67 ng/ml aprotinin, 1 ng pepstatin, 0.16 mM TLCK [*N* α -ptosyl-L-lysine chloromethyl ketone], 1 mM phenylmethylsulfonyl fluoride [PMSF]), and scraped into PBS containing protease inhibitors. The cells were pelleted at 3,000 rpm for 10 minutes at 4°C and resuspended in cold SDS lysis buffer (100 μ l per million cells) containing protease inhibitors (1% SDS, 10mM EDTA, 50mM Tris-HCl [pH8.1], 4 μ g/ml aprotinin, 2 μ g/ml pepstatin, 0.15mM TLCK, and 0.6mM PMSF), and incubated on ice for 30 minutes. All other procedures were as described. The antibodies used were anti-histone H3 (Abcam, ab1791), anti-histone H4 (Millipore, 05-858), anti-acetyl histone H3 (Millipore, 06-599), anti-acetyl histone H4 (Millipore, 06-866), anti-trimethyl histone H3 lysine 9 (Millipore, 07-422), anti-dimethyl histon H3 lysine 4 (Millipore, 07-030) and anti-heterochromatin protein 1 γ (Millipore, 05-690). A “no-antibody control” was

included for each ChIP experiment and the value for the no-antibody control was subtracted from the immunoprecipitation results before the percent input of immunoprecipitation was calculated.

4.3.3 RNA isolation and reverse transcription

RNA was isolated with the Ambion RNaqueous -4PCR kit, following the included protocol. Briefly, 5×10^6 MRC-5 cells in 100mm plates were infected at an MOI of 10 by d109 for one week and superinfected as in the ChIP experiments. RNA was harvested at the indicated time points by adding 500 μ l Lysis/Binding Buffer. Cells were scraped and vortexed. An equal volume of 67% ethanol was added, and the solution was added to a filter, which was centrifuged at 12,500 RPM at 4°C for 1 minute. The bound RNA was washed with wash buffers 1 and 2/3. RNA was eluted with 60 μ l 65°C Elution Solution. The RNA was treated with DNase I at 37°C for 30 minutes to degrade any residual DNA.

Reverse transcription was performed using the Ambion reverse transcription kit and following the included instructions. 2 μ g total RNA was reverse transcribed in a reaction volume of 20 μ l containing RNase inhibitor, oligo(dT) primers, 1 μ l MMLV-RT and 2 μ l 10x reaction buffer. The reaction tube was incubated at 85°C for 3 minutes to remove RNA secondary structure, and the reverse transcription reaction was carried out for 1 hour at 44°C. After the reverse transcription reaction was complete, the reaction tube was incubated at 95°C for 10 minutes in order to inactivate the reverse transcriptase. 8 μ l of cDNA was diluted 1:8 by adding 40 μ l DNase/RNase free H₂O for use in qPCR reactions. Additionally, 1 μ g RNA was diluted into a total of 60 μ l DNase/RNase free H₂O for use as a negative control in qPCR reactions.

4.3.4 qPCR

Reactions for ChIP or cDNA quantification were performed in triplicate using 2.5 μ l of DNA for each reaction as described (213), with a few modifications. Before setting up the 96-well reaction plate, a master mix containing 0.3125 μ l of each primer (stock concentration, 1 mM), 6.25 μ l Applied Biosystems SYBR green super mix with 1.0 μ M 6-carboxy-X-rhodamine (Bio-Rad), and 3.125 μ l of water for a total of 10 μ l for each reaction was made. The final reaction volume was 12.5 μ l, including the DNA. The primers used for ChIP and cDNA quantification and their locations relative to the transcription start site of the gene to be analyzed are as previously published (66). d106 DNA was also included in each plate, in a standard curve of 1:10 dilutions from 250,000 to 25 copies per well, which covers the threshold cycle values for the ChIP DNA samples tested. qPCR was run on a StepOne Plus Real Time PCR machine. The conditions for the run were as follows: stage 1, 95°C for 10 min; and stage 2, 40 cycle repeats of 95°C for 15 seconds and 60°C for 1 min. At the end of the run, a dissociation curve was completed to determine the purity of the amplified products. Results were analyzed using the StepOne v2.1 software from Applied Biosystems.

4.4 RESULTS

4.4.1 Plaque-forming ability of ICP0 mutants

HSV-1 that does not express ICP0 displays a deficiency in plaque formation in non-complementing cells. The requirement for ICP0 is dispensed with in U2OS cells (278), which are likely to be missing a pathway or protein required for repression of incoming HSV-1 genomes (89). Additionally, L7 cells, which are Vero cells stably transfected with ICP0 (212), are able to complement ICP0-negative viruses and give true titers of infectious virus. We compared the ability of n212, RF, R8507, R8508, and KOS to form plaques on L7 cells, U2OS cells and Vero cells (Table 2).

Comparing L7 cell to Vero cell plaqueing ability can give a rough estimate of the defects caused by the various mutations in ICP0. n212, which is completely lacking ICP0 expression, showed approximately a 100-fold defect in plaque formation on Vero cells. KOS and R8508; which are wild-type ICP0, and mutated ICP0 showing no deficiency, respectively; plaqued at essentially the same efficiency on both Vero and L7 cells. RF, containing point mutations in the RING finger region that abrogate its function, had an approximately 30-fold plaque-forming defect on Vero cells, while R8507, which cannot bind CoREST, had a plaque-forming defect on Vero cells of slightly less than 3-fold. These results imply that while most of the function of ICP0 is contained in the RING finger region, that CoREST binding is important for part of ICP0's function.

Table 2. Comparison of plaque-forming ability in L7 and Vero cells.

Virus	L7 : Vero Ratio	Standard Error
n212	105.0	10.7
RF	28.5	4.1
R8507	2.7	0.4
R8508	1.1	0.1
KOS	1.2	0.1

4.4.2 RNA expression from quiescent genomes upon reactivation by ICP0 mutants

Much of the work concerning mutations in ICP0 has been focused on lytic infection. In order to determine how the RING finger and CoREST binding regions affect gene expression and chromatin structure upon reactivation from a highly repressed state, a quiescent cell culture model was employed. Previously, it was seen that MRC-5 cells were among the cell types that were most repressive to HSV-1 gene expression in the absence of ICP0 (246). Quiescence in MRC-5 cells was established with the viral mutant d109, which expresses no IE genes and contains a GFP reporter gene under control of the HCMV IE promoter (211). Cells were infected with d109, placed at 37°C for 24 hours, then moved to 34°C for 6 days. d109-infected cells were then either mock superinfected or superinfected with HSV-1 mutants lacking ICP0 (n212), the RING finger mutant (RF), a CoREST binding mutant (R8507), a control mutant with mutations in the CoREST binding region which do not affect CoREST binding (R8508), or wild-type KOS. Superinfected cells were placed at 37°C, and 4 hpi, before the onset of viral replication, RNA was harvested for analysis by RT-PCR (Figure 17A).

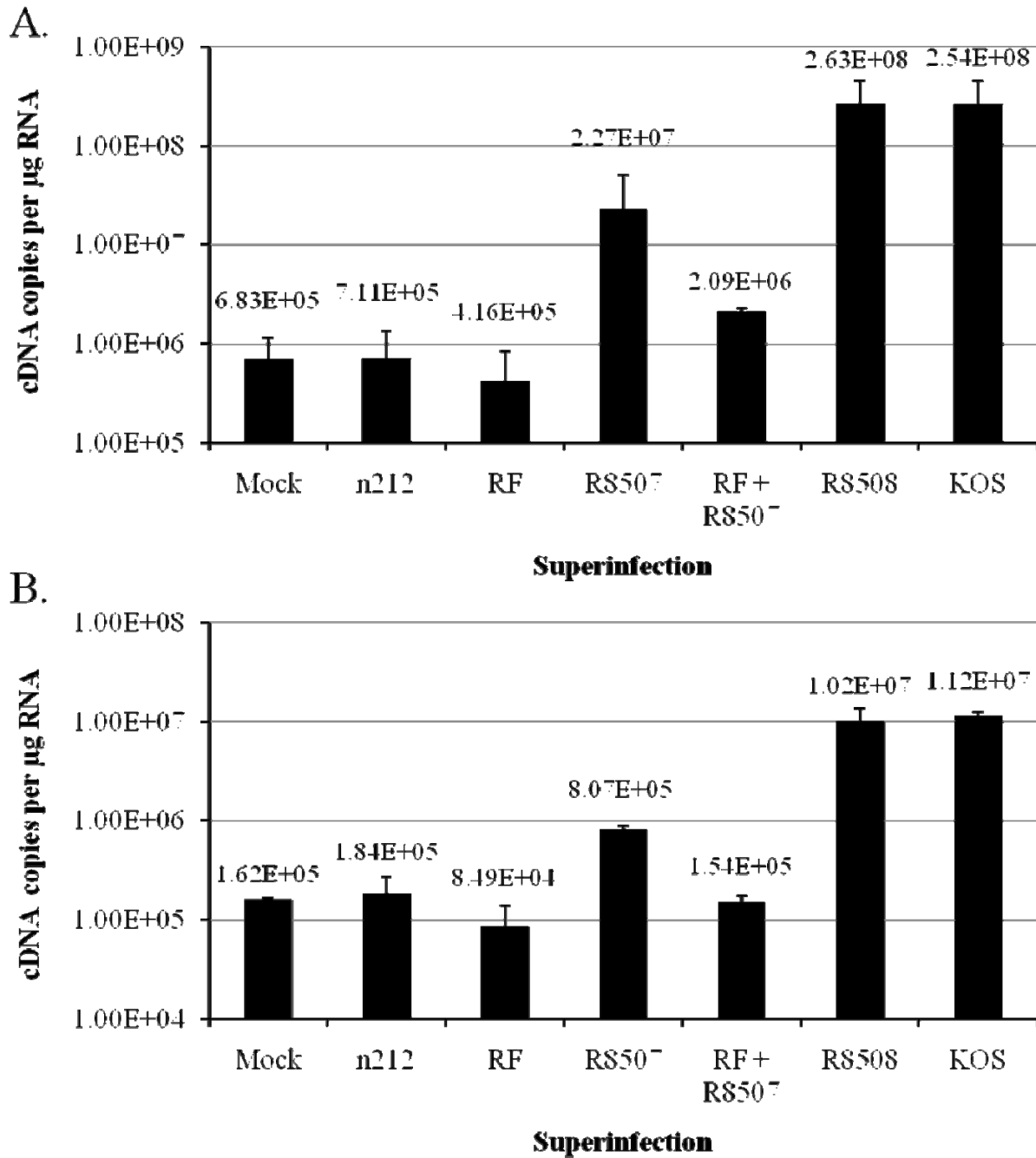


Figure 17. Abundance of GFP mRNA in d109-infected MRC-5 cells (A) or Vero cells (B) after superinfection.

Infections, RNA isolation, cDNA preparation, and RT-PCR were performed as described in Materials and Methods. Quiescent infection by d109 was established for 1 week. The graphs indicate the number of RNA molecules of GFP per μg RNA at 4 h p.i. after superinfection by the indicated virus.

One week after d109 infection, expression of GFP RNA reached a steady state level of approximately 5×10^5 copies per μg of total RNA. Superinfection with n212 caused no increase in RNA expression. This was also the case for RF, indicating that in the absence of a functional RING finger, the other domains of ICP0 are unable to activate gene expression from repressed viral genomes. In contrast, superinfection with R8508 or KOS led to a 1000-fold increase of GFP RNA. Superinfection with R8507 caused an intermediate amount of reactivation. ICP0 lacking CoREST binding activated expression from quiescent d109 by 2 orders of magnitude, but remained 10-fold lower than the reactivation of gene expression induced by wild-type ICP0. These results indicated that some of the ability of ICP0 to reactivate gene expression from highly repressed genomes was lost when CoREST binding was abrogated, but that the RING finger was absolutely required for any ICP0 function. This led us to test whether RF and R8507 could complement one another in *trans*. Somewhat surprisingly, the two ICP0 mutants were not able to efficiently complement one another in *trans*, indicating that both functions of ICP0 must reside on the same molecule for full reactivation of quiescent genomes.

Previously, it had been shown that Vero cells were less repressive to HSV-1 gene expression than MRC-5 cells (66, 246). In order to determine whether the RF or R8507 mutants were able to overcome a less repressive state, d109 quiescence was established for one week in Vero cells, followed by superinfection (Figure 17B). The steady state level of GFP RNA per μg total RNA appeared slightly lower in Vero cells than in MRC-5, but this was due to the lack of contact inhibition and overgrowth of cells in the week following infection with d109. While this fact made the quantitative change in gene expression appear less pronounced, the qualitative changes in gene expression induced by the various ICP0 mutants mimicked those seen in MRC-5 cells. n212 and RF did not increase the level of GFP RNA, while R8508 and KOS derepressed

quiescent d109 and allowed an increase in GFP RNA of 2 orders of magnitude. R8507 was able to partially activate GFP expression from repressed d109, increasing RNA levels 5-fold over mock infection, but this level of RNA was approximately 14-fold less than that induced by wild-type ICP0. The RF and R8507 mutants were again not able to complement each other.

Since it appeared that both Vero and MRC-5 cells had fully established repression of d109 by 7 days post infection, the ability of the various mutants to reactivate d109 GFP expression after d109 quiescence was established for one day was tested (Figure 18). In MRC-5 cells, the baseline level of GFP expression from d109 was approximately 10-fold greater at one day than at 7 days post infection (Figure 18A). Thus, it takes greater than 24 hours for MRC-5 cells to fully establish repression on quiescent genomes. However, the level of activation from wild-type ICP0 was similar to that seen when repression was fully established after 1 week. This indicates that even after full epigenetic repression of d109, wild-type ICP0 was able to completely remove barriers to gene expression. RF and R8507 showed similar phenotypes to the more highly repressed state, with RF being unable to reactivate gene expression, R8507 displaying a partial ability to reactivate GFP expression, and the mutants unable to complement one another.

Vero cells have not fully repressed d109 at 24 hpi (66). The baseline level of GFP expression was thus much higher – approximately 2 orders of magnitude – than in cells infected for 7 days (Figure 18B). Thus, it was difficult to discern changes in gene expression induced by ICP0, since full expression induced by wild-type ICP0 was only 10-fold greater than in the absence of ICP0. The qualitative findings remained the same, however. RF failed to activate GFP expression from d109, there was a slight increase in expression upon superinfection with R8507, and the two mutants failed to complement one another.

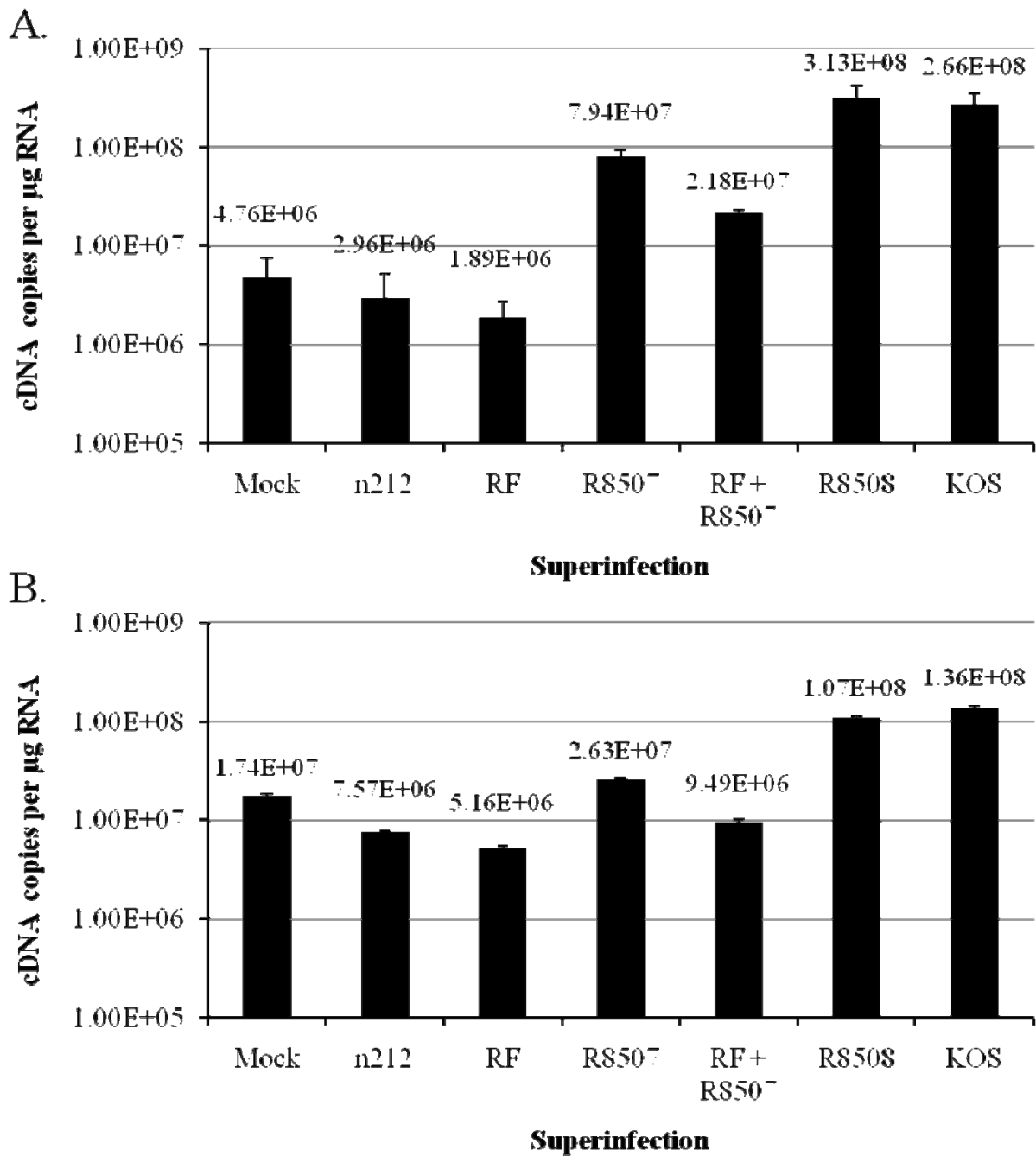


Figure 18. Abundance of GFP mRNA in d109-infected MRC-5 cells (A) or Vero cells (B) after superinfection.

Infections, RNA isolation, cDNA preparation, and RT-PCR were performed as described in Materials and Methods. Quiescent infection by d109 was established for 24 hours. The graphs indicate the number of RNA molecules of GFP per µg RNA at 4 h p.i. after superinfection by the indicated virus.

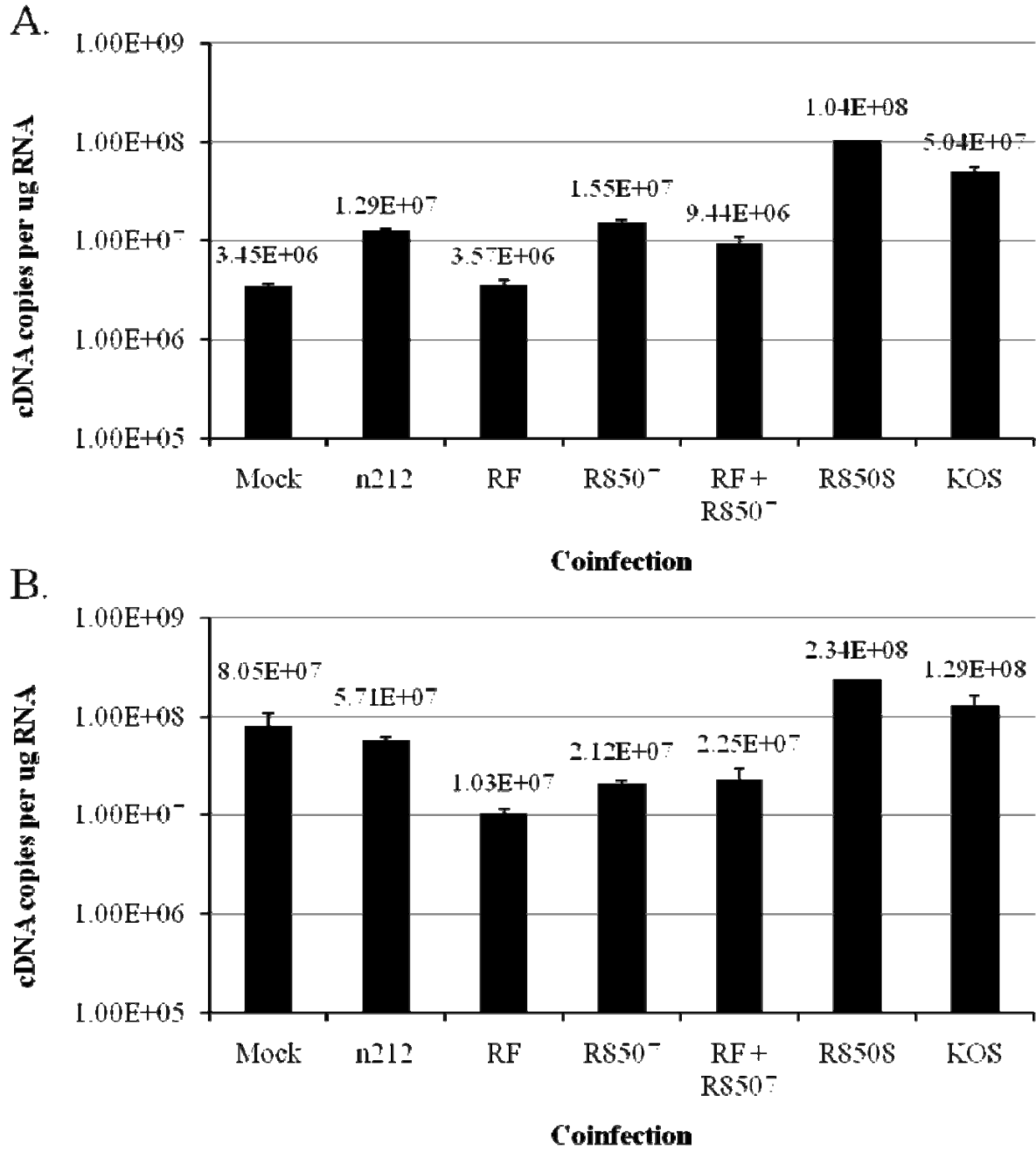


Figure 19. Abundance of GFP mRNA in d109-infected MRC-5 cells (A) or Vero cells (B) after superinfection.

Infections, RNA isolation, cDNA preparation, and RT-PCR were performed as described in Materials and Methods. The graphs indicate the number of RNA molecules of GFP per μg RNA at 4 h p.i. after coinfection by the indicated viruses.

Finally, in order to determine the effects on completely unrepressed genomes, the level of GFP expression induced by the various forms of ICP0 when coinfecting with d109 was established (Figure 19). In MRC-5 cells, coinfection with d109 and HSV-1 expressing wild-type ICP0 yielded a 330-fold increase in GFP RNA at 4 hpi as compared to infection with d109 alone (Figure 19A). RF did activate gene expression, and there was at best a small increase in GFP expression induced by coinfection with R8507. In Vero cells, where repression is delayed, there was only a 2-to-3-fold increase in GFP expression when d109 was coinfecting with HSV-1 expressing wild-type ICP0, and there was no increase in gene expression in the presence of any of the ICP0 mutants (Figure 19B). These results indicate that both the RING finger and CoREST binding regions of ICP0 are involved in derepression of quiescent virus, which is increasingly repressed, likely by chromatin structure, over time. Thus, we explored the ability of the various forms of ICP0 to affect the chromatin structure of highly repressed, quiescent d109 in MRC-5 cells.

4.4.3 Changes in chromatin structure of highly repressed quiescent d109 induced by ICP0 mutants

Previously it has been shown that ICP0 expression prevents the accumulation of higher-order chromatin structure, repressive histone modifications, and histones on viruses entering quiescence (66). In order to determine the effects of ICP0 mutants on the chromatin structure of quiescent virus, MRC-5 cells were infected with d109, and one week later, were either mock superinfected or superinfected with n212, RF, R8507, R8508, or KOS. 4hpi, ChIP was performed.

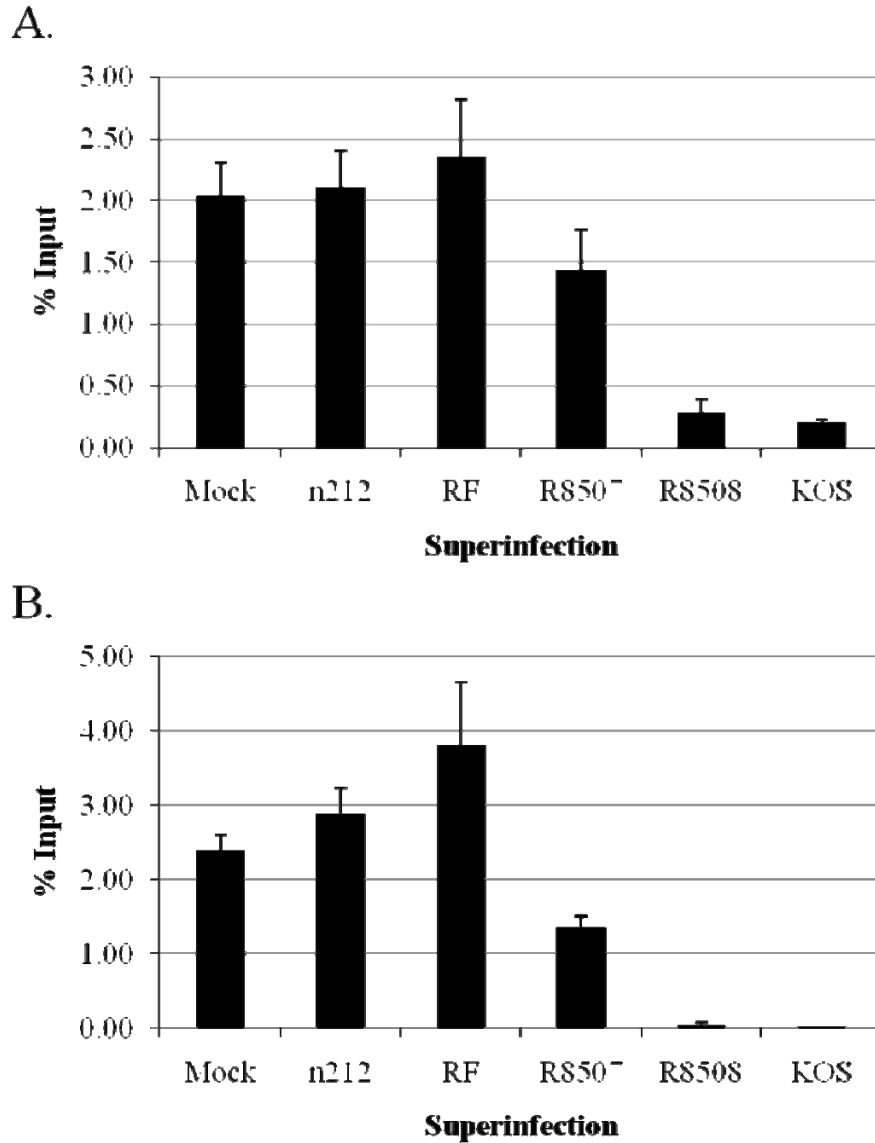


Figure 20. Repressive chromatin modifications associated with the HCMV promoter of d109 in MRC-5 cells after superinfection.

Quiescent infection by d109 was established for 1 week. Chromatin Immunoprecipitation (ChIP) with antibodies to HP1 γ (A) and H3K9me3 (B), and followed by RT-PCR were performed as described in the Materials and Methods. Graphs show the percentages of total genomes bound after superinfection with the indicated virus at 4 h post superinfection with the indicated virus. Error bars represent standard error of the mean from multiple experiments.

We first looked at the ability of the various mutants to remove HP1 γ (Figure 20A). In a previous study, after 24 hours in HEL cells, HP1 γ was found on approximately 0.7% of the viral

genomes (66). In contrast, by day 7 post-d109 infection, HP1 γ was bound to almost 2.5% of HCMV promoters. Superinfection with the ICP0-negative mutant n212, as well as the RF mutant, did not cause the removal of HP1 γ from quiescent d109 genomes. KOS and R8508 superinfection led to an almost complete removal of HP1 γ from d109, while R8507 superinfection resulted in an approximately 25% reduction of HP1 γ from the d109 genome. These results correlate with GFP expression.

Modification of histone tails are associated with changes in transcriptional permissiveness, and some of these modification allow for the recruitment of proteins involved in transcriptional activation or repression (112). Trimethylation of histone H3 lysine 9 (H3K9me3) is associated with repression and serves as a docking site for HP1 γ (201, 218). Using ChIP, the relative abilities of ICP0 mutants to cause the removal of this heterochromatin mark were assessed (Figure 20B). Superinfection with n212 or RF was not able to cause the removal of H3K9me3, and RF superinfection may in fact have resulted in a slight increase in H3K9me3 on the d109 HCMV promoter. R8507 superinfection resulted in an approximately 40% decrease in H3K9me3, while R8508 and KOS superinfection resulted in a complete loss of H3K9me3 from the d109 HCMV promoter.

ICP0 expression prevents histone H3 association with the viral genome during the entry into quiescence (66), and during lytic infection (29). The various ICP0 mutants were tested for their ability to remove histones H3 and H4 from the quiescent d109 genome (Figure 21). As in previous experiments, n212 and RF were not able to remove either histone H3 (Figure 21A) or H4 (Figure 21B). Similarly to H3K9me3, RF superinfection may have caused a slight increase in histone levels on the d109 HCMV promoter. Again, while KOS and R8508 superinfection

caused an almost complete reduction in histone levels on the d109 HCMV promoter, R8507 superinfection resulted in a partial reduction in histone H3 (~30%) and histone H4 (~55%).

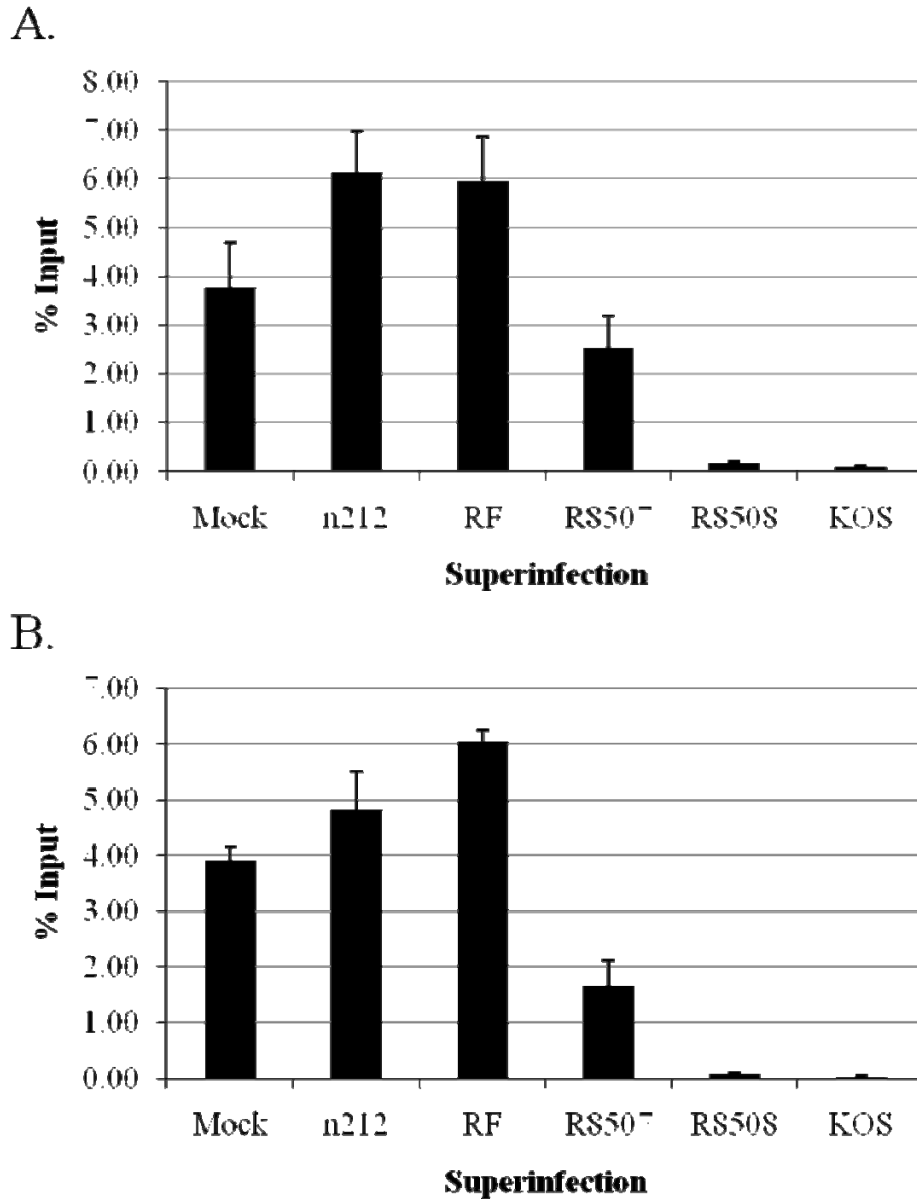


Figure 21. Binding of histones H3 and H4 to the HCMV promoter of d109 in MRC-5 cells after superinfection.

ChIP with antibodies to histones H3 and H4, and RT-PCR were performed as described in the legend to Figure 20 to determine the percentages of genomes bound by histones H3 (A) and H4 (B). Graphs show the percent of total genomes bound at 4 h post superinfection with the indicated virus. Error bars represent standard error of the mean from multiple experiments.

Since the R8507 mutant does not disrupt the REST/CoREST/HDAC1/2/LSD1 repressive complex, it was of interest to investigate the effects of the mutations in ICP0 on histone acetylation levels and histone H3 lysine 4 dimethylation. In order to account for the drastically different levels of histones on d109 after superinfection with each virus, levels of AcH3 (Figure 22A) and H3K4me2 (Figure 23) were normalized to total histone H3 (Figure 21A), and levels of AcH4 (Figure 22B) were normalized to total histone H4 (Figure 21B). Levels of AcH3 on quiescent d109 were extremely low, and superinfection with R8508 or KOS resulted in a 10-fold increase in hyperacetylation of histone H3 (Figure 22A). n212, RF, and R8507 superinfection did not result in an increase in hyperacetylation of histone H3. Essentially the same results were seen when hyperacetylation of histone H4 on the quiescent d109 genome was measured, although the quantitative changes differed slightly (Figure 22B). R8508 superinfection resulted in an approximately 75-fold increase in hyperacetylation of the d109 promoter, while KOS superinfection resulted in a 150-fold increase. RF and n212 superinfection led to no increase in H4 hyperacetylation, and there was at most a 4 fold increase of H4 hyperacetylation on the d109 HCMV promoter after R8507 superinfection.

Since LSD1 is a component of the CoREST repressor complex, and LSD1 is responsible for a removal of H3K4me2, levels of this mark of active transcription were also assayed by ChIP (Figure 23). Quiescent d109 genomes had undetectable levels of H3K4me2 on the HCMV promoter, and n212 did not affect the level of H3K4me2. RF and R8507 superinfection resulted in very little increase in the amount of bound histone H3 bearing this mark. R8508 superinfection resulted in a 2-to-3-fold increase in the levels of H3K4me2, while KOS superinfection increased the levels of histone H3 bearing H3K4me2 by 10-fold. The results from

ChIP are consistent with the RNA expression patterns seen upon superinfection with viruses providing mutant ICP0.

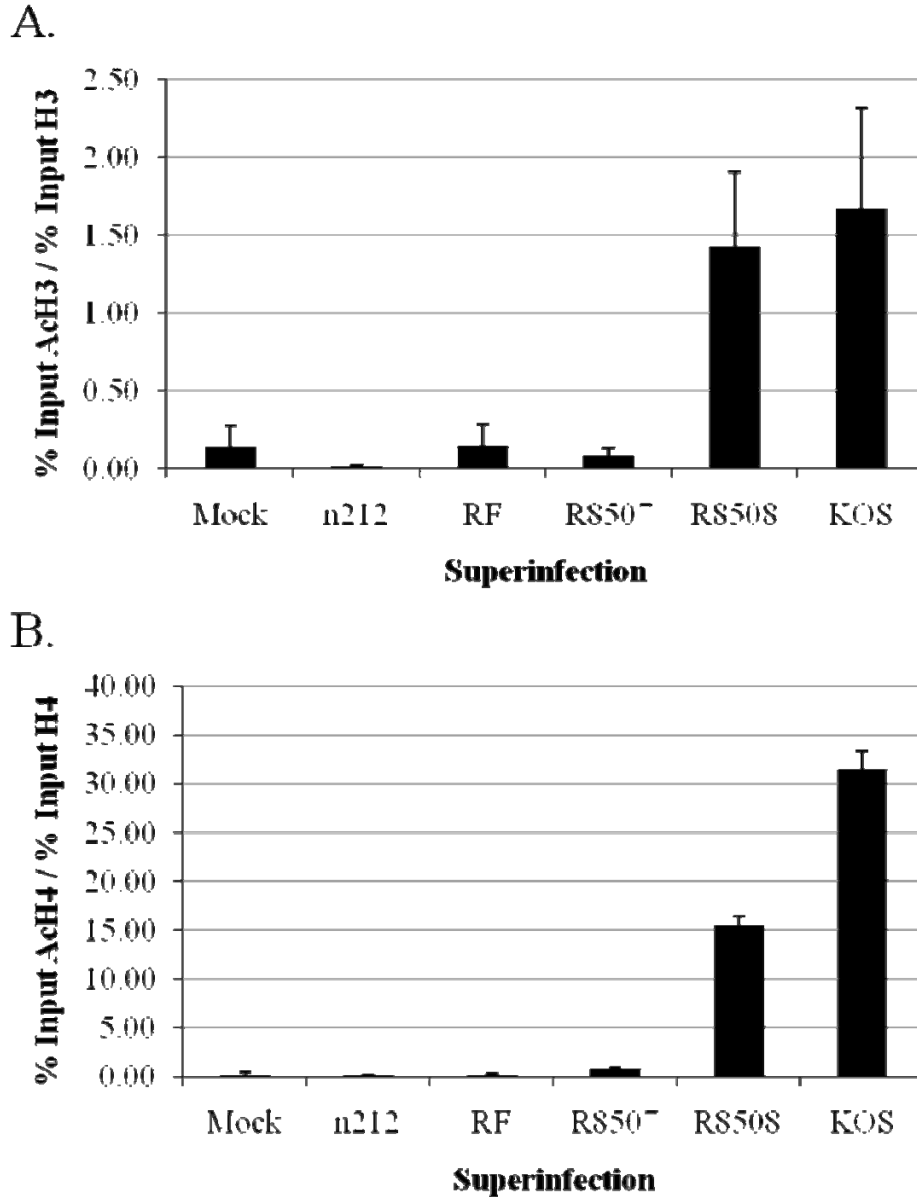


Figure 22. Binding of hyperacetylated histone H3 (AcH3) and hyperacetylated H4 (AcH4) to the HCMV promoter of d109 in MRC-5 cells after superinfection.

ChIP with an antibody to AcH3 (A) and AcH4 (B) and RT-PCR were performed as described in Figure 20 to determine the percentage of d109 genomes bound by AcH3 or AcH4 at 4 h post superinfection with the indicated virus. In order to compensate for the changing amounts of total histone H3 and H4, AcH3 was normalized to the amount of histone H3 (A) and AcH4 was normalized to the amount of histone H4 (B) on the genome by dividing the percent of acetylated histone by the percent of total histone (Figure 21). Error bars represent standard deviations from multiple experiments.

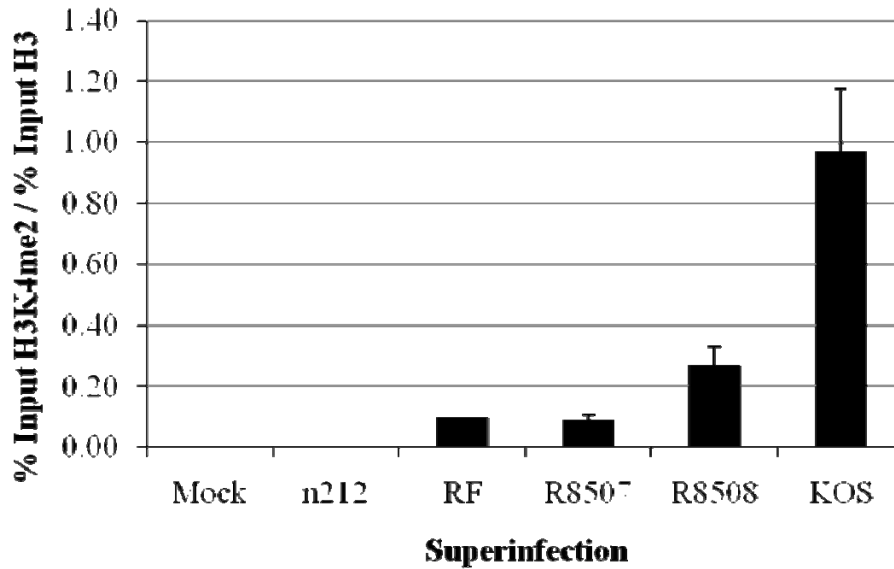


Figure 23. Binding of histone H3 dimethyl lysine 4 (H3K4me2) to the HCMV promoter of d109 in MRC-5 cells after superinfection.

ChIP with an antibody to H3K4me2 and RT-PCR were performed as described in Figure 20 to determine the percentage of d109 genomes bound by H3K4me2 at 4 h post superinfection with the indicated virus. In order to compensate for the changing amounts of total histone H3, H3K4me2 was normalized to the amount of histone H3 on the genome by dividing the percent of acetylated histone by the percent of total histone (Figure 21). Error bars represent standard deviations from multiple experiments.

4.5 DISCUSSION

ICP0 is multifunctional protein, with several seemingly distinct functional domains, each contributing to its overall effects. The E3 ubiquitinating ligase function of the ICP0 RING finger in exon 2 has been shown to cause the degradation of numerous proteins, the most relevant to this study being components of the ND10 bodies, including PML and Sp100 (25). Additionally, the C-terminus of ICP0 is required for its full function, and has been shown to interact with, and disrupt, the transcriptionally repressive complex REST/CoREST/HDAC1/2/LSD1 (78, 80, 81, 83). Through these, and possibly other, functions, ICP0 is able to prevent the accumulation of

heterochromatin on viruses entering quiescence (66). Since ICP0 is required for the efficient reactivation of quiescent HSV-1, it was of interest to determine the ability of various mutants of ICP0 to reactivate gene expression and cause changes in chromatin structure of highly repressed and chromatinized HSV-1. Both the ND10 bodies and the CoREST repressive complex are implicated in repression of transcription from HSV-1, and it is likely that this repression is mediated through an increase in heterochromatin on the quiescent genomes. We therefore used mutant viruses that were either lacking the RING finger activity, or the ability to disrupt the CoREST repressive complex, and compared their ability to alter chromatin to reactivate gene expression from the HCMV promoter on the GFP reporter gene found in quiescent d109 genomes.

Initially, expression of the GFP reporter gene was characterized in MRC-5 cells, one week after infection with d109. In the absence of superinfecting virus, the steady state-GFP level was approximately 10 copies per cell. 4 hours after superinfection with KOS or R8508, the level of GFP was 10^4 copies per cell. The ICP0-negative mutant n212 was not able to activate gene expression from quiescent d109, and the RING finger mutated virus RF was also unable to reactivate gene expression. R8507 was able to reactivate GFP expression to a level 10-fold lower than wild-type ICP0, but 100-fold higher than the level of GFP produced by quiescent d109 (Figure 17).

Since it has been previously shown that cell type and time-post-infection are important factors in epigenetic repression of HSV-1 (66), and since primary human fibroblast cells, such as MRC-5 cells, are the most repressive cell type to HSV-1 gene expression in the absence of ICP0 (246), Vero cells were also tested to determine if a less repressed state was more easily reactivated by the various mutants of ICP0 (Figure 18). Additionally, the ability of the ICP0

mutants to activate GFP expression from d109 under lower levels of epigenetic repression was tested by measuring induced gene expression 1 day post d109 infection (Figure 19). The quantitative results differed somewhat among the various conditions tested, however, the qualitative abilities of RF, R8507 and wild-type ICP0 to reactivate gene expression was consistent. In both Vero and MRC-5 cells, once quiescence was established, a functional RING finger was absolutely required to reactivate GFP expression. The ability to disrupt CoREST was not required for an increase in transcription, but was required for full activation of gene expression from quiescent viruses. These data show that in the absence of a functional RING finger, disruption of the CoREST repressor complex is not sufficient to reactivate transcription.

Additionally, in no circumstances was superinfection with both RF and R8507 able to activate transcription above the level induced by R8507. Thus, both functional domains must be on the same molecule in order to fully activate transcription. This may be a result of aberrantly localized ICP0, as the RING finger mutant cannot exit the ND10 bodies (83, 182), and R8507 is delayed in ICP0 translocation to the cytoplasm (83). Alternatively, the RING finger and CoREST binding region may need to occupy the same physical space simultaneously, and location on two separate molecules may prevent this.

At all levels of repression, wild-type ICP0 activated transcription to a similar extent. This indicates that wild-type ICP0 is able to fully remove chromatin structure and activate transcription, to levels previously seen for tk and gC during lytic wild-type infection 8h p.i. (66).

One interesting difference was seen when d109 was coinfecting with the ICP0-mutant viruses, which results in no time for epigenetic repression to be established before provision of ICP0. In both MRC-5 and Vero cells, neither RF, nor R8507 was able to significantly activate GFP expression (Figure 19). This points to a role for the CoREST binding region of ICP0 in

transcription during the lytic phase of the viral life-cycle that may differ from its role in reactivation from quiescence.

It has been established that quiescent virus can be found in a heterochromatic state, and is associated with higher-order chromatin proteins, such as HP1 α and HP1 γ (32, 66). In order to determine the relative ability of the ICP0 mutants to affect this structure in relation to their abilities to reactivate transcription, ChIP was performed. Superinfection with n212 or RF had no effect on the association of HP1 γ with the d109 genome, while KOS and R8508 superinfection caused an almost complete removal of HP1 γ (Figure 20A). R8507 superinfection resulted in a partial removal of HP1 γ from d109. The same pattern was seen for H3K9me3 (Figure 20B), a mark of repressive chromatin that serves as a binding site for HP1 γ .

ICP0 expression has been shown to prevent histone H3 association with the HSV-1 genome, both during lytic infection, and during the entry into quiescence (29, 66). The abilities of the various ICP0 mutants to cause the removal of histone H3 and histone H4 mimicked their abilities to remove heterochromatin, with n212 and RF unable to cause histone removal, R8508 and KOS superinfection resulting in almost complete removal, and R8507 causing an intermediate removal of histones (Figure 21).

The inability of the RING finger mutant to remove chromatin structure from d109 is consistent with its lack of transcriptional activation. The available evidence indicates that degradation of cellular proteins mediated by the RING finger is required before the action(s) of the ICP0 C-terminus are able to cause an increase in transcriptional activity. The RING finger is responsible for the degradation of the ND10 organizing proteins PML and Sp100. The ND10 bodies have been implicated in viral silencing (50), and there is a significant link between components of these bodies and epigenetic regulation of transcription. Members of the HP1

family are associated with Sp100, forming a link between ND10 bodies and chromatin. Both HP1 and the splice variant Sp100-HMG have the ability to act as transcriptional repressors when bound to a promoter (220). Additionally, ND10 components ATRX and hDaxx can also be found at heterochromatin, interact with one another, and are members of a repressive complex that has SWI/SNF chromatin remodeling activity (107, 243, 277). Depletion of PML, Sp100, ATRX, or hDaxx (62, 63, 155) can increase the transcription from ICP0-negative HSV-1 mutants, directly implicating disruption of ND10 bodies with changes in the chromatin state of quiescent viral genomes.

The intermediate phenotype of R8507 is also consistent with previous findings that show a decrease, but not complete elimination, of transcription from viral promoters due to various C-terminal truncations (21-23). Further evidence that ND10 bodies play an important role in the maintenance of heterochromatin on quiescent genomes is that R8507, which eventually causes the degradation of PML, is delayed for this activity (83). Additionally, the ICP0 mutants D13 and D14, which contain deletions of the amino acids 633-680 and 680-720, respectively, are impaired in ND10 localization (160). These deletions overlap the portion of ICPO required to bind CoREST, which falls between amino acids 668-718 of ICPO. The amino acid substitutions of R8507 are D671A/E673A, further implicating the region between amino acids 633 and 720 in partially increased transcription, as well as an intermediate decrease in heterochromatin.

Since R8507 is deficient in disruption of the CoREST repressor complex, it follows that this would lead to a decrease in acetylated histones by the HDAC1/2 portion of this complex, as well as a decrease in H3K4me₂, a mark of active transcription that is removed by LSD1. By ChIP, it was found that the histone H3 remaining bound to the d109 genome was hypoacetylated, and that n212, RF, and R8507 were unable to cause acetylation of histone H3 bound to d109

(Figure 22A). In contrast, there was a greater than 10-fold increase in hyperacetylation of d109-bound histones after KOS superinfection. The hyperacetylation of histone H4 followed a somewhat similar pattern: RF and n212 superinfection failed to induce histone H4 acetylation, in this case R8507 superinfection upregulated AcH4 very slightly (approximately 4-fold), while KOS superinfection caused a 150-fold increase in acetylation of the histones bound to d109 (Figure 22B).

There is a small increase in the dimethylation of d109-bound histone H3K4 after superinfection with both RF and R8507, as compared to superinfection with n212, whereas KOS superinfection leads to an approximately 10-fold upregulation in H3K4me2 over RF and R8507 (Figure 23). R8508 superinfection caused large, but not wild-type level increases in hyperacetylation of both histone H3 and H4, and a small increase in H3K4me2, suggesting that although the mutations in the CoREST binding region do not impair CoREST repressor disruption or transcription in cell culture, there may be other, more subtle, effects on its function.

The inability of R8507, with a functional RING finger, to cause a significant increase in hyperacetylation of histones is consistent with an important, but not required role for the disruption of the CoREST repressor complex in derepression of quiescent genomes. It may be that once heterochromatin is removed from the genome, that hyperacetylation of histones and H3K4 dimethylation are important in maintaining a euchromatic state.

Our results add to the hypothesis that the ND10 bodies are linked to the chromatin compartment through multiple protein interactions, and that ICP0 targets the ND10 bodies as a mechanism to remove heterochromatin, both in lytic infection and during the reactivation from latency. Additionally, this study confirms a function for the disruption of the REST/CoREST/HDAC1/2/LSD1 repressor complex, and suggests that there may be more

functions associated with the C-terminal region of ICP0. The RF is necessary and sufficient for reactivation of quiescent genomes, but for full removal of heterochromatin, increase in euchromatin, and activation of transcription, the disruption of the CoREST repressor is required. Previously, it was seen that in the absence of ICP0, quiescent genomes were impaired in rescue by reactivation or recombination with replicating HSV-1, and that this effect was amplified when quiescence was established for three days. Additionally, as time progressed after d109 infection, the ability of the HDAC inhibitor TSA to reactivate GFP expression gradually decreased (246). These observations, along with the results of the current study, support a model in which quiescent HSV-1 is increasingly heterochromatinized as time progresses, that this higher-order chromatin structure prevents access to the genome by transcription factors and proteins involved in viral replication, that expression of ICP0 causes the removal of heterochromatin from the viral genome through the action of the RING finger, and that ICP0 maintains a euchromatic state on the genome by interfering with multiple cellular pathways, thus allowing a generalized increase of viral transcription.

5.0 SUMMARY AND GENERAL DISCUSSION

5.1 SUMMARY OF RESULTS

ICP0 is a promiscuous transactivator of gene expression, which mediates its effects through indirect mechanisms. As such, study of this molecule gives insight into cellular pathways targeted by Herpes Simplex Virus Type 1 (HSV-1) to increase its gene expression and counteract the host response to incoming viral genomes. The study presented here models the effects of chromatin structure on viral gene expression, both during the entry into quiescence, and during reactivation from a repressed state. Additionally, the effects of cell type and ICP0 expression on viral chromatin structure were determined.

A cell culture model of quiescence modeling aspects of *in vivo* latency was used to probe the effects of cell type and ICP0 expression on the entry of HSV-1 into quiescence (66). It has been shown that, in the absence of ICP0, HEL cells are among the most repressive to viral gene expression, while Vero cells are able to repress viral gene expression to an intermediate extent (246). Either HEL or Vero cells were infected with the viral mutants d109 or d106, followed by analysis of gene expression and chromatin structure. The viral mutant d109 lacks all 5 immediate early (IE) genes. It expresses a GFP reporter under control of the HCMV promoter. d109 is non-toxic to cells and can establish long-term quiescent infection in cell culture. Gene

expression from d109 can be reactivated by provision of ICP0 in *trans*. d106 expresses the GFP transgene, as well as ICP0, but is deleted for the other 4 IE genes (211).

Real Time PCR was used to characterize gene expression from the model promoters HCMV, an extremely strong promoter; tk, an early (E) gene; and gC, a late (L) gene. For all three genes and in both cell types, d109 expression decreased over time, indicating an increasing repression of viral gene expression. In d106 infection, GFP and tk expression increased over time, while gC expression decreased. In all cases, expression in the presence of ICP0 (d106) was greater than in the absence of ICP0 (d109). Additionally, expression was generally greater in Vero cells than in HEL cells.

Since HSV-1 DNA is not extensively methylated, and viral gene expression is globally repressed during latency, it has been hypothesized that gene expression is controlled by chromatin structure (128). We therefore explored the chromatin structure of d109 and d106 in Vero and HEL cells by micrococcal nuclease digestion and chromatin immunoprecipitation (ChIP).

Although nucleosomes can be found on latent HSV-1 genomes (110), the presence of nucleosomes has not been established during productive HSV-1 infection (95, 96, 117, 136, 172). In order to determine the nucleosomal association with viruses entering quiescence, micrococcal nuclease digestion was employed. The pattern of digestion suggested that while some of the genomes may have been contained in a nucleosomal structure, most of the genomes were irregularly associated with chromatin and, at early times post infection, many viral genomes entering quiescence did not have a fully established chromatin structure.

To determine the association of histones with HSV genomes in a more direct manner, ChIP was employed. It was seen that histone H3 was found on d109 in both cell types and

increased over time, and that ICP0 expression from d106 reduced histone association and prevented it from increasing. The amount of gene expression did not correlate to the association of histone H3, indicating that histone H3 was not simply being removed as a consequence of transcription. Additionally, the histones that were bound to the d106 genome were hyperacetylated, which is a mark of active transcription.

In order to characterize the increase in heterochromatin over time, which correlated with a decrease in transcription, the amounts of repressive chromatin mark histone H3 trimethyl lysine 9 (H3K9me3), and heterochromatin protein 1 γ (HP1 γ) were measured by ChIP. ICP0 expression caused a large decrease in the amount of both H3K9me3 and HP1 γ in both cell types examined, while d109 was increasingly associated with both marks of repressive chromatin in HEL cells. In Vero cells, only the gC promoter of d109 acquired significant HP1 γ association. This correlated with the gene expression data, and the greater ability of d109 to express the GFP transgene in Vero cells than in HEL cells.

The study of chromatin structure and gene expression upon entry into quiescence demonstrated that the level and kinetics of epigenetic repression vary by cell type, and that ICP0 has numerous functions in addition to increasing the acetylation of histones. It may act as a central epigenetic switch early in infection in determining chromatin structure of the virus. Expression of ICP0 prevented HP1 γ association with the virus in both cell types on all promoters. It may do this by increasing acetylation of histones, specifically on H3K9, thus decreasing H3K9me3 and preventing HP1 γ association. ICP0 expression also prevented histone H3 association with the virus. This is a function not previously ascribed to ICP0 and may reflect interference with histone chaperones. After the removal of chromatin, the level of gene expression is dependent on promoter strength.

In order to determine the effects of ICP0 expression on previously established heterochromatin, d109 was allowed to establish quiescence in MRC-5 cells which, like HEL cells, are primary human fibroblasts that are highly repressive to HSV-1 gene expression in the absence of ICP0. One week after d109 infection, ICP0 was expressed *in trans* by superinfection to reactivate gene expression. ICP0 was provided either by d105, which, like d106, overexpresses ICP0, but does not contain the GFP transgene, or by an adenovirus, Ad.S11E4(ICP0), expressing ICP0 at levels similar to those during the first several hours of wild-type infection.

By 2 hours after superinfection with d105, the level of GFP expression from d109 was increased approximately 10-fold, and by 24 hours post-d105 infection, the level of GFP was 3 orders of magnitude greater than mock-superinfected cells. Ad.S11E4(ICP0) superinfection also increased the level of GFP RNA by approximately 1000-fold over superinfection with empty vector, indicating that even a small amount of ICP0 can fully reactivate gene expression from quiescent genomes, and that no other HSV-1 proteins are required for reactivation of gene expression. Additionally, ICP0 expression from Ad.S11E4(ICP0) resulted in large increases of gene expression from the model E and L genes tk and gC, indicating that the effect of ICP0 is general across the viral genome, and not specifically linked to the HCMV promoter.

Utilizing ChIP to determine the chromatin structure of quiescent d109 upon d105-mediated reactivation, it was seen that heterochromatin was removed upon ICP0 expression, and that the removal of HP1 γ and H3K9me3 was coincident with the induction of gene expression. By using Ad.S11E4(ICP0), it was also determined that expression of small amounts of ICP0 resulted in the removal of heterochromatin from quiescent d109, and that this effect was general across the viral genome.

Since ICP0 expression resulted in a decrease in histone H3 association with HSV-1 genomes entering quiescence (66), the effects of ICP0 expression on histone H3 and H4 association with quiescent d109 were quantified by ChIP. As with heterochromatin, upon d105 superinfection, both histones H3 and H4 are removed from the quiescent d109 HCMV promoter. Micrococcal nuclease digestion was used to further visualize the effects of ICP0 expression on quiescent d109 chromatin structure. The GFP gene of quiescent d109 genomes was highly resistant to micrococcal nuclease digestion, indicating that quiescent genomes were in a chromatin structure that was less accessible to the enzyme than general cellular DNA. This was consistent with the ChIP data indicating a highly heterochromatinized state of d109. Superinfection with d105 resulted in a chromatin structure of the d109 GFP gene that was rapidly degraded by micrococcal nuclease, and may have been even more susceptible to degradation than the general cellular DNA. These results were complementary to the ChIP data, demonstrating that ICP0 expression results in removal of chromatin from quiescent HSV-1 genomes.

Interestingly, Ad.S11E4(ICP0) expression of small amounts of ICP0 did not result in the removal of histone H3 from the d109 genome, and histone H4 was removed only to a small extent. This is consistent with a previous report that characterized the effects of an adenovirus expressed ICP0 on histone H3 association (32). Although Ad.S11E4(ICP0) expression of ICP0 did not result in histone H3 removal from quiescent d109, GFP expression was equivalent to that induced by d105 superinfection. This indicates that histone removal is not absolutely required for reactivation of gene expression.

Both d105 and Ad.S11E4(ICP0) superinfection resulted in a small increase in the acetylation of remaining histones on d109. However, after d105 superinfection, acetylation of

histones followed derepression of gene expression, suggesting that this is either a bystander effect of ICP0 on chromatin structure, or that acetylation of histones is a means by which the virus maintains a euchromatic state during reactivation.

In order to further investigate the effects of ICP0 on quiescent HSV-1 chromatin structure, and to delve further into the mechanism by which these effects are mediated, a series of superinfections with HSV-1 carrying mutations in ICP0 was carried out, and changes in gene expression and chromatin structure were characterized with RT-PCR and ChIP. ICP0 is a RING finger E3 ubiquitin ligase, with the RING finger domain found in exon 2 (7, 48, 52, 61). A number of proteins are degraded in a RING finger- and proteasome-dependent manner upon expression of ICP0, among which are major constituents of ND10 bodies PML and Sp100 (79) and centromeric structural proteins (55, 151, 152). ICP0 also interacts with and inhibits the activity of some class II histone deacetylases in a RING finger-independent manner (153). The C-terminus of ICP0 has also been shown to disrupt the repressive complex REST/CoREST/HDAC1/2/LSD1 (78, 80, 81, 83), leading to relocalization of some constituents of the complex.

The viral mutants n212 (does not express ICP0) (23), RF (RING finger function is disrupted) (146), R8507 (disruption of CoREST repressor complex abrogated) (83), R8508 (silent mutations in the CoREST binding region) (83) and the wild-type virus KOS were used to superinfect MRC-5 cells harboring quiescent d109, and test the effects of mutations in ICP0 on its ability to reactivate GFP expression and alter quiescent viral chromatin structure. Neither n212, nor RF were able to reactivate GFP gene expression from quiescent d109, while both R8508 and KOS reactivated gene expression by approximately 1000-fold. R8507 reactivated GFP expression an intermediate amount, 100-fold. RF and R8507 coinfection were unable to

complement each other. This pattern of reactivation ability was seen in multiple levels of epigenetic repression induced by different lengths of establishment of d109 quiescence in different cell types.

The ability of these ICP0 mutants to alter the chromatin structure of quiescent d109 was also characterized. Neither n212, nor RF superinfection was able to cause removal of heterochromatin from the d109 HCMV promoter, as measured by HP1 γ and H3K9me3 association. RF and n212 superinfection also did not result in the removal of histone H3 or H4. Both R8508 and KOS were able to cause the removal of heterochromatin and histones, while R8507 superinfection caused a partial removal of HP1 γ , H3K9me3, histone H3, and histone H4. These results are consistent with the gene expression data.

Since R8507 is responsible for the disruption of the CoREST repressor complex, we also measured the ability of the various HSV-1 mutants to cause the hyperacetylation of histones and an increase in H3K4me2, a mark of active transcription that can be removed by LSD1 (224). As expected, neither n212 nor RF superinfection resulted in hyperacetylation of histones, while both R8508 and KOS superinfections increased the acetylation of both histone H3 and H4. Interestingly, R8507 superinfection did not result in hyperacetylation of histone H3, and only slight hyperacetylation of histone H4. Additionally, superinfection with RF or R8507 yielded only slight increases of H3K4me2 on d109, while KOS superinfection resulted in a large increase in H3K4me2. This is consistent with an active CoREST repressor complex functioning during R8507 infection, and a need for the RING finger and C-terminus of ICP0 to work in tandem for full ICP0 activity.

The results of these studies point to multiple roles for ICP0 in increasing gene expression. ICP0 expression results in a decrease in chromatin association on incoming genomes entering

quiescence, as well as a removal of previously established chromatin structure on quiescent genomes. Additionally, expression of ICP0 results in the increase of marks of active transcription on the viral genome. These functions appear to intersect in removal of repression introduced by the cellular response to incoming viral DNA.

5.2 ICP0 ACTS AT THE INTERSECTION OF INTERFERON, CHROMATIN, CELL-CYCLE, AND DNA DAMAGE RESPONSE PATHWAYS

ICP0 is required for efficient reactivation from latency (86). Additionally, in a transgenic mouse model, stressors that are known to cause HSV-1 reactivation, such as UV irradiation and hyperthermic stress, were shown to upregulate transcription from the ICP0 promoter (148). It has been hypothesized that VP-16, which activates IE gene expression, coordinates the exit from latency (248). Even if ICP0 expression is not the trigger for reactivation, it would still be the case that the activity of ICP0 is essential for removal of viral chromatin structure, allowing access to viral promoters, efficient reactivation of viral gene expression, and the production of progeny virus. The study of ICP0 gives insight into multiple pathways that cells use to control gene expression, including the interferon response, chromatin control of gene expression, cellular antiviral mechanisms, and DNA break response pathways.

In this study, we have used a cell culture model of quiescence to demonstrate the importance of cell type and ICP0 expression in the epigenetic control of gene transcription during HSV-1 latency. During the entry into quiescence, ICP0 may act as an epigenetic switch, allowing lytic replication to proceed in cells in which ICP0 is expressed, and allowing viral genomes to be heterochromatinized in cells in which ICP0 expression is repressed. Upon

reactivation from quiescence, expression of ICP0 is able to cause the removal of heterochromatin. While this function is largely dependent on the ability of the RING finger domain of ICP0 to mediate the degradation of a number of proteins, the C-terminal region, and the disruption of the CoREST/REST/HDAC1/2/LSD1 repressor complex are required for its full activity.

These studies imply that ICP0 expression disrupts repression of viral transcription. This activity occurs through multiple functional domains of ICP0. The RING finger domain is an E3 ubiquitin ligase which causes the degradation of a number of proteins, including two that are critical for organizing the ND10 bodies: Sp100 and PML (248). ND10 bodies are thought to be part of the innate cellular response to viral DNA (50), and incoming HSV-1 DNA localizes adjacent to ND10 bodies (59, 64, 105, 161). Several proteins responsible for formation of repressive chromatin are found in ND10 bodies, including HP1 γ , ATRX, and hDaxx. HP1 γ binds to the repressive chromatin mark H3K9me₃, has been shown to repress transcription and helps to form higher-order chromatin structure (149). ATRX and hDaxx are members of a repressive complex that has SWI/SNF chromatin remodeling activity and can be found associated with heterochromatin (107, 243, 277). Thus, the removal of heterochromatin structure shown in ChIP assays and micrococcal nuclease digestion is most likely due to the degradation of a number of proteins by the RING finger of ICP0.

ICP0 expression has also been shown to cause the acetylation of histones associated with viral genomes (29, 32, 66). This may be an effect due to disruption of repressive complexes containing HDACs, rather than actively increasing acetylation. By disrupting HDAC-containing complexes, ICP0 is preventing repression by abrogating the removal of acetylation from histones. ICP0 interacts with, and causes the redistribution of, class II HDACs (153). ICP0 also

interacts with, and causes the disruption of the HDAC-containing repressor complex REST/CoREST/HDAC1/2/LSD1 (78, 80, 81, 83). When point mutations in the CoREST binding region (R8507) render ICP0 unable to disrupt this complex, hyperacetylation of histones on quiescent genomes was not observed. Thus, the changes in chromatin induced by ICP0 expression are likely the result of multiple interactions through several functional domains of ICP0, as well as the degradation of multiple proteins.

While it appears that ICP0 is primarily involved in preventing or removing epigenetic repression of viral gene expression, it may also have an active role in increasing gene expression. In some cell types, ICP0 has been shown to degrade the catalytic subunit of DNAPK, DNAPKcs (133, 188). DNAPKcs is a repressor of the activity of GCN5, which is a histone acetyltransferase (6). Thus, degradation of DNAPKcs may be a means by which ICP0 further increases gene expression through epigenetic mechanisms. This possibility, and the mechanisms by which ICP0 exerts its effects, require additional study.

The effect of ICP0 on chromatin structure is intimately linked with its other functions. Viruses lacking ICP0 are hypersensitive to interferon (91, 169), and the mutants RF and R8507 have also been shown to exhibit this phenotype (83). ICP0 blocks the action of interferon through multiple mechanisms, including preventing the upregulation of interferon stimulated genes through IRF3 and IRF7 signaling (144, 165, 166). Interferon has been shown to upregulate the components of ND10 bodies (54, 244, 245), which ICP0 also targets for degradation and dispersal, and are crucial to the shutdown of viral gene expression (62, 63, 65, 160, 161). Additionally, the CoREST repressor complex targeted by the C-terminus of ICP0 localizes adjacent to ND10 (80), as do incoming viral genomes.

ICP0 also causes the degradation of the centromeric proteins CENP-A (152), CENP-B (151), and CENP-C (55). This may be an important aspect of ICP0 function, or it may be a tangential effect caused by the destruction of ND10 bodies. HP1, which is removed from viral genomes upon ICP0 expression, as well as ATRX and hDaxx, which are constituents of ND10, localize both to ND10 bodies and the centromeres (56), linking destruction of centromeric proteins by ICP0 with the destruction of ND10 bodies.

ICP0 also has been shown to inhibit the circularization of viral genomes (108), and interferes with the DNA break repair pathway by degrading the H2A ubiquitinating ligases RNF8 and RNF 168 and interfering with the localization of DNA repair proteins (143). Additionally, DNA repair proteins are recruited to viral replication compartments (50). The cellular protein p53 senses multiple types of DNA damage (145), is at the hub of the DNA damage response and acts as a checkpoint protein that can cause cell cycle arrest . ICP0 interacts with, and ubiquitinates, p53, although it does not cause large scale degradation of p53 (15). ICP0 expression results in cell cycle arrest at both the G1/S and G2/M checkpoints, and upregulation of the p53 responsive genes p21, mdm2, and gadd45 in both a p53-dependent and p53-independent manner (97). ICP0 also interacts with and stabilizes cyclin D3 (116), and causes it to localize in the vicinity of ND10 bodies (257), further contributing to the effects of ICP0 on the cell cycle.

These findings, together with the results of the current study, demonstrate the complexity of cellular pathways leading to the chromatinization of incoming viral genomes. As a multifunctional protein with numerous interaction domains, as well as enzymatic function, ICP0 is able to perturb cellular metabolism in a number of ways that results in the removal of chromatin from the viral genome. Further study of the mechanisms of ICP0 action, as well as

the cellular response to incoming viral genomes, will yield greater understanding of the intersection of transcriptional regulation with numerous cellular pathways.

BIBLIOGRAPHY

1. **Amelio, A. L., N. V. Giordani, N. J. Kubat, E. O'Neil J, and D. C. Bloom.** 2006. Deacetylation of the herpes simplex virus type 1 latency-associated transcript (LAT) enhancer and a decrease in LAT abundance precede an increase in ICP0 transcriptional permissiveness at early times postexplant. *J Virol* **80**:2063-8.
2. **Amelio, A. L., P. K. McAnany, and D. C. Bloom.** 2006. A chromatin insulator-like element in the herpes simplex virus type 1 latency-associated transcript region binds CCCTC-binding factor and displays enhancer-blocking and silencing activities. *J Virol* **80**:2358-68.
3. **Aranda-Anzaldo, A.** 1992. Altered chromatin higher-order structure in cells infected by herpes simplex virus type 1. *Arch Virol* **124**:245-53.
4. **Arthur, J. L., C. G. Scarpini, V. Connor, R. H. Lachmann, A. M. Tolkovsky, and S. Efstathiou.** 2001. Herpes simplex virus type 1 promoter activity during latency establishment, maintenance, and reactivation in primary dorsal root neurons in vitro. *J Virol* **75**:3885-95.
5. **Bannister, A. J., P. Zegerman, J. F. Partridge, E. A. Miska, J. O. Thomas, R. C. Allshire, and T. Kouzarides.** 2001. Selective recognition of methylated lysine 9 on histone H3 by the HP1 chromo domain. *Nature* **410**:120-4.
6. **Barlev, N. A., V. Poltoratsky, T. Owen-Hughes, C. Ying, L. Liu, J. L. Workman, and S. L. Berger.** 1998. Repression of GCN5 histone acetyltransferase activity via bromodomain-mediated binding and phosphorylation by the Ku-DNA-dependent protein kinase complex. *Mol Cell Biol* **18**:1349-58.
7. **Barlow, P. N., B. Luisi, A. Milner, M. Elliott, and R. Everett.** 1994. Structure of the C3HC4 domain by 1H-nuclear magnetic resonance spectroscopy. A new structural class of zinc-finger. *J Mol Biol* **237**:201-11.
8. **Barski, A., S. Cuddapah, K. Cui, T. Y. Roh, D. E. Schones, Z. Wang, G. Wei, I. Chepelev, and K. Zhao.** 2007. High-resolution profiling of histone methylations in the human genome. *Cell* **129**:823-37.

9. **Barton, E. S., D. W. White, J. S. Cathelyn, K. A. Brett-McClellan, M. Engle, M. S. Diamond, V. L. Miller, and H. W. t. Virgin.** 2007. Herpesvirus latency confers symbiotic protection from bacterial infection. *Nature* **447**:326-9.
10. **Batterson, W., and B. Roizman.** 1983. Characterization of the herpes simplex virion-associated factor responsible for the induction of alpha genes. *J Virol* **46**:371-7.
11. **Block, T., S. Barney, J. Masonis, J. Maggioncalda, T. Valyi-Nagy, and N. W. Fraser.** 1994. Long term herpes simplex virus type 1 infection of nerve growth factor-treated PC12 cells. *J Gen Virol* **75 (Pt 9)**:2481-7.
12. **Block, T. M., S. Deshmane, J. Masonis, J. Maggioncalda, T. Valyi-Nagi, and N. W. Fraser.** 1993. An HSV LAT null mutant reactivates slowly from latent infection and makes small plaques on CV-1 monolayers. *Virology* **192**:618-30.
13. **Block, T. M., J. G. Spivack, I. Steiner, S. Deshmane, M. T. McIntosh, R. P. Lirette, and N. W. Fraser.** 1990. A herpes simplex virus type 1 latency-associated transcript mutant reactivates with normal kinetics from latent infection. *J Virol* **64**:3417-26.
14. **Blondeau, J. M., F. Y. Aoki, and G. B. Glavin.** 1993. Stress-induced reactivation of latent herpes simplex virus infection in rat lumbar dorsal root ganglia. *J Psychosom Res* **37**:843-9.
15. **Boutell, C., and R. D. Everett.** 2003. The herpes simplex virus type 1 (HSV-1) regulatory protein ICP0 interacts with and Ubiquitinates p53. *J Biol Chem* **278**:36596-602.
16. **Boutell, C., A. Orr, and R. D. Everett.** 2003. PML residue lysine 160 is required for the degradation of PML induced by herpes simplex virus type 1 regulatory protein ICP0. *J Virol* **77**:8686-94.
17. **Boutell, C., S. Sadis, and R. D. Everett.** 2002. Herpes simplex virus type 1 immediate-early protein ICP0 and its isolated RING finger domain act as ubiquitin E3 ligases in vitro. *J Virol* **76**:841-50.
18. **Branco, F. J., and N. W. Fraser.** 2005. Herpes simplex virus type 1 latency-associated transcript expression protects trigeminal ganglion neurons from apoptosis. *J Virol* **79**:9019-25.
19. **Buschhausen, G., M. Graessmann, and A. Graessmann.** 1985. Inhibition of herpes simplex thymidine kinase gene expression by DNA methylation is an indirect effect. *Nucleic Acids Res* **13**:5503-13.
20. **Buschhausen, G., B. Wittig, M. Graessmann, and A. Graessmann.** 1987. Chromatin structure is required to block transcription of the methylated herpes simplex virus thymidine kinase gene. *Proc Natl Acad Sci U S A* **84**:1177-81.

21. **Cai, W., T. L. Astor, L. M. Liptak, C. Cho, D. M. Coen, and P. A. Schaffer.** 1993. The herpes simplex virus type 1 regulatory protein ICP0 enhances virus replication during acute infection and reactivation from latency. *J Virol* **67**:7501-12.
22. **Cai, W., and P. A. Schaffer.** 1992. Herpes simplex virus type 1 ICP0 regulates expression of immediate-early, early, and late genes in productively infected cells. *J Virol* **66**:2904-15.
23. **Cai, W. Z., and P. A. Schaffer.** 1989. Herpes simplex virus type 1 ICP0 plays a critical role in the de novo synthesis of infectious virus following transfection of viral DNA. *J Virol* **63**:4579-89.
24. **Campbell, M. E., J. W. Palfreyman, and C. M. Preston.** 1984. Identification of herpes simplex virus DNA sequences which encode a trans-acting polypeptide responsible for stimulation of immediate early transcription. *J Mol Biol* **180**:1-19.
25. **Chelbi-Alix, M. K., and H. de The.** 1999. Herpes virus induced proteasome-dependent degradation of the nuclear bodies-associated PML and Sp100 proteins. *Oncogene* **18**:935-41.
26. **Chen, Q., L. Lin, S. Smith, J. Huang, S. L. Berger, and J. Zhou.** 2007. CTCF-dependent chromatin boundary element between the latency-associated transcript and ICP0 promoters in the herpes simplex virus type 1 genome. *J Virol* **81**:5192-201.
27. **Ciufo, D. M., M. A. Mullen, and G. S. Hayward.** 1994. Identification of a dimerization domain in the C-terminal segment of the IE110 transactivator protein from herpes simplex virus. *J Virol* **68**:3267-82.
28. **Clements, G. B., and N. D. Stow.** 1989. A herpes simplex virus type 1 mutant containing a deletion within immediate early gene 1 is latency-competent in mice. *J Gen Virol* **70 (Pt 9)**:2501-6.
29. **Cliffe, A. R., and D. M. Knipe.** 2008. Herpes simplex virus ICP0 promotes both histone removal and acetylation on viral DNA during lytic infection. *J Virol* **82**:12030-8.
30. **Colberg-Poley, A. M., H. Isom, and F. Rapp.** 1979. Experimental HSV latency using phosphonoacetic acid. *Proc Soc Exp Biol Med* **162**:235-7.
31. **Colberg-Poley, A. M., H. C. Isom, and F. Rapp.** 1979. Reactivation of herpes simplex virus type 2 from a quiescent state by human cytomegalovirus. *Proc Natl Acad Sci U S A* **76**:5948-51.
32. **Coleman, H. M., V. Connor, Z. S. Cheng, F. Grey, C. M. Preston, and S. Efstathiou.** 2008. Histone modifications associated with herpes simplex virus type 1 genomes during quiescence and following ICP0-mediated de-repression. *J Gen Virol* **89**:68-77.
33. **Conn, K. L., M. J. Hendzel, and L. M. Schang.** 2008. Linker histones are mobilized during infection with herpes simplex virus type 1. *J Virol* **82**:8629-46.

34. **Crouch, N. A., and F. Rapp.** 1972. Cell-dependent differences in the production of infectious herpes simplex virus at a supraoptimal temperature. *J Virol* **9**:223-30.
35. **Crouch, N. A., and F. Rapp.** 1972. Differential effect of temperature on the replication of herpes simplex virus type 1 and type 2. *Virology* **50**:939-41.
36. **Danaher, R. J., R. J. Jacob, M. D. Chorak, C. S. Freeman, and C. S. Miller.** 1999. Heat stress activates production of herpes simplex virus type 1 from quiescently infected neurally differentiated PC12 cells. *J Neurovirol* **5**:374-83.
37. **Danaher, R. J., R. J. Jacob, and C. S. Miller.** 1999. Establishment of a quiescent herpes simplex virus type 1 infection in neurally-differentiated PC12 cells. *J Neurovirol* **5**:258-67.
38. **Danaher, R. J., R. J. Jacob, and C. S. Miller.** 2006. Reactivation from quiescence does not coincide with a global induction of herpes simplex virus type 1 transactivators. *Virus Genes* **33**:163-7.
39. **Danaher, R. J., R. J. Jacob, M. R. Steiner, W. R. Allen, J. M. Hill, and C. S. Miller.** 2005. Histone deacetylase inhibitors induce reactivation of herpes simplex virus type 1 in a latency-associated transcript-independent manner in neuronal cells. *J Neurovirol* **11**:306-17.
40. **Daujat, S., U. M. Bauer, V. Shah, B. Turner, S. Berger, and T. Kouzarides.** 2002. Crosstalk between CARM1 methylation and CBP acetylation on histone H3. *Curr Biol* **12**:2090-7.
41. **Decman, V., P. R. Kinchington, S. A. Harvey, and R. L. Hendricks.** 2005. Gamma interferon can block herpes simplex virus type 1 reactivation from latency, even in the presence of late gene expression. *J Virol* **79**:10339-47.
42. **Delius, H., and J. B. Clements.** 1976. A partial denaturation map of herpes simplex virus type 1 DNA: evidence for inversions of the unique DNA regions. *J Gen Virol* **33**:125-33.
43. **Deshmane, S. L., and N. W. Fraser.** 1989. During latency, herpes simplex virus type 1 DNA is associated with nucleosomes in a chromatin structure. *J Virol* **63**:943-7.
44. **Diao, L., B. Zhang, J. Fan, X. Gao, S. Sun, K. Yang, D. Xin, N. Jin, Y. Geng, and C. Wang.** 2005. Herpes virus proteins ICP0 and BICP0 can activate NF-kappaB by catalyzing IkkappaBalph ubiquitination. *Cell Signal* **17**:217-29.
45. **Dressler, G. R., D. L. Rock, and N. W. Fraser.** 1987. Latent herpes simplex virus type 1 DNA is not extensively methylated in vivo. *J Gen Virol* **68 (Pt 6)**:1761-5.
46. **Efstathiou, S., A. C. Minson, H. J. Field, J. R. Anderson, and P. Wildy.** 1986. Detection of herpes simplex virus-specific DNA sequences in latently infected mice and in humans. *J Virol* **57**:446-55.

47. **Egger, G., G. Liang, A. Aparicio, and P. A. Jones.** 2004. Epigenetics in human disease and prospects for epigenetic therapy. *Nature* **429**:457-63.
48. **Everett, R. D.** 2000. ICP0 induces the accumulation of colocalizing conjugated ubiquitin. *J Virol* **74**:9994-10005.
49. **Everett, R. D.** 2000. ICP0, a regulator of herpes simplex virus during lytic and latent infection. *Bioessays* **22**:761-70.
50. **Everett, R. D.** 2006. Interactions between DNA viruses, ND10 and the DNA damage response. *Cell Microbiol* **8**:365-74.
51. **Everett, R. D.** 1984. Trans activation of transcription by herpes virus products: requirement for two HSV-1 immediate-early polypeptides for maximum activity. *Embo J* **3**:3135-41.
52. **Everett, R. D., P. Barlow, A. Milner, B. Luisi, A. Orr, G. Hope, and D. Lyon.** 1993. A novel arrangement of zinc-binding residues and secondary structure in the C3HC4 motif of an alpha herpes virus protein family. *J Mol Biol* **234**:1038-47.
53. **Everett, R. D., C. Boutell, and A. Orr.** 2004. Phenotype of a herpes simplex virus type 1 mutant that fails to express immediate-early regulatory protein ICP0. *J Virol* **78**:1763-74.
54. **Everett, R. D., and M. K. Chelbi-Alix.** 2007. PML and PML nuclear bodies: implications in antiviral defence. *Biochimie* **89**:819-30.
55. **Everett, R. D., W. C. Earnshaw, J. Findlay, and P. Lomonte.** 1999. Specific destruction of kinetochore protein CENP-C and disruption of cell division by herpes simplex virus immediate-early protein Vmw110. *Embo J* **18**:1526-38.
56. **Everett, R. D., W. C. Earnshaw, A. F. Pluta, T. Sternsdorf, A. M. Ainsztein, M. Carmena, S. Ruchaud, W. L. Hsu, and A. Orr.** 1999. A dynamic connection between centromeres and ND10 proteins. *J Cell Sci* **112 (Pt 20)**:3443-54.
57. **Everett, R. D., P. Freemont, H. Saitoh, M. Dasso, A. Orr, M. Kathoria, and J. Parkinson.** 1998. The disruption of ND10 during herpes simplex virus infection correlates with the Vmw110- and proteasome-dependent loss of several PML isoforms. *J Virol* **72**:6581-91.
58. **Everett, R. D., M. Meredith, and A. Orr.** 1999. The ability of herpes simplex virus type 1 immediate-early protein Vmw110 to bind to a ubiquitin-specific protease contributes to its roles in the activation of gene expression and stimulation of virus replication. *J Virol* **73**:417-26.
59. **Everett, R. D., and J. Murray.** 2005. ND10 components relocate to sites associated with herpes simplex virus type 1 nucleoprotein complexes during virus infection. *J Virol* **79**:5078-89.

60. **Everett, R. D., J. Murray, A. Orr, and C. M. Preston.** 2007. Herpes simplex virus type 1 genomes are associated with ND10 nuclear substructures in quiescently infected human fibroblasts. *J Virol* **81**:10991-1004.
61. **Everett, R. D., A. Orr, and C. M. Preston.** 1998. A viral activator of gene expression functions via the ubiquitin-proteasome pathway. *Embo J* **17**:7161-9.
62. **Everett, R. D., C. Parada, P. Gripon, H. Sirma, and A. Orr.** 2008. Replication of ICP0-null mutant herpes simplex virus type 1 is restricted by both PML and Sp100. *J Virol* **82**:2661-72.
63. **Everett, R. D., S. Rechter, P. Papior, N. Tavalai, T. Stamminger, and A. Orr.** 2006. PML contributes to a cellular mechanism of repression of herpes simplex virus type 1 infection that is inactivated by ICP0. *J Virol* **80**:7995-8005.
64. **Everett, R. D., G. Sourvinos, C. Leiper, J. B. Clements, and A. Orr.** 2004. Formation of nuclear foci of the herpes simplex virus type 1 regulatory protein ICP4 at early times of infection: localization, dynamics, recruitment of ICP27, and evidence for the de novo induction of ND10-like complexes. *J Virol* **78**:1903-17.
65. **Everett, R. D., and A. Zafiropoulos.** 2004. Visualization by live-cell microscopy of disruption of ND10 during herpes simplex virus type 1 infection. *J Virol* **78**:11411-5.
66. **Ferenczy, M. W., and N. A. DeLuca.** 2009. Epigenetic modulation of gene expression from quiescent herpes simplex virus genomes. *J Virol* **83**:8514-24.
67. **Freeman, M. L., B. S. Sheridan, R. H. Bonneau, and R. L. Hendricks.** 2007. Psychological Stress Compromises CD8+ T Cell Control of Latent Herpes Simplex Virus Type 1 Infections. *J Immunol* **179**:322-8.
68. **Freemont, P. S.** 1993. The RING finger. A novel protein sequence motif related to the zinc finger. *Ann N Y Acad Sci* **684**:174-92.
69. **Freemont, P. S., I. M. Hanson, and J. Trowsdale.** 1991. A novel cysteine-rich sequence motif. *Cell* **64**:483-4.
70. **Friedmann, A., J. Shlomai, and Y. Becker.** 1977. Electron microscopy of herpes simplex virus DNA molecules isolated from infected cells by centrifugation in CsCl density gradients. *J Gen Virol* **34**:507-22.
71. **Gaffney, D. F., J. McLauchlan, J. L. Whitton, and J. B. Clements.** 1985. A modular system for the assay of transcription regulatory signals: the sequence TAATGARAT is required for herpes simplex virus immediate early gene activation. *Nucleic Acids Res* **13**:7847-63.
72. **Gelman, I. H., and S. Silverstein.** 1985. Identification of immediate early genes from herpes simplex virus that transactivate the virus thymidine kinase gene. *Proc Natl Acad Sci U S A* **82**:5265-9.

73. **Giordani, N. V., D. M. Neumann, D. L. Kwiatkowski, P. S. Bhattacharjee, P. K. McAnany, J. M. Hill, and D. C. Bloom.** 2008. During Hsv-1 Infection of Rabbits, the Ability to Express the Lat Increases Latent-Phase Transcription of Lytic Genes. *J Virol*.
74. **Goetze, S., J. Mateos-Langerak, and R. van Driel.** 2007. Three-dimensional genome organization in interphase and its relation to genome function. *Semin Cell Dev Biol* **18**:707-14.
75. **Grant, P. A., A. Eberharter, S. John, R. G. Cook, B. M. Turner, and J. L. Workman.** 1999. Expanded lysine acetylation specificity of Gen5 in native complexes. *J Biol Chem* **274**:5895-900.
76. **Green, M. T., J. E. Knesek, E. C. Dunkel, and G. K. SeGall.** 1987. Localization of 3H-thymidine-labeled HSV-1 in latently infected rabbit trigeminal ganglion cells. *Invest Ophthalmol Vis Sci* **28**:394-7.
77. **Gregory, D. A., and S. L. Bachenheimer.** 2008. Characterization of mre11 loss following HSV-1 infection. *Virology* **373**:124-36.
78. **Gu, H., Y. Liang, G. Mandel, and B. Roizman.** 2005. Components of the REST/CoREST/histone deacetylase repressor complex are disrupted, modified, and translocated in HSV-1-infected cells. *Proc Natl Acad Sci U S A* **102**:7571-6.
79. **Gu, H., and B. Roizman.** 2003. The degradation of promyelocytic leukemia and Sp100 proteins by herpes simplex virus 1 is mediated by the ubiquitin-conjugating enzyme UbcH5a. *Proc Natl Acad Sci U S A* **100**:8963-8.
80. **Gu, H., and B. Roizman.** 2009. Engagement of the Lysine Specific Demethylase/HDAC1/CoREST/REST Complex by Herpes Simplex Virus 1. *J Virol*.
81. **Gu, H., and B. Roizman.** 2007. Herpes simplex virus-infected cell protein 0 blocks the silencing of viral DNA by dissociating histone deacetylases from the CoREST-REST complex. *Proc Natl Acad Sci U S A* **104**:17134-9.
82. **Gu, H., and B. Roizman.** 2007. Herpes simplex virus-infected cell protein 0 blocks the silencing of viral DNA by dissociating histone deacetylases from the CoREST REST complex. *Proc Natl Acad Sci U S A*.
83. **Gu, H., and B. Roizman.** 2009. The two functions of herpes simplex virus 1 ICP0, inhibition of silencing by the CoREST/REST/HDAC complex and degradation of PML, are executed in tandem. *J Virol* **83**:181-7.
84. **Hagglund, R., and B. Roizman.** 2004. Role of ICP0 in the strategy of conquest of the host cell by herpes simplex virus 1. *J Virol* **78**:2169-78.
85. **Halford, W. P., C. D. Kemp, J. A. Isler, D. J. Davido, and P. A. Schaffer.** 2001. ICP0, ICP4, or VP16 expressed from adenovirus vectors induces reactivation of latent herpes

- simplex virus type 1 in primary cultures of latently infected trigeminal ganglion cells. *J Virol* **75**:6143-53.
86. **Halford, W. P., and P. A. Schaffer.** 2001. ICP0 is required for efficient reactivation of herpes simplex virus type 1 from neuronal latency. *J Virol* **75**:3240-9.
 87. **Hammer, S. M., J. C. Kaplan, B. R. Lowe, and M. S. Hirsch.** 1982. Alpha interferon and acyclovir treatment of herpes simplex virus in lymphoid cell cultures. *Antimicrob Agents Chemother* **21**:634-40.
 88. **Hammer, S. M., B. S. Richter, and M. S. Hirsch.** 1981. Activation and suppression of herpes simplex virus in a human T lymphoid cell line. *J Immunol* **127**:144-8.
 89. **Hancock, M. H., J. A. Corcoran, and J. R. Smiley.** 2006. Herpes simplex virus regulatory proteins VP16 and ICP0 counteract an innate intranuclear barrier to viral gene expression. *Virology* **352**:237-52.
 90. **Happel, N., and D. Doenecke.** 2009. Histone H1 and its isoforms: contribution to chromatin structure and function. *Gene* **431**:1-12.
 91. **Harle, P., B. Sainz, Jr., D. J. Carr, and W. P. Halford.** 2002. The immediate-early protein, ICP0, is essential for the resistance of herpes simplex virus to interferon-alpha/beta. *Virology* **293**:295-304.
 92. **Harris, R. A., R. D. Everett, X. X. Zhu, S. Silverstein, and C. M. Preston.** 1989. Herpes simplex virus type 1 immediate-early protein Vmw110 reactivates latent herpes simplex virus type 2 in an in vitro latency system. *J Virol* **63**:3513-5.
 93. **Harris, R. A., and C. M. Preston.** 1991. Establishment of latency in vitro by the herpes simplex virus type 1 mutant in1814. *J Gen Virol* **72 (Pt 4)**:907-13.
 94. **Hayward, G. S., R. J. Jacob, S. C. Wadsworth, and B. Roizman.** 1975. Anatomy of herpes simplex virus DNA: evidence for four populations of molecules that differ in the relative orientations of their long and short components. *Proc Natl Acad Sci U S A* **72**:4243-7.
 95. **Herrera, F. J., and S. J. Triezenberg.** 2004. VP16-dependent association of chromatin-modifying coactivators and underrepresentation of histones at immediate-early gene promoters during herpes simplex virus infection. *J Virol* **78**:9689-96.
 96. **Hobbs, W. E., D. E. Brough, I. Kovesdi, and N. A. DeLuca.** 2001. Efficient activation of viral genomes by levels of herpes simplex virus ICP0 insufficient to affect cellular gene expression or cell survival. *J Virol* **75**:3391-403.
 97. **Hobbs, W. E., and N. A. DeLuca.** 1999. Perturbation of cell cycle progression and cellular gene expression as a function of herpes simplex virus ICP0. *J Virol* **73**:8245-55.

98. **Hoggan, M. D., and B. Roizman.** 1959. The effect of the temperature of incubation on the formation and release of herpes simplex virus in infected FL cells. *Virology* **8**:508-24.
99. **Honess, R. W., and B. Roizman.** 1974. Regulation of herpesvirus macromolecular synthesis. I. Cascade regulation of the synthesis of three groups of viral proteins. *J Virol* **14**:8-19.
100. **Honess, R. W., and B. Roizman.** 1975. Regulation of herpesvirus macromolecular synthesis: sequential transition of polypeptide synthesis requires functional viral polypeptides. *Proc Natl Acad Sci U S A* **72**:1276-80.
101. **Hsu, W. L., and R. D. Everett.** 2001. Human neuron-committed teratocarcinoma NT2 cell line has abnormal ND10 structures and is poorly infected by herpes simplex virus type 1. *J Virol* **75**:3819-31.
102. **Huang, C. J., M. K. Rice, G. B. Devi-Rao, and E. K. Wagner.** 1994. The activity of the pseudorabies virus latency-associated transcript promoter is dependent on its genomic location in herpes simplex virus recombinants as well as on the type of cell infected. *J Virol* **68**:1972-6.
103. **Huang, J., J. R. Kent, B. Placek, K. A. Whelan, C. M. Hollow, P. Y. Zeng, N. W. Fraser, and S. L. Berger.** 2006. Trimethylation of histone H3 lysine 4 by Set1 in the lytic infection of human herpes simplex virus 1. *J Virol* **80**:5740-6.
104. **Idowu, A. D., E. B. Fraser-Smith, K. L. Poffenberger, and R. C. Herman.** 1992. Deletion of the herpes simplex virus type 1 ribonucleotide reductase gene alters virulence and latency in vivo. *Antiviral Res* **17**:145-56.
105. **Ishov, A. M., and G. G. Maul.** 1996. The periphery of nuclear domain 10 (ND10) as site of DNA virus deposition. *J Cell Biol* **134**:815-26.
106. **Ishov, A. M., A. G. Sotnikov, D. Negorev, O. V. Vladimirova, N. Neff, T. Kamitani, E. T. Yeh, J. F. Strauss, 3rd, and G. G. Maul.** 1999. PML is critical for ND10 formation and recruits the PML-interacting protein daxx to this nuclear structure when modified by SUMO-1. *J Cell Biol* **147**:221-34.
107. **Ishov, A. M., O. V. Vladimirova, and G. G. Maul.** 2004. Heterochromatin and ND10 are cell-cycle regulated and phosphorylation-dependent alternate nuclear sites of the transcription repressor Daxx and SWI/SNF protein ATRX. *J Cell Sci* **117**:3807-20.
108. **Jackson, S. A., and N. A. DeLuca.** 2003. Relationship of herpes simplex virus genome configuration to productive and persistent infections. *Proc Natl Acad Sci U S A* **100**:7871-6.
109. **Jacob, R. J., and B. Roizman.** 1977. Anatomy of herpes simplex virus DNA VIII. Properties of the replicating DNA. *J Virol* **23**:394-411.

110. **Jamieson, D. R., L. H. Robinson, J. I. Daksis, M. J. Nicholl, and C. M. Preston.** 1995. Quiescent viral genomes in human fibroblasts after infection with herpes simplex virus type 1 Vmw65 mutants. *J Gen Virol* **76 (Pt 6):**1417-31.
111. **Javier, R. T., J. G. Stevens, V. B. Dissette, and E. K. Wagner.** 1988. A herpes simplex virus transcript abundant in latently infected neurons is dispensable for establishment of the latent state. *Virology* **166:**254-7.
112. **Jenuwein, T., and C. D. Allis.** 2001. Translating the histone code. *Science* **293:**1074-80.
113. **Jordan, R., and P. A. Schaffer.** 1997. Activation of gene expression by herpes simplex virus type 1 ICP0 occurs at the level of mRNA synthesis. *J Virol* **71:**6850-62.
114. **Kawaguchi, Y., R. Bruni, and B. Roizman.** 1997. Interaction of herpes simplex virus 1 alpha regulatory protein ICP0 with elongation factor 1delta: ICP0 affects translational machinery. *J Virol* **71:**1019-24.
115. **Kawaguchi, Y., M. Tanaka, A. Yokoyama, G. Matsuda, K. Kato, H. Kagawa, K. Hirai, and B. Roizman.** 2001. Herpes simplex virus 1 alpha regulatory protein ICP0 functionally interacts with cellular transcription factor BMAL1. *Proc Natl Acad Sci U S A* **98:**1877-82.
116. **Kawaguchi, Y., C. Van Sant, and B. Roizman.** 1997. Herpes simplex virus 1 alpha regulatory protein ICP0 interacts with and stabilizes the cell cycle regulator cyclin D3. *J Virol* **71:**7328-36.
117. **Kent, J. R., P. Y. Zeng, D. Atanasiu, J. Gardner, N. W. Fraser, and S. L. Berger.** 2004. During lytic infection herpes simplex virus type 1 is associated with histones bearing modifications that correlate with active transcription. *J Virol* **78:**10178-86.
118. **Khanna, K. M., R. H. Bonneau, P. R. Kinchington, and R. L. Hendricks.** 2003. Herpes simplex virus-specific memory CD8+ T cells are selectively activated and retained in latently infected sensory ganglia. *Immunity* **18:**593-603.
119. **Knipe, D. M., and A. Cliffe.** 2008. Chromatin control of herpes simplex virus lytic and latent infection. *Nat Rev Microbiol.*
120. **Knotts, F. B., M. L. Cook, and J. G. Stevens.** 1973. Latent herpes simplex virus in the central nervous system of rabbits and mice. *J Exp Med* **138:**740-4.
121. **Koch, C. M., R. M. Andrews, P. Flicek, S. C. Dillon, U. Karaoz, G. K. Clelland, S. Wilcox, D. M. Beare, J. C. Fowler, P. Couttet, K. D. James, G. C. Lefebvre, A. W. Bruce, O. M. Dovey, P. D. Ellis, P. Dhami, C. F. Langford, Z. Weng, E. Birney, N. P. Carter, D. Vetric, and I. Dunham.** 2007. The landscape of histone modifications across 1% of the human genome in five human cell lines. *Genome Res* **17:**691-707.
122. **Kondo, Y., Y. Yura, H. Iga, T. Yanagawa, H. Yoshida, N. Furumoto, and M. Sato.** 1990. Effect of hexamethylene bisacetamide and cyclosporin A on recovery of herpes

- simplex virus type 2 from the in vitro model of latency in a human neuroblastoma cell line. *Cancer Res* **50**:7852-7.
123. **Kornberg, R. D.** 1974. Chromatin structure: a repeating unit of histones and DNA. *Science* **184**:868-71.
 124. **Kosz-Vnenchak, M., D. M. Coen, and D. M. Knipe.** 1990. Restricted expression of herpes simplex virus lytic genes during establishment of latent infection by thymidine kinase-negative mutant viruses. *J Virol* **64**:5396-402.
 125. **Kouzarides, T.** 2007. Chromatin modifications and their function. *Cell* **128**:693-705.
 126. **Kramer, M. F., and D. M. Coen.** 1995. Quantification of transcripts from the ICP4 and thymidine kinase genes in mouse ganglia latently infected with herpes simplex virus. *J Virol* **69**:1389-99.
 127. **Kubat, N. J., A. L. Amelio, N. V. Giordani, and D. C. Bloom.** 2004. The herpes simplex virus type 1 latency-associated transcript (LAT) enhancer/rcr is hyperacetylated during latency independently of LAT transcription. *J Virol* **78**:12508-18.
 128. **Kubat, N. J., R. K. Tran, P. McAnany, and D. C. Bloom.** 2004. Specific histone tail modification and not DNA methylation is a determinant of herpes simplex virus type 1 latent gene expression. *J Virol* **78**:1139-49.
 129. **Kuo, M. H., and C. D. Allis.** 1999. In vivo cross-linking and immunoprecipitation for studying dynamic Protein:DNA associations in a chromatin environment. *Methods* **19**:425-33.
 130. **Lacasse, J. J., and L. M. Schang.** 2009. During lytic infections, Herpes Simplex Virus Type 1 DNA is in complexes with the properties of unstable nucleosomes. *J Virol*.
 131. **Lachner, M., D. O'Carroll, S. Rea, K. Mechtler, and T. Jenuwein.** 2001. Methylation of histone H3 lysine 9 creates a binding site for HP1 proteins. *Nature* **410**:116-20.
 132. **Lancz, G. J., and T. L. Zetzlemoyer.** 1976. Restricted replication of herpes simplex virus in neural cells. *Proc Soc Exp Biol Med* **152**:302-6.
 133. **Lees-Miller, S. P., M. C. Long, M. A. Kilvert, V. Lam, S. A. Rice, and C. A. Spencer.** 1996. Attenuation of DNA-dependent protein kinase activity and its catalytic subunit by the herpes simplex virus type 1 transactivator ICP0. *J Virol* **70**:7471-7.
 134. **Lehming, N., A. Le Saux, J. Schuller, and M. Ptashne.** 1998. Chromatin components as part of a putative transcriptional repressing complex. *Proc Natl Acad Sci U S A* **95**:7322-6.
 135. **Leib, D. A., D. M. Coen, C. L. Bogard, K. A. Hicks, D. R. Yager, D. M. Knipe, K. L. Tyler, and P. A. Schaffer.** 1989. Immediate-early regulatory gene mutants define

- different stages in the establishment and reactivation of herpes simplex virus latency. *J Virol* **63**:759-68.
136. **Leinbach, S. S., and W. C. Summers.** 1980. The structure of herpes simplex virus type 1 DNA as probed by micrococcal nuclease digestion. *J Gen Virol* **51**:45-59.
 137. **Lentine, A. F., and S. L. Bachenheimer.** 1990. Intracellular organization of herpes simplex virus type 1 DNA assayed by staphylococcal nuclease sensitivity. *Virus Res* **16**:275-92.
 138. **Li, B., M. Carey, and J. L. Workman.** 2007. The role of chromatin during transcription. *Cell* **128**:707-19.
 139. **Li, W., W. Cun, L. Liu, M. Hong, L. Wang, L. Wang, C. Dong, and Q. Li.** 2009. The transactivating effect of HSV-1 ICP0 is enhanced by its interaction with the PCAF component of histone acetyltransferase. *Arch Virol*.
 140. **Liedtke, W., B. Opalka, C. W. Zimmermann, and E. Lignitz.** 1993. Age distribution of latent herpes simplex virus 1 and varicella-zoster virus genome in human nervous tissue. *J Neurol Sci* **116**:6-11.
 141. **Liesegang, T. J., L. J. Melton, 3rd, P. J. Daly, and D. M. Ilstrup.** 1989. Epidemiology of ocular herpes simplex. Incidence in Rochester, Minn, 1950 through 1982. *Arch Ophthalmol* **107**:1155-9.
 142. **Lilley, C. E., C. T. Carson, A. R. Muotri, F. H. Gage, and M. D. Weitzman.** 2005. DNA repair proteins affect the lifecycle of herpes simplex virus 1. *Proc Natl Acad Sci U S A* **102**:5844-9.
 143. **Lilley, C. E., M. S. Chaurushiya, C. Boutell, S. Landry, J. Suh, S. Panier, R. D. Everett, G. S. Stewart, D. Durocher, and M. D. Weitzman.** A viral E3 ligase targets RNF8 and RNF168 to control histone ubiquitination and DNA damage responses. *Embo J* **29**:943-55.
 144. **Lin, R., R. S. Noyce, S. E. Collins, R. D. Everett, and K. L. Mossman.** 2004. The herpes simplex virus ICP0 RING finger domain inhibits IRF3- and IRF7-mediated activation of interferon-stimulated genes. *J Virol* **78**:1675-84.
 145. **Liu, Y., and M. Kulesz-Martin.** 2001. p53 protein at the hub of cellular DNA damage response pathways through sequence-specific and non-sequence-specific DNA binding. *Carcinogenesis* **22**:851-60.
 146. **Lium, E. K., and S. Silverstein.** 1997. Mutational analysis of the herpes simplex virus type 1 ICP0 C3HC4 zinc ring finger reveals a requirement for ICP0 in the expression of the essential alpha27 gene. *J Virol* **71**:8602-14.

147. **Locker, H., and N. Frenkel.** 1979. BamI, KpnI, and Sall restriction enzyme maps of the DNAs of herpes simplex virus strains Justin and F: occurrence of heterogeneities in defined regions of the viral DNA. *J Virol* **32**:429-41.
148. **Loiacono, C. M., N. S. Taus, and W. J. Mitchell.** 2003. The herpes simplex virus type 1 ICP0 promoter is activated by viral reactivation stimuli in trigeminal ganglia neurons of transgenic mice. *J Neurovirol* **9**:336-45.
149. **Lomberk, G., L. Wallrath, and R. Urrutia.** 2006. The Heterochromatin Protein 1 family. *Genome Biol* **7**:228.
150. **Lomonte, P., and R. D. Everett.** 1999. Herpes simplex virus type 1 immediate-early protein Vmw110 inhibits progression of cells through mitosis and from G(1) into S phase of the cell cycle. *J Virol* **73**:9456-67.
151. **Lomonte, P., and E. Morency.** 2007. Centromeric protein CENP-B proteasomal degradation induced by the viral protein ICP0. *FEBS Lett* **581**:658-62.
152. **Lomonte, P., K. F. Sullivan, and R. D. Everett.** 2001. Degradation of nucleosome-associated centromeric histone H3-like protein CENP-A induced by herpes simplex virus type 1 protein ICP0. *J Biol Chem* **276**:5829-35.
153. **Lomonte, P., J. Thomas, P. Texier, C. Caron, S. Khochbin, and A. L. Epstein.** 2004. Functional interaction between class II histone deacetylases and ICP0 of herpes simplex virus type 1. *J Virol* **78**:6744-57.
154. **Luger, K., A. W. Mader, R. K. Richmond, D. F. Sargent, and T. J. Richmond.** 1997. Crystal structure of the nucleosome core particle at 2.8 Å resolution. *Nature* **389**:251-60.
155. **Lukashchuk, V., and R. D. Everett.** Regulation of ICP0-null mutant herpes simplex virus type 1 infection by ND10 components ATRX and hDaxx. *J Virol* **84**:4026-40.
156. **Maillet, S., T. Naas, S. Crepin, A. M. Roque-Afonso, F. Lafay, S. Efstathiou, and M. Labetoulle.** 2006. Herpes simplex virus type 1 latently infected neurons differentially express latency-associated and ICP0 transcripts. *J Virol* **80**:9310-21.
157. **Maison, C., and G. Almouzni.** 2004. HP1 and the dynamics of heterochromatin maintenance. *Nat Rev Mol Cell Biol* **5**:296-304.
158. **Marshall, K. R., R. H. Lachmann, S. Efstathiou, A. Rinaldi, and C. M. Preston.** 2000. Long-term transgene expression in mice infected with a herpes simplex virus type 1 mutant severely impaired for immediate-early gene expression. *J Virol* **74**:956-64.
159. **Maul, G. G.** 1998. Nuclear domain 10, the site of DNA virus transcription and replication. *Bioessays* **20**:660-7.

160. **Maul, G. G., and R. D. Everett.** 1994. The nuclear location of PML, a cellular member of the C3HC4 zinc-binding domain protein family, is rearranged during herpes simplex virus infection by the C3HC4 viral protein ICP0. *J Gen Virol* **75 (Pt 6)**:1223-33.
161. **Maul, G. G., A. M. Ishov, and R. D. Everett.** 1996. Nuclear domain 10 as preexisting potential replication start sites of herpes simplex virus type-1. *Virology* **217**:67-75.
162. **McMahon, R., and D. Walsh.** 2008. Efficient quiescent infection of normal human diploid fibroblasts with wild-type herpes simplex virus type 1. *J Virol* **82**:10218-30.
163. **Meignier, B., R. Longnecker, P. Mavromara-Nazos, A. E. Sears, and B. Roizman.** 1988. Virulence of and establishment of latency by genetically engineered deletion mutants of herpes simplex virus 1. *Virology* **162**:251-4.
164. **Mellerick, D. M., and N. W. Fraser.** 1987. Physical state of the latent herpes simplex virus genome in a mouse model system: evidence suggesting an episomal state. *Virology* **158**:265-75.
165. **Melroe, G. T., N. A. DeLuca, and D. M. Knipe.** 2004. Herpes simplex virus 1 has multiple mechanisms for blocking virus-induced interferon production. *J Virol* **78**:8411-20.
166. **Melroe, G. T., L. Silva, P. A. Schaffer, and D. M. Knipe.** 2007. Recruitment of activated IRF-3 and CBP/p300 to herpes simplex virus ICP0 nuclear foci: Potential role in blocking IFN-beta induction. *Virology* **360**:305-21.
167. **Minagawa, H., and Y. Yanagi.** 2000. Latent herpes simplex virus-1 infection in SCID mice transferred with immune CD4+T cells: a new model for latency. *Arch Virol* **145**:2259-72.
168. **Minaker, R. L., K. L. Mossman, and J. R. Smiley.** 2005. Functional inaccessibility of quiescent herpes simplex virus genomes. *Virol J* **2**:85.
169. **Mossman, K. L., H. A. Saffran, and J. R. Smiley.** 2000. Herpes simplex virus ICP0 mutants are hypersensitive to interferon. *J Virol* **74**:2052-6.
170. **Mossman, K. L., and J. R. Smiley.** 1999. Truncation of the C-terminal acidic transcriptional activation domain of herpes simplex virus VP16 renders expression of the immediate-early genes almost entirely dependent on ICP0. *J Virol* **73**:9726-33.
171. **Mouttet, M. E., D. Guetard, and J. M. Bechet.** 1979. Random cleavage of intranuclear herpes simplex virus DNA by micrococcal nuclease. *FEBS Lett* **100**:107-9.
172. **Muggeridge, M. I., and N. W. Fraser.** 1986. Chromosomal organization of the herpes simplex virus genome during acute infection of the mouse central nervous system. *J Virol* **59**:764-7.

173. **Mullen, M. A., D. M. Ciuffo, and G. S. Hayward.** 1994. Mapping of intracellular localization domains and evidence for colocalization interactions between the IE110 and IE175 nuclear transactivator proteins of herpes simplex virus. *J Virol* **68**:3250-66.
174. **Nakayama, J., J. C. Rice, B. D. Strahl, C. D. Allis, and S. I. Grewal.** 2001. Role of histone H3 lysine 9 methylation in epigenetic control of heterochromatin assembly. *Science* **292**:110-3.
175. **Negorev, D., and G. G. Maul.** 2001. Cellular proteins localized at and interacting within ND10/PML nuclear bodies/PODs suggest functions of a nuclear depot. *Oncogene* **20**:7234-42.
176. **Neumann, D. M., P. S. Bhattacharjee, N. V. Giordani, D. C. Bloom, and J. M. Hill.** 2007. In Vivo Changes in the Patterns of Chromatin Structure Associated with the Latent HSV-1 Genome in the Mouse Trigeminal Ganglia Can Be Detected at Early Times after Butyrate Treatment. *J Virol*.
177. **Nielsen, A. L., M. Oulad-Abdelghani, J. A. Ortiz, E. Remboutsika, P. Chambon, and R. Losson.** 2001. Heterochromatin formation in mammalian cells: interaction between histones and HP1 proteins. *Mol Cell* **7**:729-39.
178. **Nilheden, E., S. Jeansson, and A. Vahlne.** 1985. Herpes simplex virus latency in a hyperresistant clone of mouse neuroblastoma (C1300) cells. *Arch Virol* **83**:319-25.
179. **Nishiyama, Y., and F. Rapp.** 1981. Latency in vitro using irradiated herpes simplex virus. *J Gen Virol* **52**:113-9.
180. **O'Hare, P., and G. S. Hayward.** 1985. Evidence for a direct role for both the 175,000- and 110,000-molecular-weight immediate-early proteins of herpes simplex virus in the transactivation of delayed-early promoters. *J Virol* **53**:751-60.
181. **O'Neill, F. J.** 1977. Prolongation of herpes simplex virus latency in cultured human cells by temperature elevation. *J Virol* **24**:41-6.
182. **O'Rourke, D., G. Elliott, M. Papworth, R. Everett, and P. O'Hare.** 1998. Examination of determinants for intranuclear localization and transactivation within the RING finger of herpes simplex virus type 1 IE110k protein. *J Gen Virol* **79 (Pt 3)**:537-48.
183. **Oh, J., and N. W. Fraser.** 2008. Temporal association of the herpes simplex virus genome with histone proteins during a lytic infection. *J Virol* **82**:3530-7.
184. **Okuwaki, M., and K. Nagata.** 1998. Template activating factor-I remodels the chromatin structure and stimulates transcription from the chromatin template. *J Biol Chem* **273**:34511-8.

185. **Openshaw, H., L. V. Asher, C. Wohlenberg, T. Sekizawa, and A. L. Notkins.** 1979. Acute and latent infection of sensory ganglia with herpes simplex virus: immune control and virus reactivation. *J Gen Virol* **44**:205-15.
186. **Padgett, D. A., J. F. Sheridan, J. Dorne, G. G. Berntson, J. Candelora, and R. Glaser.** 1998. Social stress and the reactivation of latent herpes simplex virus type 1. *Proc Natl Acad Sci U S A* **95**:7231-5.
187. **Park, Y. J., and K. Luger.** 2008. Histone chaperones in nucleosome eviction and histone exchange. *Curr Opin Struct Biol* **18**:282-9.
188. **Parkinson, J., S. P. Lees-Miller, and R. D. Everett.** 1999. Herpes simplex virus type 1 immediate-early protein vmw110 induces the proteasome-dependent degradation of the catalytic subunit of DNA-dependent protein kinase. *J Virol* **73**:650-7.
189. **Perry, L. J., F. J. Rixon, R. D. Everett, M. C. Frame, and D. J. McGeoch.** 1986. Characterization of the IE110 gene of herpes simplex virus type 1. *J Gen Virol* **67 (Pt 11)**:2365-80.
190. **Pinnoji, R. C., G. R. Bedadala, B. George, T. C. Holland, J. M. Hill, and S. C. Hsia.** 2007. Repressor element-1 silencing transcription factor/neuronal restrictive silencer factor (REST/NRSF) can regulate HSV-1 immediate-early transcription via histone modification. *Virology* **4**:56.
191. **Pluta, A. F., W. C. Earnshaw, and I. G. Goldberg.** 1998. Interphase-specific association of intrinsic centromere protein CENP-C with HDaxx, a death domain-binding protein implicated in Fas-mediated cell death. *J Cell Sci* **111 (Pt 14)**:2029-41.
192. **Poffenberger, K. L., A. D. Idowu, E. B. Fraser-Smith, P. E. Raichlen, and R. C. Herman.** 1994. A herpes simplex virus type 1 ICP22 deletion mutant is altered for virulence and latency in vivo. *Arch Virol* **139**:111-9.
193. **Poffenberger, K. L., and B. Roizman.** 1985. A noninverting genome of a viable herpes simplex virus 1: presence of head-to-tail linkages in packaged genomes and requirements for circularization after infection. *J Virol* **53**:587-95.
194. **Poon, A. P., H. Gu, and B. Roizman.** 2006. ICP0 and the US3 protein kinase of herpes simplex virus 1 independently block histone deacetylation to enable gene expression. *Proc Natl Acad Sci U S A* **103**:9993-8.
195. **Poon, A. P., Y. Liang, and B. Roizman.** 2003. Herpes simplex virus 1 gene expression is accelerated by inhibitors of histone deacetylases in rabbit skin cells infected with a mutant carrying a cDNA copy of the infected-cell protein no. 0. *J Virol* **77**:12671-8.
196. **Preston, C. M., R. Mabbs, and M. J. Nicholl.** 1997. Construction and characterization of herpes simplex virus type 1 mutants with conditional defects in immediate early gene expression. *Virology* **229**:228-39.

197. **Preston, C. M., and M. J. Nicholl.** 2008. Induction of cellular stress overcomes the requirement of herpes simplex virus type 1 for immediate-early protein ICP0 and reactivates expression from quiescent viral genomes. *J Virol* **82**:11775-83.
198. **Preston, C. M., and M. J. Nicholl.** 1997. Repression of gene expression upon infection of cells with herpes simplex virus type 1 mutants impaired for immediate-early protein synthesis. *J Virol* **71**:7807-13.
199. **Preston, C. M., J. Russell, R. A. Harris, and D. R. Jamieson.** 1994. Herpes simplex virus latency in tissue culture cells. *Gene Ther* **1 Suppl 1**:S49-50.
200. **Quinlan, M. P., and D. M. Knipe.** 1985. Stimulation of expression of a herpes simplex virus DNA-binding protein by two viral functions. *Mol Cell Biol* **5**:957-63.
201. **Rea, S., F. Eisenhaber, D. O'Carroll, B. D. Strahl, Z. W. Sun, M. Schmid, S. Opravil, K. Mechtler, C. P. Ponting, C. D. Allis, and T. Jenuwein.** 2000. Regulation of chromatin structure by site-specific histone H3 methyltransferases. *Nature* **406**:593-9.
202. **Rice, J. C., and C. D. Allis.** 2001. Histone methylation versus histone acetylation: new insights into epigenetic regulation. *Curr Opin Cell Biol* **13**:263-73.
203. **Rock, D. L., and N. W. Fraser.** 1983. Detection of HSV-1 genome in central nervous system of latently infected mice. *Nature* **302**:523-5.
204. **Roizman, B.** 1979. The structure and isomerization of herpes simplex virus genomes. *Cell* **16**:481-94.
205. **Roizman, B., H. Gu, and G. Mandel.** 2005. The first 30 minutes in the life of a virus: unREST in the nucleus. *Cell Cycle* **4**:1019-21.
206. **Roizman, B., D. M. Knipe, and R. J. Whitley.** 2007. Herpes Simplex Viruses, p. 2501-2601. *In* D. M. Knipe, P. M. Howley, D. E. Griffin, R. A. Lamb, M. A. Martin, B. Roizman, and S. E. Strauss (ed.), *Fields Virology*, 5th ed. Lippincott Williams & Wilkins, Philadelphia.
207. **Roizman, B., and A. E. Sears.** 2001. Herpes Simplex Viruses and Their Replication, p. 2231-2295. *In* B. N. Fields, D. M. Knipe, P. M. Howley, and D. E. Griffin (ed.), *Fields' Virology*, 4th ed. Lippincott Williams & Wilkins, Philadelphia.
208. **Russell, J., and C. M. Preston.** 1986. An in vitro latency system for herpes simplex virus type 2. *J Gen Virol* **67 (Pt 2)**:397-403.
209. **Russell, J., N. D. Stow, E. C. Stow, and C. M. Preston.** 1987. Herpes simplex virus genes involved in latency in vitro. *J Gen Virol* **68 (Pt 12)**:3009-18.
210. **Sacks, W. R., and P. A. Schaffer.** 1987. Deletion mutants in the gene encoding the herpes simplex virus type 1 immediate-early protein ICP0 exhibit impaired growth in cell culture. *J Virol* **61**:829-39.

211. **Samaniego, L. A., L. Neiderhiser, and N. A. DeLuca.** 1998. Persistence and expression of the herpes simplex virus genome in the absence of immediate-early proteins. *J Virol* **72**:3307-20.
212. **Samaniego, L. A., N. Wu, and N. A. DeLuca.** 1997. The herpes simplex virus immediate-early protein ICP0 affects transcription from the viral genome and infected-cell survival in the absence of ICP4 and ICP27. *J Virol* **71**:4614-25.
213. **Sampath, P., and N. A. Deluca.** 2008. Binding of ICP4, TATA-binding protein, and RNA polymerase II to herpes simplex virus type 1 immediate-early, early, and late promoters in virus-infected cells. *J Virol* **82**:2339-49.
214. **Sawtell, N. M., and R. L. Thompson.** 2004. Comparison of herpes simplex virus reactivation in ganglia in vivo and in explants demonstrates quantitative and qualitative differences. *J Virol* **78**:7784-94.
215. **Schacker, T.** 2001. The role of HSV in the transmission and progression of HIV. *Herpes* **8**:46-9.
216. **Schang, L. M., A. Bantly, and P. A. Schaffer.** 2002. Explant-induced reactivation of herpes simplex virus occurs in neurons expressing nuclear cdk2 and cdk4. *J Virol* **76**:7724-35.
217. **Scheck, A. C., B. Wigdahl, E. De Clercq, and F. Rapp.** 1986. Prolonged herpes simplex virus latency in vitro after treatment of infected cells with acyclovir and human leukocyte interferon. *Antimicrob Agents Chemother* **29**:589-93.
218. **Schotta, G., A. Ebert, V. Krauss, A. Fischer, J. Hoffmann, S. Rea, T. Jenuwein, R. Dorn, and G. Reuter.** 2002. Central role of Drosophila SU(VAR)3-9 in histone H3-K9 methylation and heterochromatic gene silencing. *Embo J* **21**:1121-31.
219. **Schueler, M. G., and B. A. Sullivan.** 2006. Structural and Functional Dynamics of Human Centromeric Chromatin. *Annu Rev Genomics Hum Genet.*
220. **Seeler, J. S., A. Marchio, D. Sitterlin, C. Transy, and A. Dejean.** 1998. Interaction of SP100 with HP1 proteins: a link between the promyelocytic leukemia-associated nuclear bodies and the chromatin compartment. *Proc Natl Acad Sci U S A* **95**:7316-21.
221. **Shahbazian, M. D., and M. Grunstein.** 2007. Functions of site-specific histone acetylation and deacetylation. *Annu Rev Biochem* **76**:75-100.
222. **Shaw, J. E., L. F. Levinger, and C. W. Carter, Jr.** 1979. Nucleosomal structure of Epstein-Barr virus DNA in transformed cell lines. *J Virol* **29**:657-65.
223. **Sheridan, B. S., J. E. Knickelbein, and R. L. Hendricks.** 2007. CD8 T cells and latent herpes simplex virus type 1: keeping the peace in sensory ganglia. *Expert Opin Biol Ther* **7**:1323-31.

224. **Shi, Y., F. Lan, C. Matson, P. Mulligan, J. R. Whetstine, P. A. Cole, R. A. Casero, and Y. Shi.** 2004. Histone demethylation mediated by the nuclear amine oxidase homolog LSD1. *Cell* **119**:941-53.
225. **Shiraki, K., and F. Rapp.** 1986. Establishment of herpes simplex virus latency in vitro with cycloheximide. *J Gen Virol* **67 (Pt 11)**:2497-500.
226. **Shirata, N., A. Kudoh, T. Daikoku, Y. Tatsumi, M. Fujita, T. Kiyono, Y. Sugaya, H. Isomura, K. Ishizaki, and T. Tsurumi.** 2005. Activation of ataxia telangiectasia-mutated DNA damage checkpoint signal transduction elicited by herpes simplex virus infection. *J Biol Chem* **280**:30336-41.
227. **Smallwood, A., P. O. Esteve, S. Pradhan, and M. Carey.** 2007. Functional cooperation between HP1 and DNMT1 mediates gene silencing. *Genes Dev* **21**:1169-78.
228. **Smith, R. L., J. M. Escudero, and C. L. Wilcox.** 1994. Regulation of the herpes simplex virus latency-associated transcripts during establishment of latency in sensory neurons in vitro. *Virology* **202**:49-60.
229. **Spivack, J. G., and N. W. Fraser.** 1987. Detection of herpes simplex virus type 1 transcripts during latent infection in mice. *J Virol* **61**:3841-7.
230. **Spivack, J. G., and N. W. Fraser.** 1988. Expression of herpes simplex virus type 1 (HSV-1) latency-associated transcripts and transcripts affected by the deletion in avirulent mutant HFEM: evidence for a new class of HSV-1 genes. *J Virol* **62**:3281-7.
231. **Spivack, J. G., and N. W. Fraser.** 1988. Expression of herpes simplex virus type 1 latency-associated transcripts in the trigeminal ganglia of mice during acute infection and reactivation of latent infection. *J Virol* **62**:1479-85.
232. **Steiner, I., J. G. Spivack, S. L. Deshmane, C. I. Ace, C. M. Preston, and N. W. Fraser.** 1990. A herpes simplex virus type 1 mutant containing a nontransducing Vmw65 protein establishes latent infection in vivo in the absence of viral replication and reactivates efficiently from explanted trigeminal ganglia. *J Virol* **64**:1630-8.
233. **Stevens, J. G., and M. L. Cook.** 1971. Latent herpes simplex virus in spinal ganglia of mice. *Science* **173**:843-5.
234. **Stevens, J. G., E. K. Wagner, G. B. Devi-Rao, M. L. Cook, and L. T. Feldman.** 1987. RNA complementary to a herpesvirus alpha gene mRNA is prominent in latently infected neurons. *Science* **235**:1056-9.
235. **Stinski, M. F., and T. J. Roehr.** 1985. Activation of the major immediate early gene of human cytomegalovirus by cis-acting elements in the promoter-regulatory sequence and by virus-specific trans-acting components. *J Virol* **55**:431-41.

236. **Stinski, M. F., D. R. Thomsen, R. M. Stenberg, and L. C. Goldstein.** 1983. Organization and expression of the immediate early genes of human cytomegalovirus. *J Virol* **46**:1-14.
237. **Stow, N. D., and E. C. Stow.** 1986. Isolation and characterization of a herpes simplex virus type 1 mutant containing a deletion within the gene encoding the immediate early polypeptide Vmw110. *J Gen Virol* **67 (Pt 12)**:2571-85.
238. **Strelow, L. I., and D. A. Leib.** 1995. Role of the virion host shutoff (vhs) of herpes simplex virus type 1 in latency and pathogenesis. *J Virol* **69**:6779-86.
239. **Su, Y. H., M. J. Moxley, A. K. Ng, J. Lin, R. Jordan, N. W. Fraser, and T. M. Block.** 2002. Stability and circularization of herpes simplex virus type 1 genomes in quiescently infected PC12 cultures. *J Gen Virol* **83**:2943-50.
240. **Sullivan, K. F., M. Hechenberger, and K. Masri.** 1994. Human CENP-A contains a histone H3 related histone fold domain that is required for targeting to the centromere. *J Cell Biol* **127**:581-92.
241. **Syrjanen, S., H. Mikola, M. Nykanen, and V. Hukkanen.** 1996. In vitro establishment of lytic and nonproductive infection by herpes simplex virus type 1 in three-dimensional keratinocyte culture. *J Virol* **70**:6524-8.
242. **Tal-Singer, R., T. M. Lasner, W. Podrzucki, A. Skokotas, J. J. Leary, S. L. Berger, and N. W. Fraser.** 1997. Gene expression during reactivation of herpes simplex virus type 1 from latency in the peripheral nervous system is different from that during lytic infection of tissue cultures. *J Virol* **71**:5268-76.
243. **Tang, J., S. Wu, H. Liu, R. Stratt, O. G. Barak, R. Shiekhattar, D. J. Picketts, and X. Yang.** 2004. A novel transcription regulatory complex containing death domain-associated protein and the ATR-X syndrome protein. *J Biol Chem* **279**:20369-77.
244. **Tavalai, N., P. Papior, S. Rechter, M. Leis, and T. Stamminger.** 2006. Evidence for a role of the cellular ND10 protein PML in mediating intrinsic immunity against human cytomegalovirus infections. *J Virol* **80**:8006-18.
245. **Taylor, J. L., D. Unverrich, W. J. O'Brien, and K. W. Wilcox.** 2000. Interferon coordinately inhibits the disruption of PML-positive ND10 and immediate-early gene expression by herpes simplex virus. *J Interferon Cytokine Res* **20**:805-15.
246. **Terry-Allison, T., C. A. Smith, and N. A. DeLuca.** 2007. Relaxed repression of herpes simplex virus type 1 genomes in Murine trigeminal neurons. *J Virol* **81**:12394-405.
247. **Theil, D., T. Derfuss, I. Paripovic, S. Herberger, E. Meinl, O. Schueler, M. Strupp, V. Arbusow, and T. Brandt.** 2003. Latent herpesvirus infection in human trigeminal ganglia causes chronic immune response. *Am J Pathol* **163**:2179-84.

248. **Thompson, R. L., C. M. Preston, and N. M. Sawtell.** 2009. De novo synthesis of VP16 coordinates the exit from HSV latency in vivo. *PLoS Pathog* **5**:e1000352.
249. **Thomsen, D. R., R. M. Stenberg, W. F. Goins, and M. F. Stinski.** 1984. Promoter-regulatory region of the major immediate early gene of human cytomegalovirus. *Proc Natl Acad Sci U S A* **81**:659-63.
250. **Tomishima, M. J., G. A. Smith, and L. W. Enquist.** 2001. Sorting and transport of alpha herpesviruses in axons. *Traffic* **2**:429-36.
251. **Tremethick, D. J.** 2007. Higher-order structures of chromatin: the elusive 30 nm fiber. *Cell* **128**:651-4.
252. **Umbach, J. L., M. F. Kramer, I. Jurak, H. W. Karnowski, D. M. Coen, and B. R. Cullen.** 2008. MicroRNAs expressed by herpes simplex virus 1 during latent infection regulate viral mRNAs. *Nature* **454**:780-3.
253. **Vahlne, A., and E. Lycke.** 1978. Herpes simplex virus infection of in vitro cultured neuronal cells (mouse neuroblastoma C 1300 cells). *J Gen Virol* **39**:321-32.
254. **Valyi-Nagy, T., S. L. Deshmane, J. G. Spivack, I. Steiner, C. I. Ace, C. M. Preston, and N. W. Fraser.** 1991. Investigation of herpes simplex virus type 1 (HSV-1) gene expression and DNA synthesis during the establishment of latent infection by an HSV-1 mutant, in1814, that does not replicate in mouse trigeminal ganglia. *J Gen Virol* **72 (Pt 3)**:641-9.
255. **van Leeuwen, H., M. Okuwaki, R. Hong, D. Chakravarti, K. Nagata, and P. O'Hare.** 2003. Herpes simplex virus type 1 tegument protein VP22 interacts with TAF-I proteins and inhibits nucleosome assembly but not regulation of histone acetylation by INHAT. *J Gen Virol* **84**:2501-10.
256. **Van Sant, C., R. Hagglund, P. Lopez, and B. Roizman.** 2001. The infected cell protein 0 of herpes simplex virus 1 dynamically interacts with proteasomes, binds and activates the cdc34 E2 ubiquitin-conjugating enzyme, and possesses in vitro E3 ubiquitin ligase activity. *Proc Natl Acad Sci U S A* **98**:8815-20.
257. **Van Sant, C., P. Lopez, S. J. Advani, and B. Roizman.** 2001. Role of cyclin D3 in the biology of herpes simplex virus 1 ICPO. *J Virol* **75**:1888-98.
258. **Verdin, E., F. Dequiedt, and H. G. Kasler.** 2003. Class II histone deacetylases: versatile regulators. *Trends Genet* **19**:286-93.
259. **Wang, Q. Y., C. Zhou, K. E. Johnson, R. C. Colgrove, D. M. Coen, and D. M. Knipe.** 2005. Herpesviral latency-associated transcript gene promotes assembly of heterochromatin on viral lytic-gene promoters in latent infection. *Proc Natl Acad Sci U S A* **102**:16055-9.

260. **Watson, R. J., and J. B. Clements.** 1980. A herpes simplex virus type 1 function continuously required for early and late virus RNA synthesis. *Nature* **285**:329-30.
261. **Wheeler, C. E.** 1958. The effect of temperature upon the production of herpes simplex virus in tissue culture. *J Immunol* **81**:98-106.
262. **Wheeler, C. E., and C. M. Canby.** 1959. Effect of temperature on the growth curves of herpes simplex virus in tissue cultures. *J Immunol* **83**:392-6.
263. **Whitley, R. J.** 2001. Herpes Simplex Viruses, p. 2461-2342. *In* B. N. Fields, D. M. Knipe, P. M. Howley, and D. E. Griffin (ed.), *Fields' Virology*, 4th ed. Lippincott Williams & Wilkins, Philadelphia.
264. **Whitley, R. J., and J. W. Gnann, Jr.** 1993. The Epidemiology and Clinical Manifestations of Herpes Simplex Virus Infections, p. 69-105. *In* B. Roizman, R. J. Whitley, and C. Lopez (ed.), *The Human Herpesviruses*. Raven Press, New York.
265. **Whitley, R. J., D. W. Kimberlin, and B. Roizman.** 1998. Herpes simplex viruses. *Clin Infect Dis* **26**:541-53; quiz 554-5.
266. **Wigdahl, B., A. C. Scheck, R. J. Ziegler, E. De Clercq, and F. Rapp.** 1984. Analysis of the herpes simplex virus genome during in vitro latency in human diploid fibroblasts and rat sensory neurons. *J Virol* **49**:205-13.
267. **Wigdahl, B., C. A. Smith, H. M. Traglia, and F. Rapp.** 1984. Herpes simplex virus latency in isolated human neurons. *Proc Natl Acad Sci U S A* **81**:6217-21.
268. **Wigdahl, B. L., H. C. Isom, and F. Rapp.** 1981. Repression and activation of the genome of herpes simplex viruses in human cells. *Proc Natl Acad Sci U S A* **78**:6522-6.
269. **Wigdahl, B. L., A. C. Scheck, E. De Clercq, and F. Rapp.** 1982. High efficiency latency and activation of herpes simplex virus in human cells. *Science* **217**:1145-6.
270. **Wilcox, C. L., L. S. Crnic, and L. I. Pizer.** 1992. Replication, latent infection, and reactivation in neuronal culture with a herpes simplex virus thymidine kinase-negative mutant. *Virology* **187**:348-52.
271. **Wilcox, C. L., and E. M. Johnson, Jr.** 1988. Characterization of nerve growth factor-dependent herpes simplex virus latency in neurons in vitro. *J Virol* **62**:393-9.
272. **Wilcox, C. L., and E. M. Johnson, Jr.** 1987. Nerve growth factor deprivation results in the reactivation of latent herpes simplex virus in vitro. *J Virol* **61**:2311-5.
273. **Wilcox, C. L., R. L. Smith, R. D. Everett, and D. Mysofski.** 1997. The herpes simplex virus type 1 immediate-early protein ICP0 is necessary for the efficient establishment of latent infection. *J Virol* **71**:6777-85.

274. **Wilcox, C. L., R. L. Smith, C. R. Freed, and E. M. Johnson, Jr.** 1990. Nerve growth factor-dependence of herpes simplex virus latency in peripheral sympathetic and sensory neurons in vitro. *J Neurosci* **10**:1268-75.
275. **Wilkinson, D. E., and S. K. Weller.** 2004. Recruitment of cellular recombination and repair proteins to sites of herpes simplex virus type 1 DNA replication is dependent on the composition of viral proteins within prereplicative sites and correlates with the induction of the DNA damage response. *J Virol* **78**:4783-96.
276. **Wolffe, A. P., and D. Guschin.** 2000. Review: chromatin structural features and targets that regulate transcription. *J Struct Biol* **129**:102-22.
277. **Xue, Y., R. Gibbons, Z. Yan, D. Yang, T. L. McDowell, S. Sechi, J. Qin, S. Zhou, D. Higgs, and W. Wang.** 2003. The ATRX syndrome protein forms a chromatin-remodeling complex with Daxx and localizes in promyelocytic leukemia nuclear bodies. *Proc Natl Acad Sci U S A* **100**:10635-40.
278. **Yao, F., and P. A. Schaffer.** 1995. An activity specified by the osteosarcoma line U2OS can substitute functionally for ICP0, a major regulatory protein of herpes simplex virus type 1. *J Virol* **69**:6249-58.
279. **Zabierowski, S., and N. A. DeLuca.** 2004. Differential cellular requirements for activation of herpes simplex virus type 1 early (tk) and late (gC) promoters by ICP4. *J Virol* **78**:6162-70.
280. **Zaret, K.** 2005. Micrococcal nuclease analysis of chromatin structure. *Curr Protoc Mol Biol* **Chapter 21**:Unit 21 1.
281. **Zhang, Y., and C. Jones.** 2001. The bovine herpesvirus 1 immediate-early protein (bICP0) associates with histone deacetylase 1 to activate transcription. *J Virol* **75**:9571-8.
282. **Zhu, X. X., J. X. Chen, C. S. Young, and S. Silverstein.** 1990. Reactivation of latent herpes simplex virus by adenovirus recombinants encoding mutant IE-0 gene products. *J Virol* **64**:4489-98.
283. **Zhu, Z., W. Cai, and P. A. Schaffer.** 1994. Cooperativity among herpes simplex virus type 1 immediate-early regulatory proteins: ICP4 and ICP27 affect the intracellular localization of ICP0. *J Virol* **68**:3027-40.